EFFECTS OF LONG DURATION EARTHQUAKES ON BRIDGE STRUCTURES

By

BLANDINE C. VALLE

A thesis submitted in partial fulfillment of
the requirements for the degree of

MASTER OF SCIENCE IN CIVIL ENGINEERING

WASHINGTON STATE UNIVERSITY
Department of Civil and Environmental Engineering

DECEMBER 2005

To the faculty of Washington State University:

The members of the Committee appointed to examine the thesis of BLANDINE VALLE find it satisfactory and recommend that it be accepted.

____
Chair

____

____

ACKNOWLEDGMENTS

This research was carried out in the Department of Civil and Environmental Engineering at Washington State University, Pullman, Washington. Funding was provided by The Washington State Department of Transportation (WSDOT).

I wish to express my gratitude to the chairman of my committee, Dr. McDaniel, for his patience, guidance and support throughout the project. Special thanks are extended to Drs. McLean and Cofer for serving on my committee. I would also like to thank Cody Cox for his generous help and advice.

I am thankful to Maureen Clausen and Vicky Ruddick for helping me with the administrative issues throughout the project.

Most of all, I would like to thank my family for supporting and encouraging me all through my studies and I am deeply grateful to Tom for his love, encouragement and advice throughout the past five years.

EFFECTS OF LONG DURATION EARTHQUAKES ON BRIDGE STRUCTURES

ABSTRACT

By Blandine C Valle, M.S.
Washington State University
December 2005

Chair: Cole C. McDaniel

The main objective of this research was to assess the response of multi-column bent bridges, with columns expected to behave primarily in shear, subject to long-duration earthquake. Recent geological evidence indicates that the potential exists for large earthquakes resulting in long-duration ground motions in the Pacific Northwest due to rupturing of the locked interface between the Juan de Fuca and the North American Plate. Three Washington State Department of Transportation bridges were selected for this study, bridges 5/227, 5/649 and 512/29. All three bridges are located in close proximity to Olympia and Seattle. Ten earthquake records with return periods ranging from 475 to 2475 years were used to study the effect of duration on bridge response; six long-duration and four short-duration.

Since the column aspect ratios were similar for the three bridges (approximately 3), other bridge characteristics were more influential on the variation of the bridge seismic responses. The bridge deck design, monolithic or non-monolithic, and the bridge geometry greatly influenced the behavior. Each bridge was unique enough that in order

to accurately assess the seismic vulnerability of each bridge, nonlinear time history analyses were needed rather than basing predictions merely on bridge member detailing, as is often the case due to limited resources.

In general, the 475-year return period earthquakes induced light to moderate cracking in the column plastic hinge regions for all bridges. The 975-year return period earthquakes created more severe cracking with bearing pad failures in one of the bridges. The 2475-year return period earthquakes induced failures in the center bent columns as well as numerous bearing pad failures for all three bridges. The damage estimations for each earthquake were based on damage recorded in experimental column testing.

Overall, long-duration earthquakes created more damage in the three bridges than short-duration earthquakes. For the smaller earthquakes, the duration had little effect on the bridge response since multiple cycles at low ductility demands did not lead to damage of the columns. As the intensity of the earthquake and the duration increased, damage in the columns increased. Therefore, both earthquake intensity and ground motion duration affect the bridge response; however, large intensity alone can lead to significant demand on the bridges, while duration is not influential on the bridge demand unless the intensity is high as well.

TABLE OF CONTENTS

Abstract ... iv

Table of Contents ... vi

List of Figures ... ix

List of Tables ... xvi

CHAPTER ONE ... 1

Introduction ... 1

1.1 Background ... 1

1.2 Objectives ... 1

1.3 Seismic Activity in the Pacific Northwest ... 2

CHAPTER TWO ... 7

Literature Review ... 7

2.1 Definition of Earthquake Duration ... 7

2.2 Damage Indices ... 11

2.3 Effect of Earthquake Duration on the Damage in Reinforced Concrete Structures ... 13

CHAPTER THREE ... 15

Bridge Modeling ... 15

3.1 Bridge Descriptions ... 15

3.1.1 Bridge 5/227 ... 15

- Geographical Location ... 15
- Bridge Properties ... 15
- Bridge Material Properties ... 20

3.1.2. Bridge 5/649 21

- Geographical Location 21
- Bridge Properties 21
- Bridge Material Properties 25

3.1.3 Bridge 512/19 26

- Geographical Location 26
- Bridge Properties 26
- Bridge Material Properties 31

3.2 Bridge Calibration 31

3.2.1 Jaradat Specimens 31

3.2.2 Scaling 33

- Scaling the Forces and Moments: 34
- Scaling the Displacements 36

3.2.3 Modeling 39

- Calculating the Spring Values 41

CHAPTER FOUR 44

Seismic Analysis 44

4.1 Seismic Excitations 44

CHAPTER FIVE 57

Bridge 5/649 Skew Comparison 57

5.1 Bridge 5/649 Skew or Straight Model 57

5.1.1 Maximum Demands 58

5.1.2 Hysteresis Curves 61

5.1.3 Time History Comparison.. 64

CHAPTER SIX 67

Bridge Response 67

6.1 Bridge 5/227.. 67

6.2 Bridge 512/19.. 83

6.3 Bridge 5/649.. 93

CHAPTER SEVEN 103

Conclusions... 103

References... 107

APPENDICES 109

APPENDIX A-1.. 110

APPENDIX A-2.. 113

A-2-1 Ruaumoko 3D Input File Calculations 114

A-2-1 Bridge 5/227 Ruaumoko Input File.. 115

A-2-2 Bridge 512/19 Ruamoko Input File.. 125

A-2-3 Bridge 5/649 Ruaumoko Input File.. 132

APPENDIX A-3.. 141

APPENDIX A-4.. 142

LIST OF FIGURES

Figure 1.3-1 Cascadia Subduction Zone (from The Pacific Northwest Seismograph Network) 3

Figure 1.3-2 Map of the Bridge Locations..... 5

Figure 2.1-1 Difference Between Rock Site and Soil Site Acceleration Spectra 9

Figure 2.1-2 Duration versus Magnitude for Rock Sites in the Western United States. .. 10

Figure 2.2-1 Reliability Index Versus Earthquake Duration from Lindt *et al.* (2004) 12

Figure 2.3-1 Expected Damage versus Normalized Duration for Representative Linear Reinforced Concrete Structure..... 14

Figure 3.1.1-1 Bridge 5/227 Location..... 15

Figure 3.1.1-2 Bridge 5/227 Plan View 16

Figure 3.1.1-3 Bridge 5/227 Elevation View..... 16

Figure 3.1.1-4 Bridge 5/227 50 ft. Series Girder 17

Figure 3.1.1-5 Bridge 5/227 Column Detail 18

Figure 3.1.1-6 Bridge 5/227 Intermediate Bent Footings 19

Figure 3.1.1-7 Bridge 5/227 Expansion Joint Detail 19

Figure 3.1.1-8 Bridge 5/227 Abutment Sub-Ground Column and Footing..... 20

Figure 3.1.2-1 Bridge 5/649 Location..... 21

Figure 3.1.2-2 Bridge 5/649 Plan View 22

Figure 3.1.2-3 Bridge 5/649 Elevation View..... 22

Figure 3.1.2-4 Bridge 5/649 Girder Detail..... 23

Figure 3.1.2-5 Bridge 5/649 Column Detail 24

Figure 3.1.2-6 Bridge 5/649 Footing Detail 24
Figure 3.1.2-7 Bridge 5/649 Abutment Footing detail: (a) Cross-section, (b) Elevation . 25
Figure 3.1.3-1 Bridge 512/19 Intersection 26
Figure 3.1.3-2 Bridge 512/19 Plan View 27
Figure 3.1.3-3 Bridge 512/19 Elevation View 27
Figure 3.1.3-4 Bridge 512/19 Girder Detail 28
Figure 3.1.3-5 Bridge 512/19 Column Detail 29
Figure 3.1.3-6 Bridge 512/19 Abutment Cross-section 30
Figure 3.1.3-7 Bridge 512/19 Girder Stop : (a) Plan View and (b) Locations 30
Figure 3.2.1-1 Specimen T2 Lateral Load-Displacement Hysteresis Curve 32
Figure 3.2.1-2 Specimen T2 Force-Displacement Envelope of Specimen T2 33
Figure 3.2.2-1 Relationship Between "D-a/2" Experimental and Model 35
Figure 3.2.2-2 Bilinear Relationship Between Moment and Curvature 37
Figure 3.2.2-3 Linear Relationship Between Φ_u - Φ_y Factor 38
Figure 3.2.3-1 Column Reinforcement Pattern 39
Figure 3.2.3-2 Comparison Between Force-Displacement Curves with Strain Penetration and Without 40
Figures 4.1-1 Time Histories for the Large Return Period Earthquakes: Chile 2475 45
Figures 4.1-2 Time Histories for the Large Return Period Earthquakes: Peru 2475 45
Figures 4.1-3 Time Histories for the Large Return Period Earthquakes: Kobe 975 45
Figures 4.1-4 Time Histories for the Large Return Period Earthquakes: Olympia 975 ... 46
Figures 4.1-5 Time Histories for the Large Return Period Earthquakes: Mexico City 975 46

Figures 4.1-6 Time Histories for the Small Return Period Earthquakes: Chile 975......... 46

Figures 4.1-7 Time Histories for the Small Return Period Earthquakes: Peru 975.......... 47

Figures 4.1-8 Time Histories for the Small Return Period Earthquakes: Kobe 475......... 47

Figures 4.1-9 Time Histories for the Small Return Period Earthquakes: Olympia 475 ... 47

Figures 4.1-10 Time Histories for the Small Return Period Earthquakes: Mexico City 475 48

Figure 4.1-11 ARS and DRS for Chile 975 and 2475 Earthquakes................................. 49

Figure 4.1-12 ARS and DRS for Peru 975 and 2475 Earthquakes.................................. 50

Figure 4.1-13 ARS and DRS for Kobe 475 and 975 Earthquakes................................... 51

Figure 4.1-14 ARS and DRS for Olympia 475 and 975 Earthquakes............................. 52

Figure 4.1-15 ARS and DRS for Mexico City 475 and 975 Earthquakes........................ 53

Figure 4.1-16 ARS for the 2001 Nisqually, Peru 2475 and Olympia 975 Earthquakes... 56

Figure 5.1-1 5/649 Bridge Spine Model with Skew 57

Figure 5.1-2 5/649 Bridge Spine Model without Skew 58

Figure 5.1.2-1 South Bent, Center Column: Hysteresis Curves for Bridge 5/649 – Without Skew; Olympia 975 EQ; Es=47.9 MPa (1000ksf); 861.9 MPa (18000 ksf) 62

Figure 5.1.2-2 South Bent, Center Column: Hysteresis Curves for Bridge 5/649 - With Skew; Olympia 975 EQ; Es=287.3 MPa (6000 ksf); 861.9 MPa (18000 ksf) 62

Figure 5.1.2-3 South Bent, Center Column: Hysteresis Curves for Bridge 5/649 - Without Skew; Peru 2475 EQ; Es=47.9 MPa (1000ksf); 861.9 MPa (18000 ksf) ... 63

Figure 5.1.2-4 South Bent, Center Column: Hysteresis Curves for Bridge 5/649 - With Skew; Peru 2475 EQ; Es=287.3 MPa (6000 ksf); 861.9 MPa (18000 ksf) 63

Figure 5.1.3-1 Displacement Versus Time for the Olympia 975 and Peru 2475 Earthquakes, 287.3 MPa Spring Models With Skew 64

Figure 5.1.3-2 Displacement Versus Time for the Olympia 975 and Peru 2475 Earthquakes, 287.3 MPa Spring Models Without Skew.. 65

Figure 5.1.3-3 Displacement Versus Time for the Olympia 975 and Peru 2475 Earthquakes, 861.9 MPa Spring Models With Skew 65

Figure 5.1.3-4 Displacement Versus Time for the Olympia 975 and Peru 2475 Earthquakes, 861.9 MPa Spring Models Without Skew.. 66

Figure 6.1-1 Center Bent, Center Column: Hysteresis Curves for Bridge 5/227; Chile 975 and Peru 975 EQ; Fixed Column Bases/Roller Abutment Boundary Conditions 73

Figure 6.1-2 Center Bent, Center Column: Hysteresis Curves for Bridge 5/227; Kobe 975 EQ, Mexico City 975 EQ; Olympia 975 EQ; Chile 2475 EQ and Peru 2475 EQ; Fixed Column Bases/Roller Abutment Boundary Conditions................................. 74

Figure 6.1-3 Center Bent, Center Column: Hysteresis Curves for Bridge 5/227; Kobe 975 EQ; Es=47.9 MPa (1000ksf); 861.9 MPa (18000 ksf) 75

Figure 6.1-4 Center Bent, Center Column: Hysteresis Curves for Bridge 5/227; Mexico City 975 EQ; Es= 47.9 MPa (1000ksf); 861.9 MPa (18000 ksf)............................. 75

Figure 6.1-5 Center Bent, Center Column: Hysteresis Curves for Bridge 5/227; Olympia 975 EQ; Es=47.9 MPa (1000ksf); 861.9 MPa (18000 ksf) 76

Figure 6.1-6 Center Bent, Center Column: Hysteresis Curves for Bridge 5/227; Chile 2475 EQ; Es=47.9 MPa (1000ksf); 861.9 MPa (18000 ksf) 76

Figure 6.1-7 Center Bent, Center Column: Hysteresis Curves for Bridge 5/227; Peru 2475 EQ; Es=47.9 MPa (1000ksf); 861.9 MPa (18000 ksf) 77

Figure 6.1-8 Center Bent, Center Column: Displacement Time History for Bridge 5/227; Peru 2475 EQ; Es=287.3 MPa 78

Figure 6.1-9 Center Bent, Center Column: Displacement Time History for Bridge 5/227; Peru 2475 EQ; Es=861.9 MPa 79

Figure 6.1-10 Specimen T2 Lateral Load-Displacement Hysteresis Curve 80

Figure 6.1-11 Spalling of the Concrete (Stapelton, 2004) 80

Figure 6.1-12 Vertical Cracks at Tension Face (Stapelton, 2004) 81

Figure 6.2-1 Center Bent, Middle East Column: Hysteresis Curves for Bridge 512/19; Chile 975 EQ and Peru 975 EQ; Fixed Column Base/Roller Abutment Boundary Conditions 85

Figure 6.2-2 Center Bent, Middle East Column: Hysteresis Curves for Bridge 512/19; Chile 975 EQ; Es=47.9 MN/m^2 (1000ksf); 861.9 MN/m^2 (18000 ksf) 86

Figure 6.2-3 Center Bent, Middle East Column: Hysteresis Curves for Bridge 512/19; Peru 975 EQ; Es=47.9 MN/m^2 (1000ksf); 861.9 MN/m^2 (18000 ksf) 86

Figure 6.2-4 Center Bent, Middle East Column: Hysteresis Curves for Bridge 512/19; Kobe 975 EQ, Mexico City 975 EQ, Olympia 975 EQ, Chile 2475 EQ and Peru 2475 EQ; Fixed Column Base/Roller Abutment Boundary Conditions 87

Figure 6.2-5 Center Bent, Middle East Column: Hysteresis Curves for Bridge 512/19; Kobe 975 EQ; Es=287.3 MN/m^2 (6000 ksf); 861.9 MN/m^2 (18000 ksf) 88

Figure 6.2-6 Center Bent, Middle East Column: Hysteresis Curves for Bridge 512/19; Mexico City 975 EQ; Es=287.3 MPa (6000 ksf); 861.9 MPa (18000 ksf) 88

Figure 6.2-7 Center Bent, Middle East Column: Hysteresis Curves for Bridge 512/19; Olympia 975 EQ; Es=287.3 MN/m^2 (6000 ksf); 861.89 MN/m^2 (18000 ksf) 89

Figure 6.2-8 Center Bent, Middle East Column: Hysteresis Curves for Bridge 512/19; Chile 2475 EQ; Es=287.3 MN/m^2 (6000 ksf); 861.9 MN/m^2 (18000 ksf) 89

Figure 6.2-9 Center Bent, Middle East Column: Hysteresis Curves for Bridge 512/19; Peru 2475 EQ; Es=287.3 MN/m^2 (6000 ksf); 861.9 Pa (18000 ksf) 90

Figure 6.2-10 Center Bent, Middle East Column: Displacement Time History for Bridge 512/19; Peru 2475 EQ; Es=287.3 MPa.. 91

Figure 6.2-11 Center Bent, Middle East Column: Displacement Time History for Bridge 512/19; Peru 2475 EQ; Es=861.9 MPa.. 91

Figure 6.3-1 South Bent, Center Column: Hysteresis Curves for Bridge 5/649 E; Chile 975 EQ, Peru 975 EQ; Fixed Column Bases/Roller Abutment Boundary Conditions 95

Figure 6.3-2 South Bent, Center Column: Hysteresis Curves for Bridge 5/649E; Chile 975 EQ; Es=287.3 MPa (6000 ksf); 861.9 MPa (18000 ksf) 95

Figure 6.3-3 South Bent, Center Column: Hysteresis Curves for Bridge 5/649E; Peru 975 EQ; Es=287.3 MPa (6000 ksf); 861.9 MPa (18000 ksf) 96

Figure 6.3-4 South Bent, Center Column: Hysteresis Curves for Bridge 5/649 E; Kobe 975 EQ, Mexico City 975 EQ, Olympia 975 EQ, Chile 2475 EQ and Peru 2475 EQ; Fixed Column Base/Roller Abutment Boundary Conditions 97

Figure 6.3-5 South Bent, Center Column: Hysteresis Curves for Bridge 5/649E; Kobe 975 EQ; Es=287.3 MPa (6000 ksf); 861.9 MPa (18000 ksf) 98

Figure 6.3-6 South Bent, Center Column: Hysteresis Curves for Bridge 5/649E; Mexico City 975 EQ; Es=287.3 MPa (6000 ksf); 861.9 MPa (18000 ksf)........................... 98

Figure 6.3-7 South Bent, Center Column: Hysteresis Curves for Bridge 5/649E; Olympia 975 EQ; Es=287.3 MPa (6000 ksf); 861.9 MPa (18000 ksf) 99

Figure 6.3-8 South Bent, Center Column: Hysteresis Curves for Bridge 5/649E; Chile 2475 EQ; Es=287.3 MPa (6000 ksf); 861.9 MPa (18000 ksf) 99

Figure 6.3-9 South Bent, Center Column: Hysteresis Curves for Bridge 5/649E; Peru 2475 EQ; Es=287.3 MPa (6000 ksf); 861.9 MPa (18000 ksf) 100

Figure 6.3-10 South Bent, Center Column: Displacement Time History for Bridge 5/649E; Peru 2475 EQ; Es=287.3 MPa 101

Figure 6.3-11 South Bent, Center Column: Displacement Time History Bridge 5/649E; Peru 2475 EQ; Es=861.9 MPa 101

Appendix A-1 Scaling calculations for the center column, center bent of Bridge 5/227. 112

Appendix A-3 Spring values for all bridges in US units 141

LIST OF TABLES

Table 3.1.1-1 Bridge 5/227 Material Properties 20

Table 3.1.2-1 Bridge 5/649 Material Properties 25

Table 3.1.3-1 Bridge 512/19 Material Properties 31

Table 3.2.1-1 Jaradat Specimen and Existing Bridge Properties 31

Table 3.2.3-1 Calculation Factors for Estimating Soil Spring Stiffness 42

Table 3.2.3-2 Spring Values for Each Bridge 43

Table 4.1-1 Bridge Periods, Spectral Accelerations and Spectral Displacement Values . 54

Table 5.1.1-1 Bridge 5/649 Displacement and Shear Force Demands Due to the Olympia 975 Earthquake 59

Table 5.1.1-2 Bridge 5/649 Displacement and Shear Force Demands Due to the Peru 2475 Earthquake 60

Table 6.1-1 Maximum Earthquake Demands for Bridge 5/227 Subject to the Olympia 975 Loading 68

Table 6.1-2 Maximum Bearing Pad Displacements for Bridge 5/227 Subject to the Olympia 975 Earthquake 69

Table 6.1-3 Maximum Earthquake demands for Bridge 5/227 Subject to the Peru 2475 Loading 70

Table 6.1-4 Maximum Bearing Pad Displacements for Bridge 5/227 Subject to the Peru 2475 Earthquake 71

Table 6.1-5 Pounding in the Deck and Abutments for Bridge 5/227 with the 287.3 MPa Soil Values 71

Table 6.1-6 Pounding in the Deck and Abutments for Bridge 5/227 with the 861.9 MPa Soil Values 72

Table 6.1-7 Pounding in the Deck and Abutments for Bridge 5/227 with Fixed Column Base Boundary Conditions 72

Table 6.2-1 Maximum Earthquake demands for Bridge 512/19 Subject to the Olympia 975 Loading 83

Table 6.2-2 Maximum Earthquake Demands for Bridge 512/19 Subject to the Peru 2475 Loading 84

Table 6.3-1 Maximum Earthquake demands for Bridge 5/649 Subject to the Olympia 975 Loading 93

Table 6.3-2 Maximum Earthquake demands for Bridge 5/649 Subject to the Peru 2475 Loading 94

CHAPTER ONE

INTRODUCTION

1.1 BACKGROUND

Recent geological studies have shown that the Pacific Northwest region may be subjected to earthquakes of large-magnitude and long-duration as the result of rupturing of the locked interface between the Juan de Fuca and the North American Plate. Bridge design has evolved in the past forty years and existing bridges have been left potentially vulnerable due to limited funds for seismic upgrade. For example, transverse reinforcement was typically No. 3 or No. 4 hoops placed at 12 in (30.5 cm) on center in pre-1975 Washington State bridge columns. Today, the code requires a minimum of No. 3 reinforcement bars spaced at 4 in. (10.2 cm) on center. Also, lap splice length has greatly increased from values ranging between $25d_b$ and $45d_b$ for columns built before 1975, to a $60d_b$ minimum splice length since 2003.

1.2 OBJECTIVES

The main goals of this research were to assess multi-column bent, concrete bridges constructed prior to 1975, located in the Seattle/Olympia regions, under long-duration seismic loading. A suite of earthquakes were used to simulate a range of possible earthquake excitation. The main objectives included:

- 3-D modeling of three existing multi-column bent, concrete bridges in the Seattle/Olympia region

- Non-linear time history analysis of the bridges under short-duration and long-duration earthquake loading
- To assess the influence of soil-structure-interaction on the bridge response
- To draw conclusions on the effect of long duration earthquakes on pre-1975 Washington State bridges.

1.3 SEISMIC ACTIVITY IN THE PACIFIC NORTHWEST

Western Washington State lies above the intersection of two tectonic plates, the North America continental plate and the Juan de Fuca plate, colliding together at a rate of approximately 2 in. (about 5 cm) per year (from *The Pacific Northwest Seismograph Network*). In addition, the Pacific plate forces the Juan de Fuca plate north.

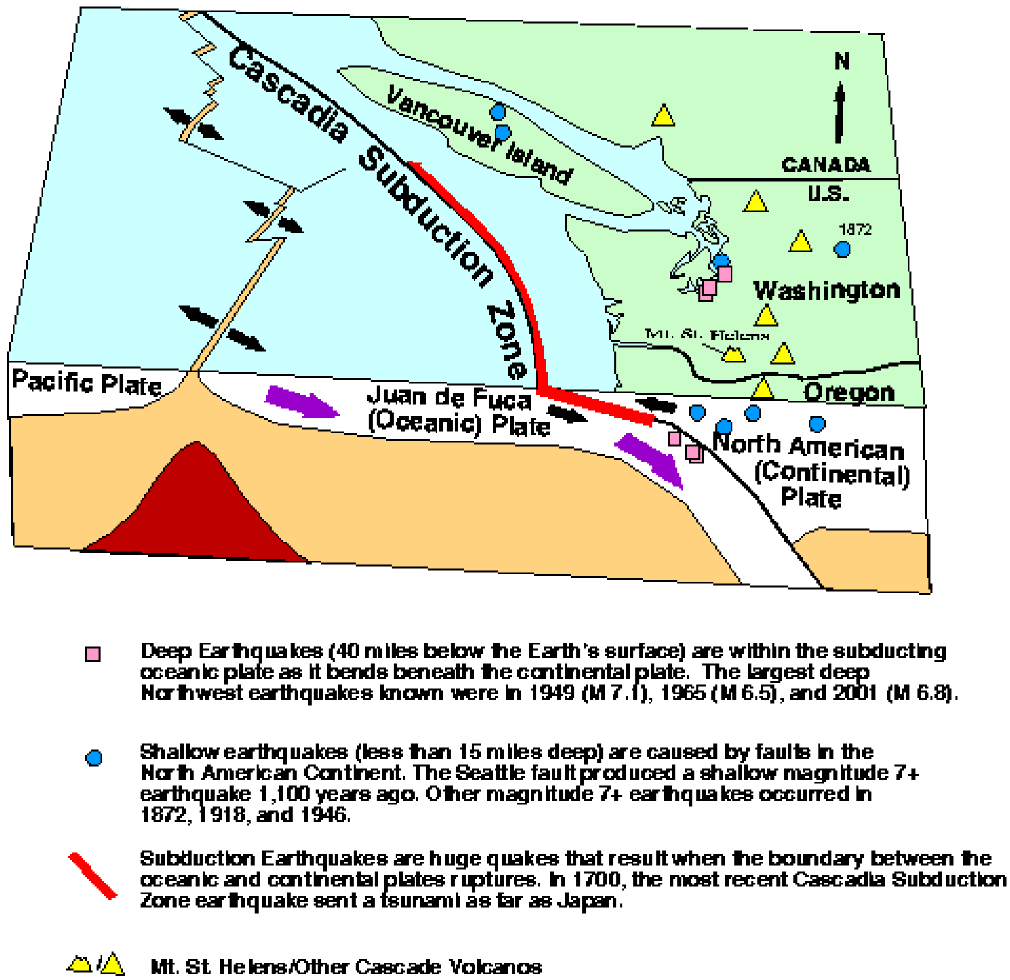

Figure 1.3-1 Cascadia Subduction Zone (from The Pacific Northwest Seismograph Network)

The most damaging earthquakes in Western Washington State in recent years have been the Nisqually Earthquake in 2001 (magnitude 6.8), Sea-Tac in 1965 (magnitude 6.5), and the 1949 Olympia earthquake (magnitude 7.1). They were respectively 52 km, 63 km and 53 km deep beneath the continent (PNSN, 2005*)*. The largest earthquake in Western Washington State since 1790, when historical recording started, occurred in 1872 in the North Cascades with a magnitude of 7.4. Subduction zone earthquakes tend to be the rarest and strongest. Geological evidence shows that this type of earthquake occurred in the region about 300 years ago. Subduction zones around the world have produced earthquakes of magnitude 8 and higher. Seismologists predict that an earthquake of this magnitude could occur again in the Pacific Northwest.

Since seismic recordings of large subduction zone earthquakes in the Pacific Northwest are not available, earthquakes from other regions of the world were used in this research and scaled to represent possible seismic activity in the Puget Sound region (Stapelton, 2004 and PanGEO Inc., 2005). These earthquakes were the Moquegua, Peru earthquake (2001), the Mexico City, Mexico earthquake (1985), the Kobe, Japan earthquake (1995), the Olympia, Washington earthquake (1949) and the Lloledo, Chile earthquake (1985).

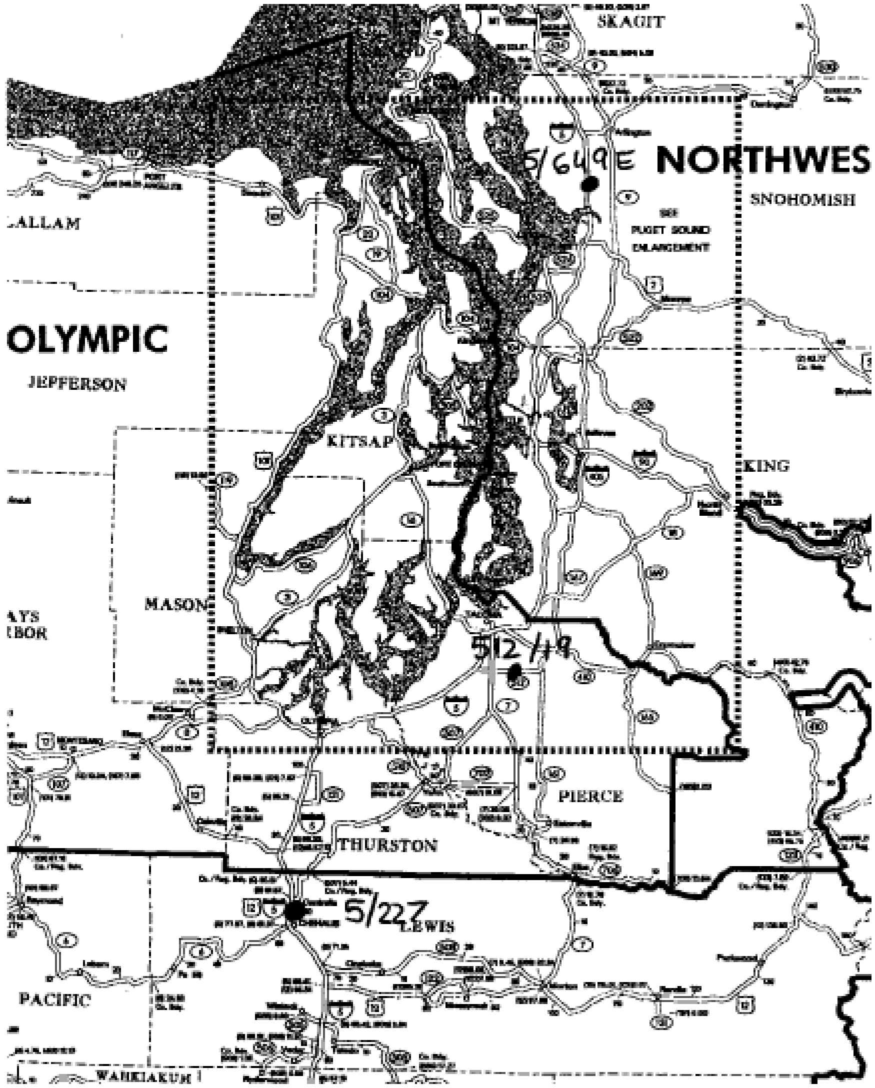

Figure 1.3-2 Map of the Bridge Locations

Bridges 5/227 and 512/19 are located 24 km (15 miles) south and 45 km (28 miles) east respectively of Olympia and bridge 5/649 is situated 56 km (35 miles) north of Seattle. Depending on the location of the bridges, the return periods for a given earthquake vary. The larger Peru and Chile records had a return period of 2475 years or greater and the smaller Peru and Chile records had a return period of 975 years or greater. We will refer to these earthquakes as Peru 2475, Chile 2475 for the large earthquakes and

Peru 975, Chile 975 for the smaller earthquakes throughout the following study. The return periods for the other earthquakes, Olympia, Kobe and Mexico City were determined by PanGeo Inc., a geotechnical subconsultant of WSDOT, and were found to be 975 years and 475 years. The origin of these records will be explained in greater depth in chapter four.

CHAPTER TWO

LITERATURE REVIEW

There are three parameters that are typically used to characterize earthquakes: the magnitude of shaking, the frequency content and the significant duration of motion. The first two have been researched more thoroughly than the last.

2.1 DEFINITION OF EARTHQUAKE DURATION

Several ways to define earthquake duration have been proposed over the last thirty years. Bolt (1973) defined "bracketed duration" as the time between the first and last accelerations of a magnitude higher than 0.05g or 0.1g. In this definition, earthquakes with a peak ground motion (PGA) smaller than 0.05g are considered as having no duration. Other definitions focus on the shape of the record rather than on numerical values. Overall, a single definition of earthquake duration has not been accepted. The most widely accepted is Abrahamson and Silva's (1996) "Arias Duration of Horizontal Strong Shaking Attenuation Relation":

$$Ln\left(D_{0.05\_I}\right) = Ln\left[\frac{\left(\dfrac{\Delta\sigma(M)}{10^{1.5M+16.05}}\right)^{-\frac{1}{3}}}{4.9\cdot 10^{6}\cdot\beta} + Sc_1 + c_2\cdot\left(r - r_c\right)\right] + \ln\left(\frac{D_{0.05\_I}}{D_{0.05\_0.75}}\right)$$

for ruptures away from fault (> 10 km or 6.2 miles)

$$Ln\left(D_{0.05\_I}\right) = Ln\left[\frac{\left(\dfrac{\Delta\sigma(M)}{10^{1.5M+16.05}}\right)^{-\frac{1}{3}}}{4.9\cdot 10^{6}\cdot\beta} + Sc_1\right] + \ln\left(\frac{D_{0.05\_I}}{D_{0.05\_0.75}}\right)$$

for near-fault rupture

Where :

$D_{0.05\_I}$ = Arias Duration (sec) from 0.05 to I Normalized Arias Itensity (typically, I=0.95)

$\Delta\sigma = \exp\left[b_1 + b_2\cdot(M - 6)\right]$

M = Moment Magnitude

$b_1 = 5.204$

$b_2 = 0.851$

$\beta = 3.2$

$S = 0$ for rock sites, or $S = 1$ for soil sites

$c_1 = 0.805$

$c_2 = 0.063$

r = closest distance to the effective fault rupture plane in km

$r_c = 10km$

$$\ln\left(\frac{D_{0.05\_I}}{D_{0.05\_0.75}}\right) = a_1 + a_2\cdot\ln\left(\frac{I - 0.05}{I - 1}\right) + a_3\cdot\left(\ln\left(\frac{I - 0.05}{I - 1}\right)\right)^2$$

$a_1 = -0.532$

$a_2 = 0.552$

$a_3 = -0.262$

SE = standard error = 0.493 for I=0.95

Duration also depends on soil conditions. R. Dobry, I. M. Idriss and E. NG (1978) studied the difference in the duration for the 1971 San Fernando horizontal strong ground motion records for a rock site and a soft-to-medium soil site. The following duration plots illustrate the differences between the two.

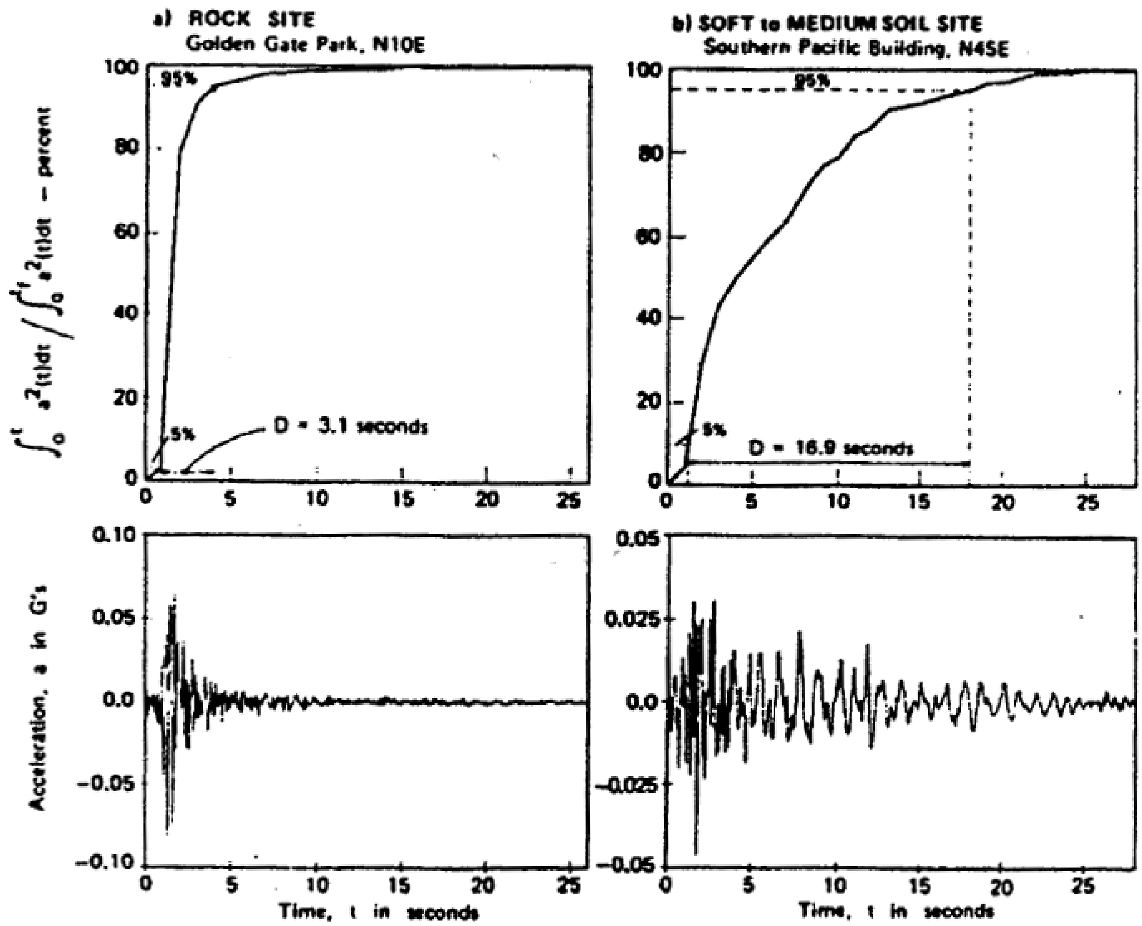

Figure 2.1-1 Difference Between Rock Site and Soil Site Acceleration Spectra

A correlation was found between the duration, D, and the magnitude, M, for rock motions, as illustrated below.

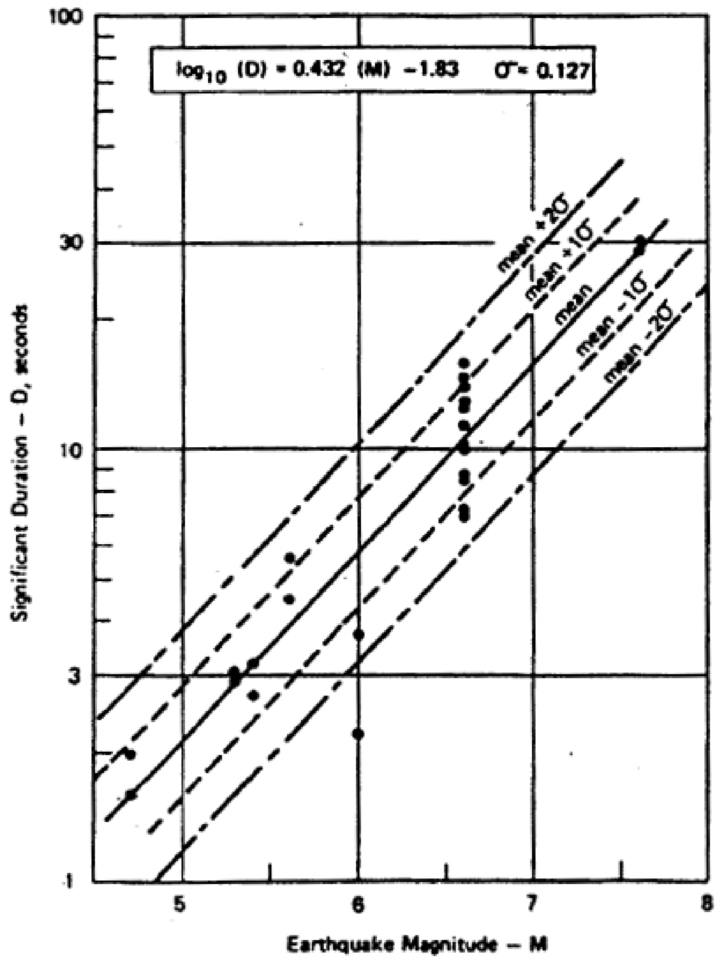

Figure 2.1-2 Duration versus Magnitude for Rock Sites in the Western United States.

The equation developed above is valid only for earthquake magnitudes of 4.5 to 7.6. For higher magnitudes, the duration of rupture at the source, d, increases much more rapidly than the significant duration of the earthquake, D, rendering the logarithmic correlation false. This study assumed a constant velocity of rupture, the dislocation at the source was considered to be an approximately continuous process (Bolt, 1970).

The following conclusion was obtained from the study: “Accelerograms at rock sites have more consistent and reasonably predictable durations, while durations of records on soil show much larger scatter, with the duration of rock being a lower bound.”

2.2 DAMAGE INDICES

Lindt *et al.* (2004) studied the effect of earthquake duration on the reliability of structures, especially for the integration of reliability indices in the LRFD code. Lindt investigated the relationship between earthquake duration and very-low-cycle damage estimates through a combination of nonlinear structural dynamics and the theory of order statistics. A suite of ten earthquakes used for this research and were based on the earthquake spectra of three US cities: Los Angeles, Seattle and Boston. The return periods used for the earthquakes were 475 years and 2475 years which correspond to a probability of occurrence of 10% and 2% in 50 years. This research concluded that earthquake duration has a significant effect on the damage of a structure, as the duration increases the reliability index decreases as shown on figure 2.3-1 below.

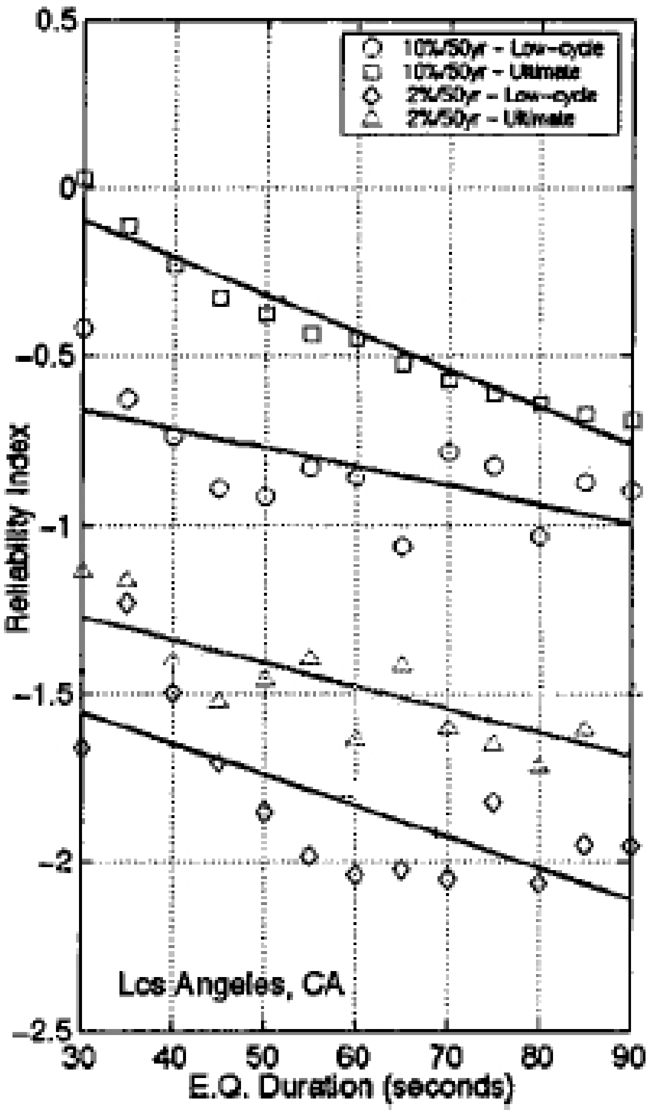

Figure 2.2-1 Reliability Index Versus Earthquake Duration from Lindt *et al.* (2004)

2.3 EFFECT OF EARTHQUAKE DURATION ON THE DAMAGE IN REINFORCED CONCRETE STRUCTURES

In 1988, Jeong *et al.* conducted a study on the damage observed in reinforced concrete and steel simple structures versus earthquake duration. The damage model used in this research was relatively crude but nevertheless qualitatively correct of the impact of damage on a structure as duration varies. The total damage for varying ductility levels was calculated with the following equations: $D = \sum_i D_i$ where $D_i = \frac{1}{C} n_i \cdot \mu_i^s$

and n_i: number of cycles

μ_i: ductility level of cycle i

C and s: positive empirical constants whose values were taken as 416 and 6 respectively for a reinforced concrete structure

Failure occurs when D reaches unity. This model was modified to take the maximum deformation and the absorbed hysteretic energy of the structure into account. Below is the final equation for the accumulative damage in a linear system for a specific earthquake duration.

$$E[D(t_d)] = \frac{-1}{C} \cdot \int_0^{t_d} \int_0^{\infty} \mu^s \frac{\partial \nu(\mu,t)}{\partial \mu} d\mu \cdot dt$$

where t_d is the duration of the excitation and $\nu(\mu,t)$ is the average frequency of up-crossings of the level μ.

Figure 2.4-1 below shows the plot of the previous equation for different values of ductility.

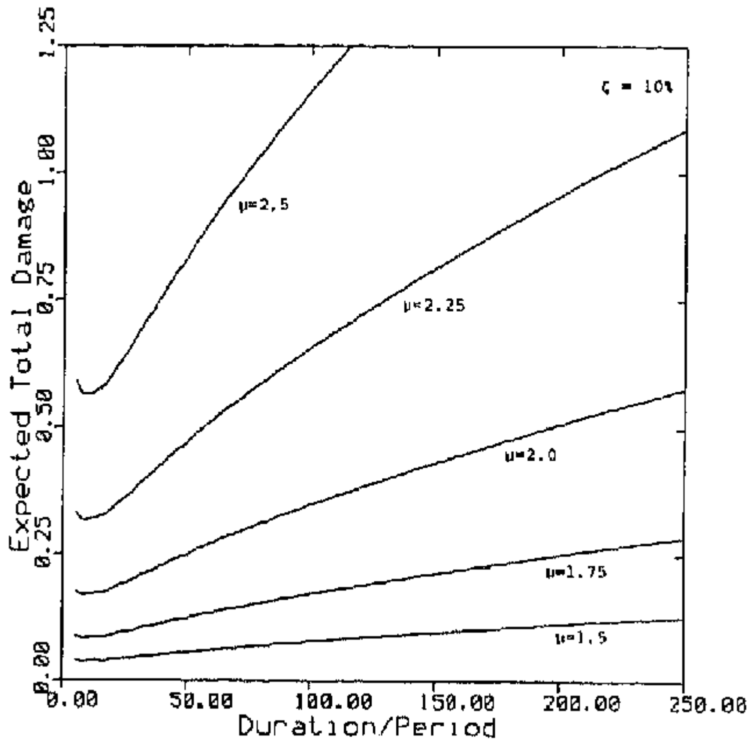

Figure 2.3-1 Expected Damage versus Normalized Duration for Representative Linear Reinforced Concrete Structure

It is clear from the above figure that total damage increases with duration. The slope of increase becomes steeper as the ductility level of the structure increases.

In 1975, Housner concluded that a large acceleration and spectral value but small duration earthquake will cause little structural damage (Housner, 1975). However, more recent studies have shown opposite trends. Jeong *et al.* (1988) showed that duration and ductility greatly affect structural damage and should therefore be taken into account when designing in seismic regions. Moreover, the study showed that for an increasing number of cycles for a given earthquake model, structural damage increases. Jeong *et al.*'s study was based on analytical excitations and not actual earthquake records.

CHAPTER THREE

BRIDGE MODELING

3.1 BRIDGE DESCRIPTIONS

3.1.1 Bridge 5/227

- Geographical Location

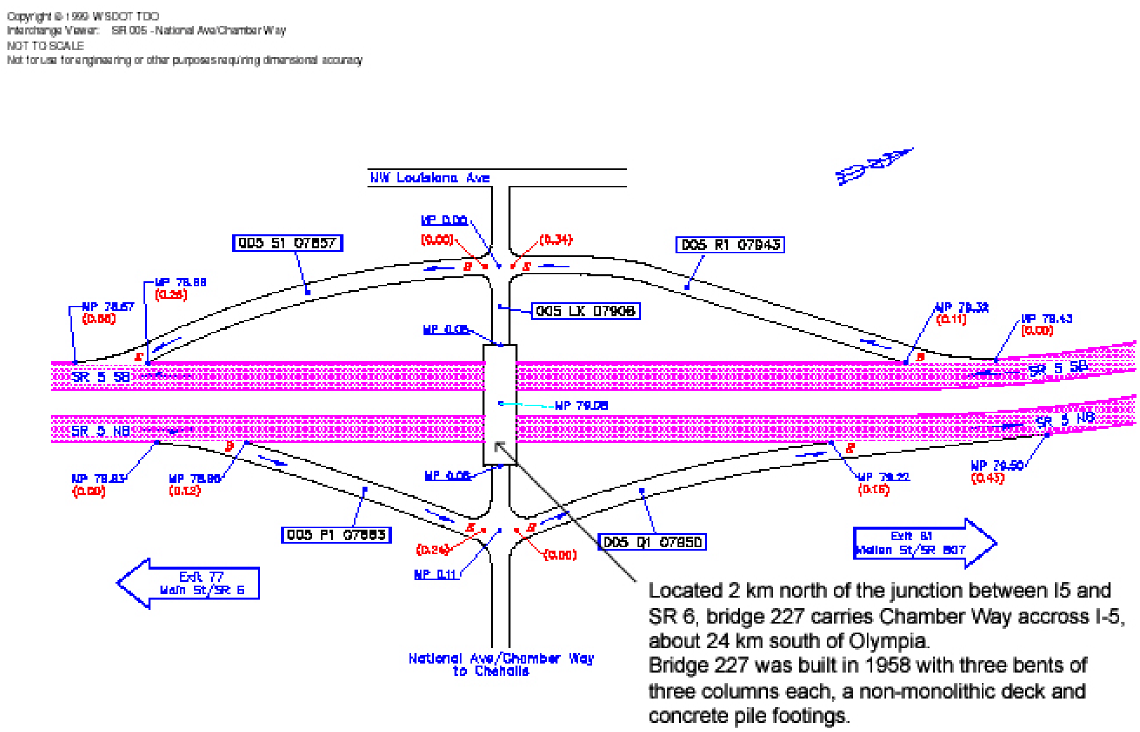

Figure 3.1.1-1 Bridge 5/227 Location

- Bridge Properties

The four span bridge has a total length of 53.24 m (184.50 ft). The outer spans are each 13.64 m (44.75 ft) long, the middle-west span is 15.7 m (51.50 ft) long and the middle-east span is 13.26 m (43.50 ft) long. The bridge elevation and plan views are shown in figures 3.1.1-2 and 3.1.1-3.

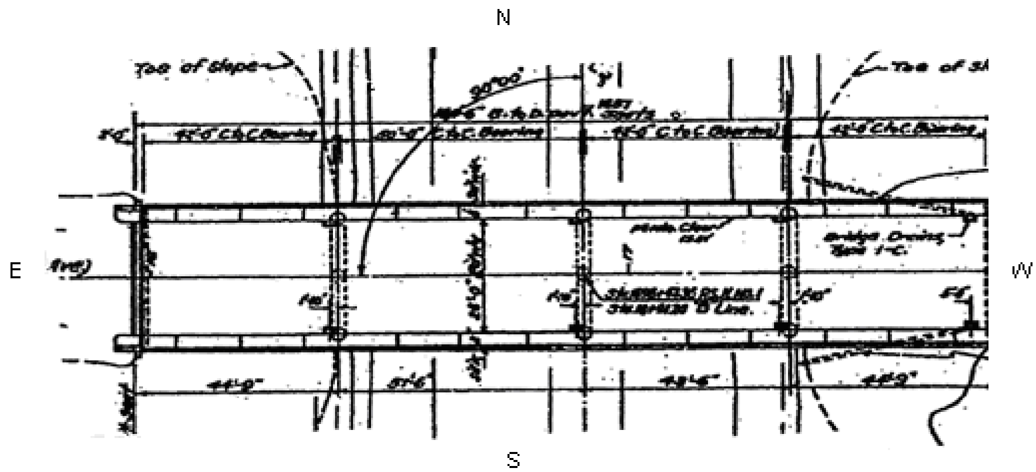

Figure 3.1.1-2 Bridge 5/227 Plan View

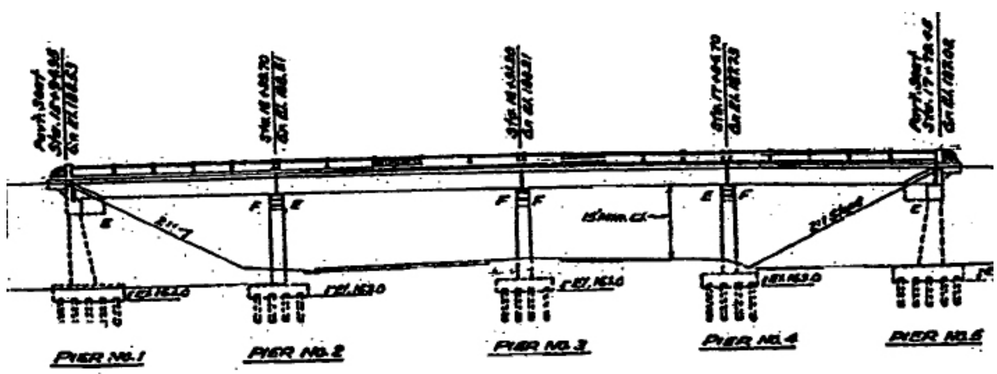

Figure 3.1.1-3 Bridge 5/227 Elevation View

The deck is supported by six 50 ft series standard WSDOT I-girders running longitudinally under each span. The girders are 1.8 m (5 ft, 11 in) on center and are pre- and post-tensioned (see figure 3.1.1-4). The girders support a 14 cm (5.5 in) thick reinforced concrete slab.

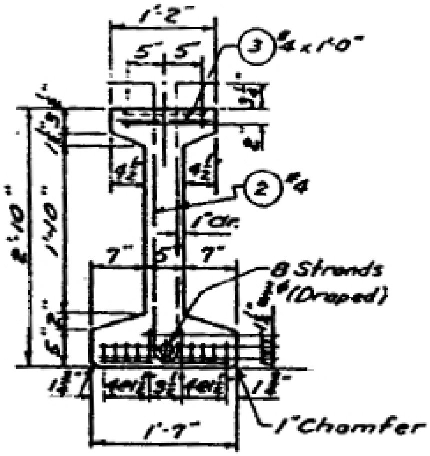

Figure 3.1.1-4 Bridge 5/227 50 ft. Series Girder

At each bent, a 91.44 cm (3 ft) by 1.22 m (4 ft) transverse crossbeam distributes the bridge loads to the three columns. The outer columns of each bent are of equal heights and the middle columns are slightly smaller. For the east bent, the outer columns are 5.68 m (18.64 ft) high and the middle columns are 5.53 m (18.14 ft) high. The middle bent outer and inner columns are 5.83 m (19.12 ft) and 5.68 m (18.62 ft) high respectively. The west bent is comprised of 5.92 m (19.42 ft) high outer columns, and a 5.77 m (18.92 ft) high inner column. The columns are 0.91 m (3 ft) in diameter with a cover of 9.2 cm ($3^{5/8}$ in), reinforced by No. 3 hoops spaced 30.48 cm (12 in) on center. Longitudinal reinforcement is comprised of eight equally spaced No. 10 bars. The lap splice length is $20d_b$ or 66 cm (2ft, 2in) along the base of each column.

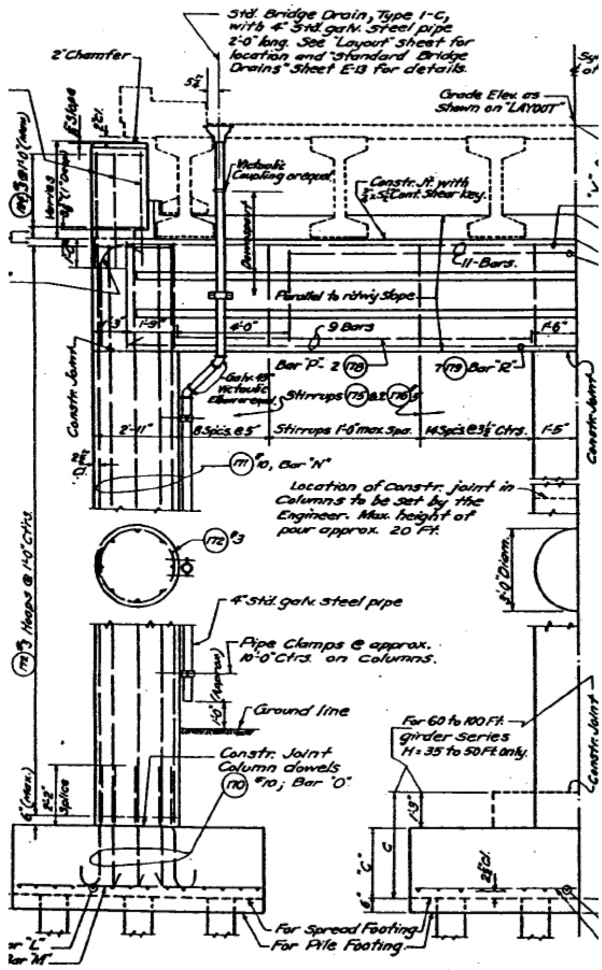

Figure 3.1.1-5 Bridge 5/227 Column Detail

The spread footings are supported by concrete piles. The exterior footings are 76.2 cm (2.5 ft) deep, 1.83 m (6 ft) wide (along the transverse direction of the bridge) and 3.66 m (12 ft) long. The interior footings are 91.44 cm (3 ft) deep, 2.74 m (9 ft) wide and 3.66 m (12 ft) long. The reinforcement for the exterior footings is a grillage of ten no. 9 bars spaced at 17.78 cm (7 in) on center along the length of the footing and twelve no. 6 bars spaced at 30.48 cm (12 in) on center along the width of the footing. For the interior footings, fourteen no. 9 bars spaced at 20.32 cm (8 in) on center longitudinally and twenty no. 6 bars spaced at 17.78 cm (7 in) on center in the transverse direction make up the reinforcement. The piles form two rows of three along the length of the exterior footings, and three rows of three longitudinally as well under the interior footings as shown in figure 3.1.1-6 below.

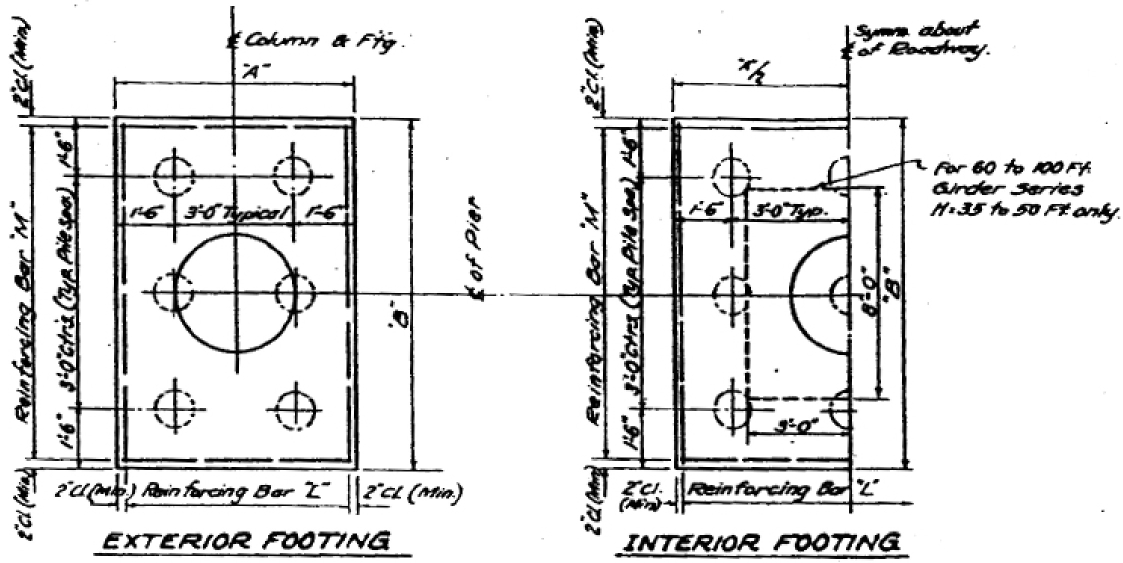

Figure 3.1.1-6 Bridge 5/227 Intermediate Bent Footings

Rubber expansion joints are situated at each bent and at the abutments. They are 5.08 cm (2 in) wide and run the width of the roadway.

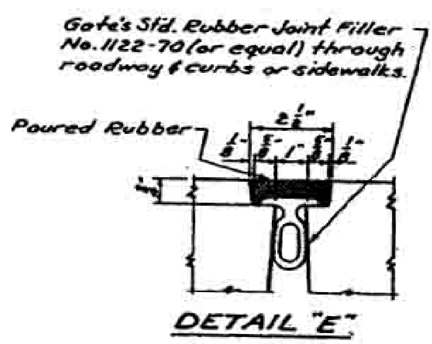

Figure 3.1.1-7 Bridge 5/227 Expansion Joint Detail

The end bents run across the width of the bridge, are 2m (6 ft, 6.5 in) deep and 30.48 cm (1 ft) long for the top half and 91.44 cm (3 ft) long for the bottom half.

Transverse and longitudinal reinforcements are placed throughout the cross-section as displayed in figure 3.1.1-8. Sub-ground columns support the abutments and run about 6.1 m (20 ft) deep below the abutment. The columns are tapered along the depth and are anchored down by a 3.7 m (12 ft) by 4.6 m (15 ft) by 84 cm (2.75 ft) reinforced concrete block. Four rows of five concrete piles support the footings as detailed in figure 3.1.1-8.

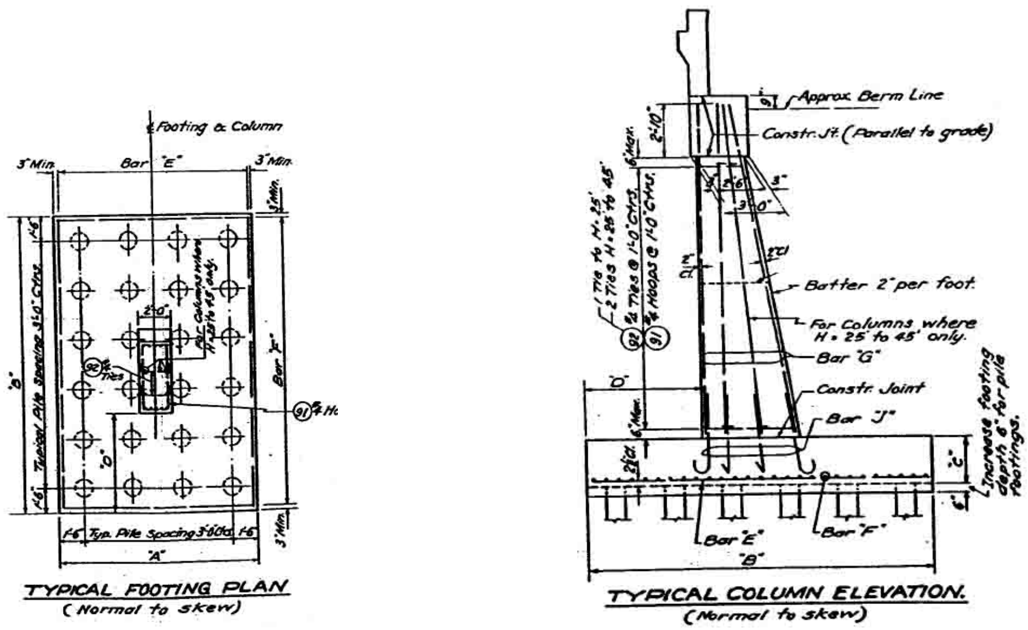

Figure 3.1.1-8 Bridge 5/227 Abutment Sub-Ground Column and Footing

- <u>Bridge Material Properties</u>

Table 3.1.1-1 Bridge 5/227 Material Properties

Material Properties	
Steel Yield Strength	44 ksi (303.5 MPa)
Steel Ultimate Strength	75 ksi (517.24 MPa)
Concrete Strength after 28 days	4 ksi (27.58 MPa)

3.1.2. Bridge 5/649

- Geographical Location

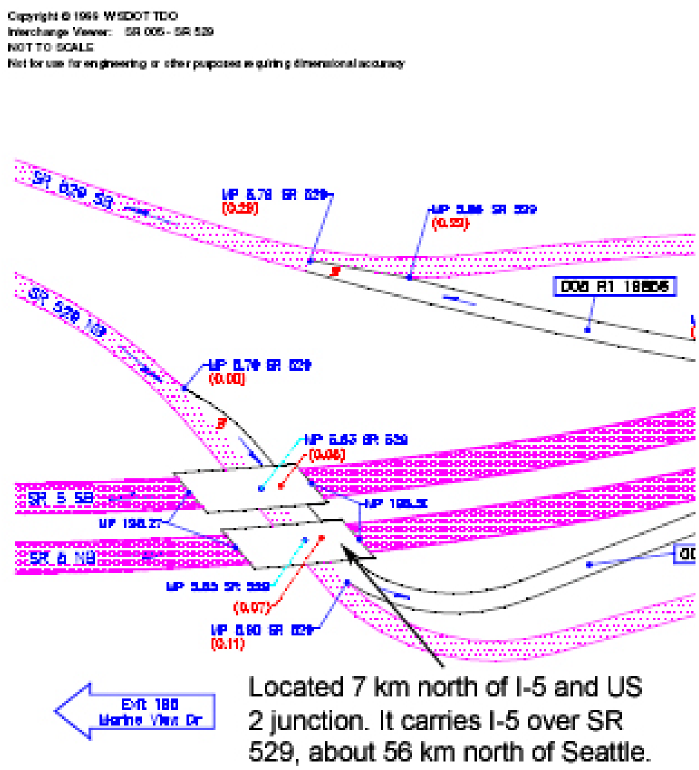

Figure 3.1.2-1 Bridge 5/649 Location

Bridge 5/649 is made up of two independent bridges. The east bridge is 4.88 m (16 ft) longer than the west bridge and therefore will be more prone to damage than the west bridge in the event of an earthquake, which is why the modeling was limited to the east bridge.

- Bridge Properties

Bridge 5/649 is made up of two bents with three columns each, supported by treated timber pile footings. The deck is 74.68 m (245 ft) long divided into three spans:

the north ramp which is 23.5 m (77 ft) long, the middle span 29.3 m (96 ft) long and the south ramp 21.95 m (72 ft) long. The bridge carries a 22.5 m (73.8 ft) wide roadway (dimension taken along the back of the pavement seat). The bridge has a 45 degree skew and no curvature.

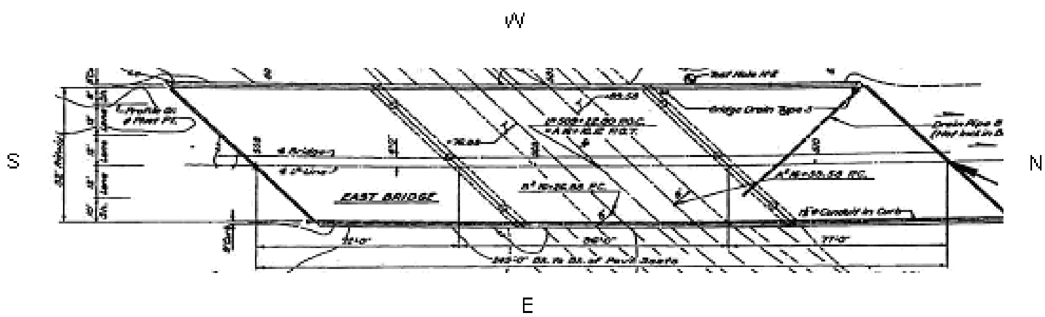

Figure 3.1.2-2 Bridge 5/649 Plan View

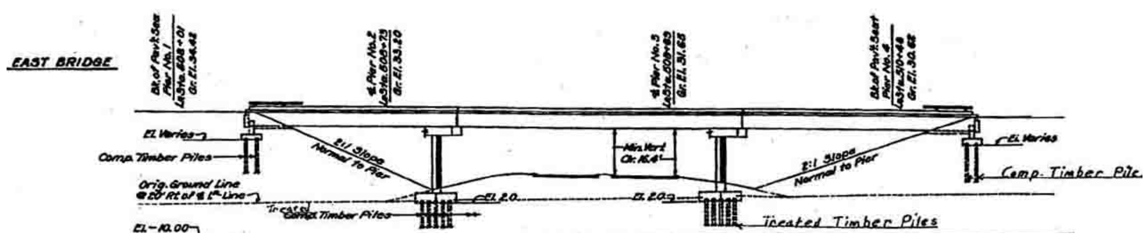

Figure 3.1.2-3 Bridge 5/649 Elevation View

The non-monolithic deck includes a 16.5 cm (6.50 in) thick reinforced concrete slab resting on a series of pre- and post-tensioned I-girders detailed in figure 3.1.2-4 below. The girder layout varies for each span. The south ramp is supported by six girders spaced at 4.3 m (14 ft, 7/8 in) on center, the middle span counts seven girders spaced at 3 m (9 ft, 11 in) on center and the north ramp has five girders spaced at 4.2 m (13 ft, 8 in) on center. The girders are reinforced by no. 4 bars longitudinally and no. 4 stirrups in the transverse direction.

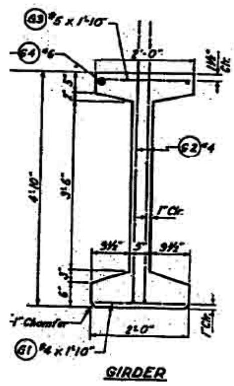

Figure 3.1.2-4 Bridge 5/649 Girder Detail

The girders rest on crossbeams that are 1.22 m (4 ft) by 1 m (3.25 ft) reinforced concrete rectangular beams than run 22.35 m (73.33 ft) across the width of the bridge.

The bridge has a downward slope creating a difference in the column heights. The north bent has three columns: the north-east column measuring 5.41 m (17.74 ft) high, the north-middle column at 5.23 m (17.15 ft) high and the north-west column at 5 m (16.35 ft) high. The south bent has a similar configuration with slightly taller columns: the south-east column is 5.9 m (19.23 ft) high, the south-middle is 5.7 m (18.7 ft) high and the south-west is 5.5 m (17.98 ft) high. Each column is reinforced longitudinally by eleven evenly spaced no. 9 bars and in the traverse direction by no. 3 hoops spaced at 30.48 cm (12 in) on center. The lap splice length is 1 m (3 ft, 4 in) which represents 35 d_b.

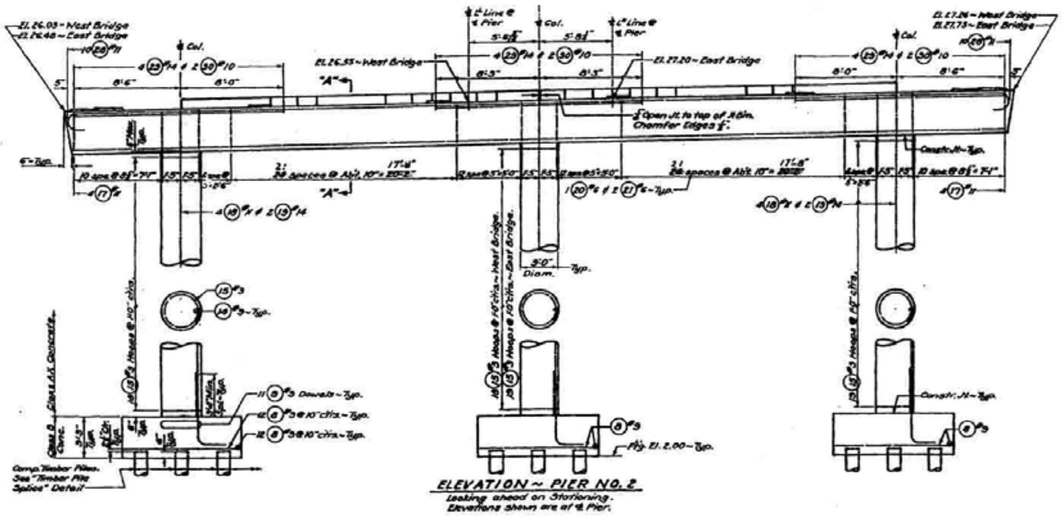

Figure 3.1.2-5 Bridge 5/649 Column Detail

Each column rests on concrete spread footings with treated timber piles. The footings are 2.9 m (9.5 ft) squares, 1 m (3.25 ft) deep. The timber piles are arranged in a grid of three rows of three.

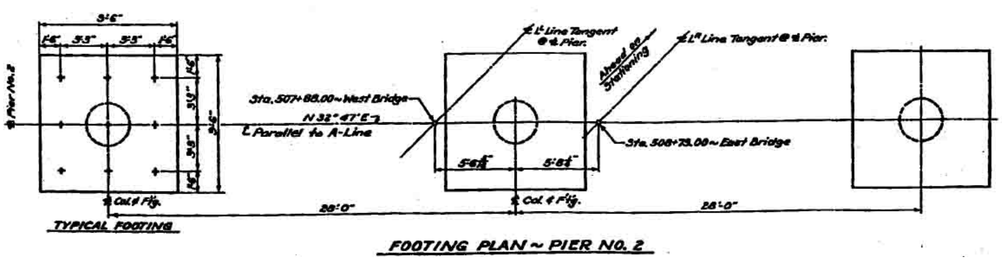

Figure 3.1.2-6 Bridge 5/649 Footing Detail

The expansion joints at each bent and at the abutments contribute to a release of energy in the longitudinal direction during seismic activity. The rubber joints are 3.17 cm (1.25 in) wide.

The abutments are inverted T-beams about 22.25 m (73 ft) long, 1.98 m (6.5 ft) wide and 1.98 m (6.5 ft) high. The stems are cut-out to support the girders and provide transverse girder stops in both directions for each girder. Two rows of ten concrete piles spaced in the transverse direction at 2.36 m (7.75 ft) on center, support each abutment.

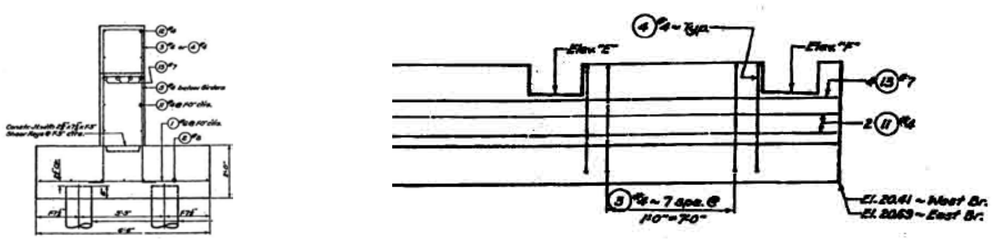

(a) (b)

Figure 3.1.2-7 Bridge 5/649 Abutment Footing detail: (a) Cross-section, (b) Elevation

- <u>Bridge Material Properties</u>

Table 3.1.2-1 Bridge 5/649 Material Properties

Material Properties	
Steel Yield Strength	44 ksi (303.5 MPa)
Steel Ultimate Strength	75 ksi (517.24 MPa)
Concrete Strength after 28 days	4 ksi (27.58 MPa)

3.1.3 Bridge 512/19

- Geographical Location

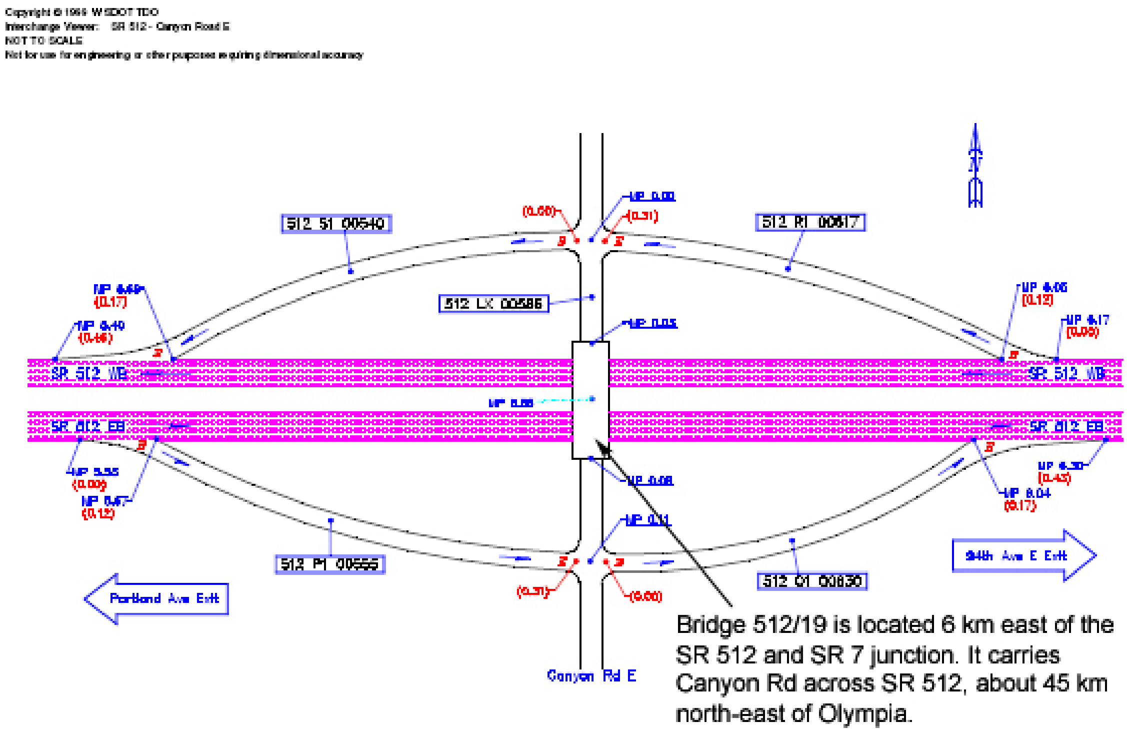

Figure 3.1.3-1 Bridge 512/19 Intersection

- Bridge Properties

This bridge is the largest of all three bridges. The roadway is 23.5 m (77 ft) wide and 75.6 m (248 ft) long. The roadway rests on three bents of four columns each anchored into the ground by concrete spread footings. The deck is monolithic and has a slight skew of about 3 degrees.

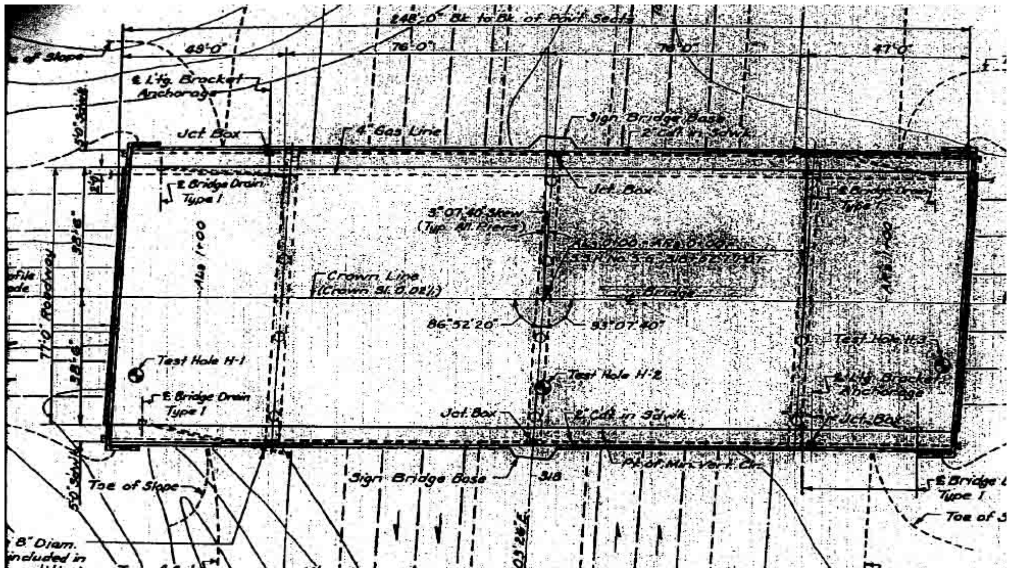

Figure 3.1.3-2 Bridge 512/19 Plan View

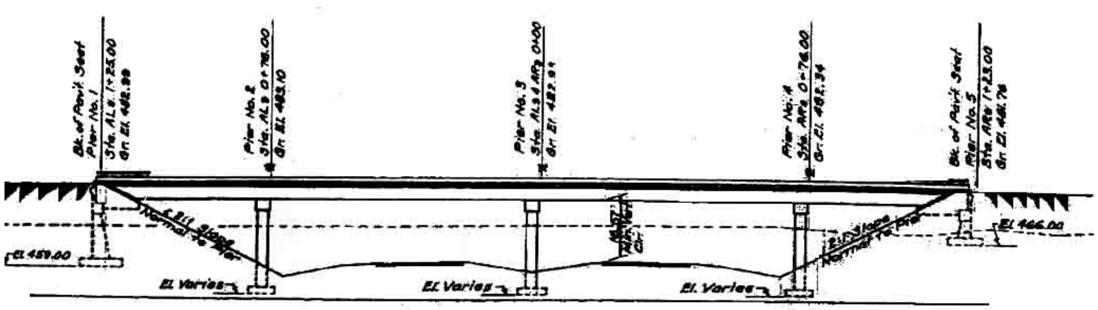

Figure 3.1.3-3 Bridge 512/19 Elevation View

The bridge is made up of four spans: the north ramp is 15 m (49 ft) long, the two middle spans are 23.16 m (76 ft) long and the south ramp is 14.33 m (47 ft) long. The slab is 16.51 cm (6.5 in) thick and is supported by twelve I-girders spaced evenly at 2.23 m (7 ft, 4 in) apart. The girders are 1.27 m (4 ft, 2 in) tall. The bottom flange is reinforced by no. 4 bars and the top flange by no. 5 bars. The stirrups are no. 4 bars.

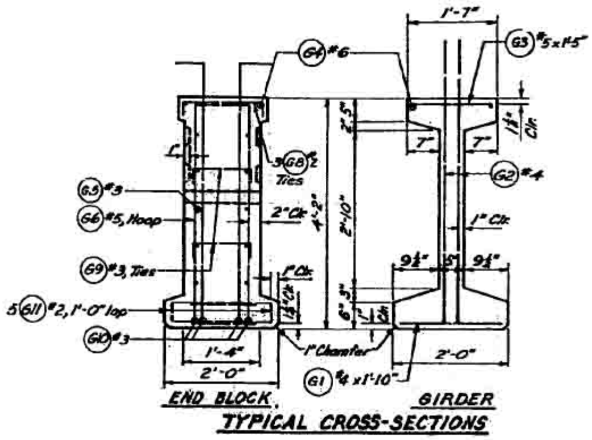

Figure 3.1.3-4 Bridge 512/19 Girder Detail

The girders rest on crossbeams at intermediate piers. These crossbeams are 1.1 m (3.5 ft) square reinforced concrete beams that run 23.47 m (77 ft) across the bridge. The crossbeams join the columns and form the bents supporting the bridge. The columns all have the same height of 6.13 m (20.1 ft). The columns are 91.44 cm (3 ft) in diameter and are reinforced longitudinally by eleven evenly spaced no. 9 bars and by no. 3 hoops spaced 30.48 cm (12 in) on center. Lap splice length is 35 d_b, which totals 1 m (3 ft, 4 in).

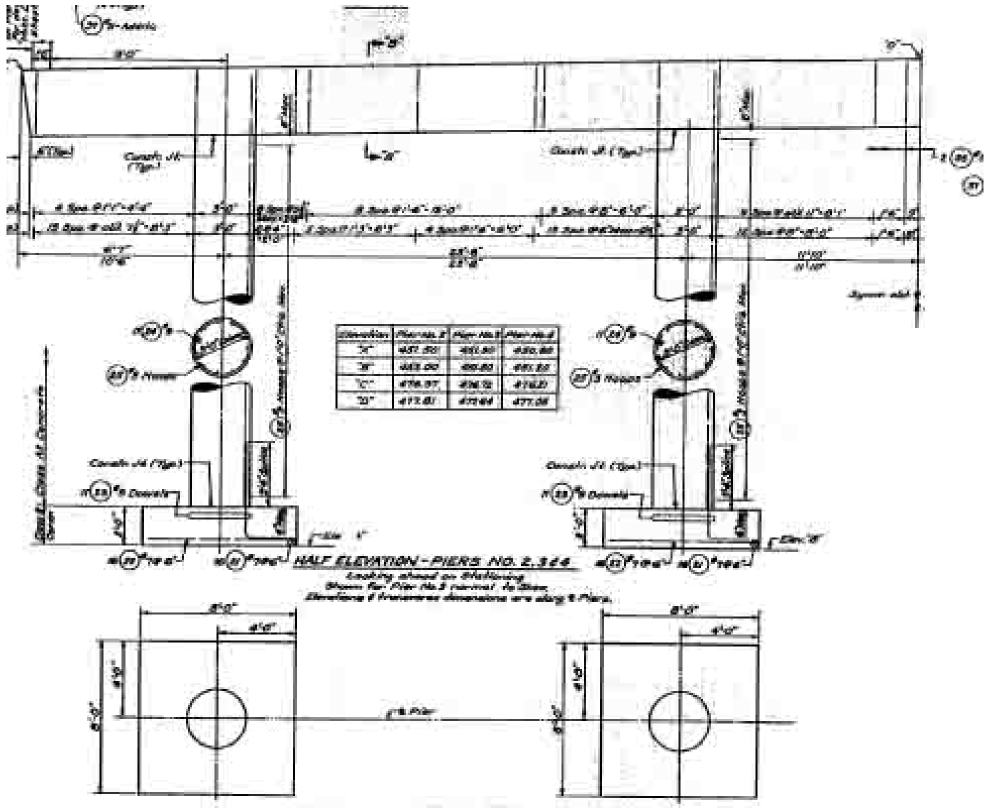

Figure 3.1.3-5 Bridge 512/19 Column Detail

The abutments are reinforced concrete piers supported by sub-ground columns of different heights. The north abutment is the deepest one at 7 m (23 ft) deep from the top of the deck, and the south abutment is 4.88 m (16 ft) deep from the top of the deck. They are L-shaped beams 2.5 m (8 ft, 2 in) high and 30.48 cm (1 ft) wide for the stem and 1.13 m (3 ft, 9 in) for the seat. The abutments are anchored into the ground by spread footings that are 2.13 m (7 ft) by 3.66 m (12 ft) by 61 cm (2 ft) concrete blocks for the north abutment and 1.83 m (6 ft) by 3.05 m (10 ft) by 61 cm (2 ft) deep reinforced concrete blocks for the south abutment.

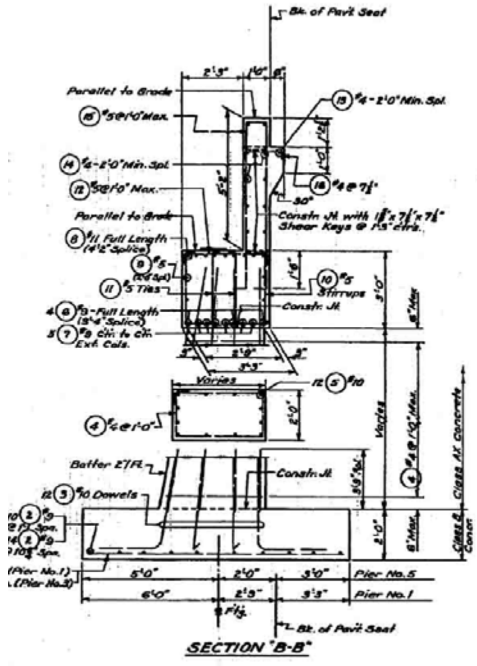

Figure 3.1.3-6 Bridge 512/19 Abutment Cross-section

The abutments were built to provide transverse support to the girders through girder stops. Four girder stops are positioned on both abutments, two in each direction. They are 45.72 cm (1.5 ft) by 50.8 cm (1 ft, 8 in) by 22.86 cm (9 in) high concrete blocks poured once the girders are in place. Figure 3.1.3-7 illustrates the locations of the girder stops along the abutments as well as a plan view.

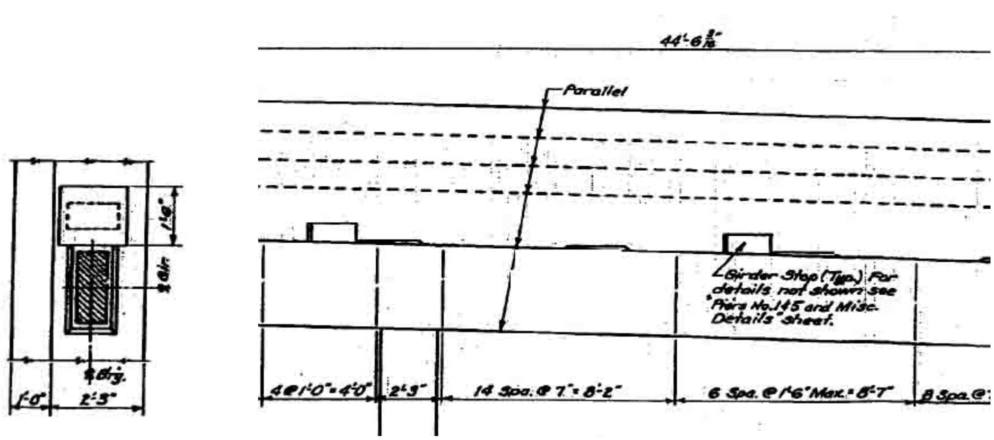

(a) **(b)**

Figure 3.1.3-7 Bridge 512/19 Girder Stop : (a) Plan View and (b) Locations

- Bridge Material Properties

Table 3.1.3-1 Bridge 512/19 Material Properties

Material Properties	
Steel Yield Strength	44 ksi (303.5 MPa)
Steel Ultimate Strength	75 ksi (517.24 MPa)
Concrete Strength after 28 days	4 ksi (27.58 MPa)

3.2 BRIDGE CALIBRATION

3.2.1 Jaradat Specimens

In order to model the bridge columns, it was necessary to compare the model to experimental data. A previous WSU graduate student, Jaradat (1996), tested several columns in the laboratory at 1/3 scale. The one that best fit the existing bridges was specimen T2. The concrete compressive strength of the bridges is specified in the plans as 4000 psi. An increase of 1.5 was recommended by WSDOT and Priestley (1991) to account for the natural gain in strength over the last 40 to 50 years.

Table 3.2.1-1 below is a presentation of the test specimen's properties compared to the bridge column properties.

Table 3.2.1-1 Jaradat Specimen and Existing Bridge Properties

	Jaradat Specimen T2	**Bridge5/649**	**Bridge 5/227**	**Bridge 512/19**
Material Properties				
Steel Yield Strength	371 MPa (53.8 ksi)	303 MPa (44 ksi)	303 MPa (44 ksi)	303 MPa (44 ksi)
Steel Ultimate Strength	578 MPa (83.9 ksi)	517 MPa (75 ksi)	517 MPa (75 ksi)	517 MPa (75 ksi)
Concrete Strength after 28 days	29 MPa (4.2 ksi)	41 MPa (6 ksi)	41 MPa (6 ksi)	41 MPa (6 ksi)
Geometric properties				
Column length	177.8 cm (70 in)	5.2 - 6.1 m (204-240 in)	5.4 - 5.9 m (211-233 in)	6.1 m (241 in)
Column diameter	25.4 cm (10 in)	91.4 cm (36 in)	91.4 cm (36 in)	91.4 cm (36 in)
Reinforcement Properties				
Longitudinal reinforcement ratio	0.011	0.0113	0.011	0.0113
Transverse reinforcement ratio	0.00194	0.00194	0.00194	0.00194
Longitudinal bars	8 #3	11 #9	8 #10	11 #9
Hoops	9 gauge (3.2 in o.c.)	#3 (12 in sp)	#3 (12 in sp)	#3 (12 in sp)
Lap splice	20 db	35 db	20 db	35 db

Specimen T2 was tested under cyclic loading with a peak lateral load of 35.6 kN (8.0 kips) and an axial load of 84.5 kN (19 kips) to represent the dead loads applied to the columns. Figure 3.2.1-1 shows the hysteresis curves obtained for specimen T2.

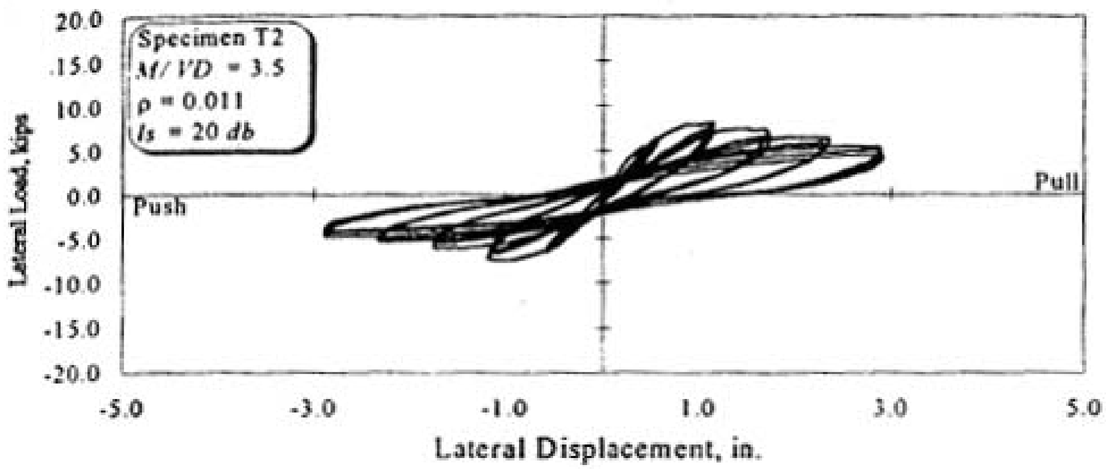

Figure 3.2.1-1 Specimen T2 Lateral Load-Displacement Hysteresis Curve

An envelope representing a force-displacement pushover curve for the specimen was extracted from this hysteresis. This envelope was used to calibrate each column of the existing bridges.

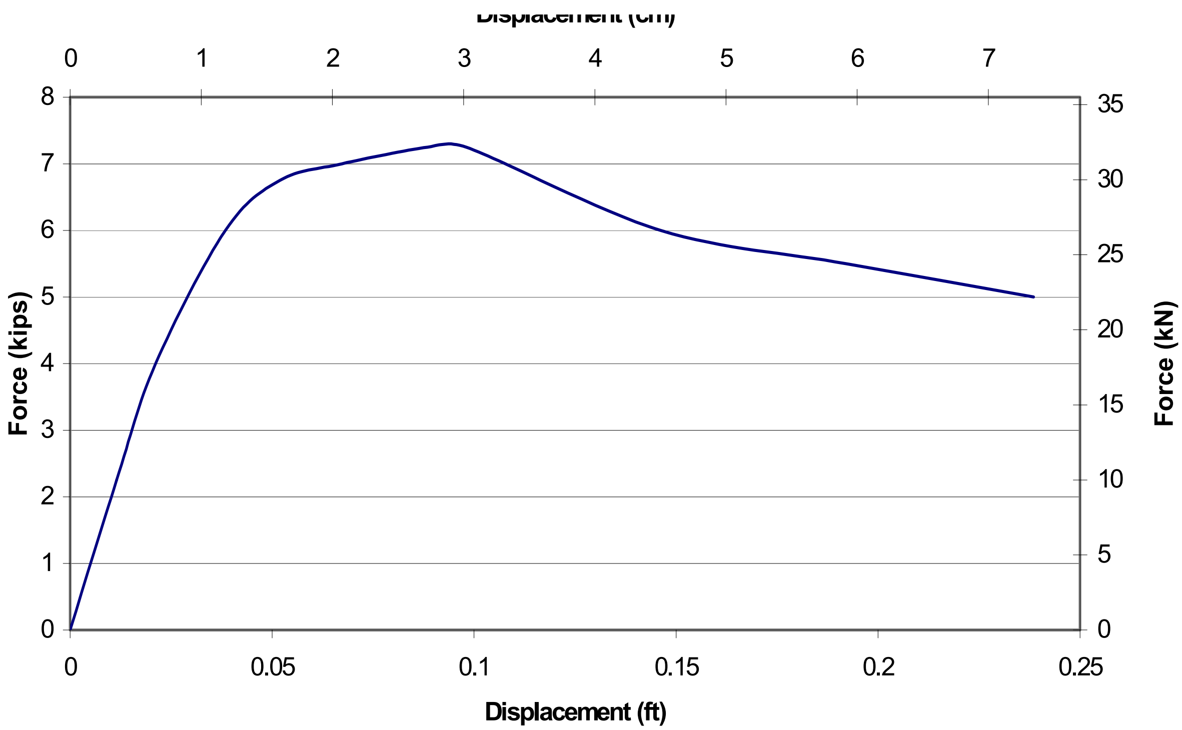

Figure 3.2.1-2 Specimen T2 Force-Displacement Envelope of Specimen T2

3.2.2 Scaling

Jaradat (1996) tested several columns under cyclic loading. These columns were scaled down to be conducted in a laboratory. Therefore, the results needed to be scaled up to fit the analytical assessment of the columns in the existing bridge. The material properties for the test and the bridge are different; therefore, each column of the bridge was modeled with the same material properties as the test column in order to compare the force-displacement prediction to the test results. Once the behavior of each column of the bridge approached the specimen's, the entire bridge model was run with the existing material properties of the bridge. In the following equations, subscript "ex" specifies the test specimen and "mod" the bridge model. Since the length and the diameter of the columns aren't scaled linearly, it is necessary to differentiate the two dimensions.

- Scaling the Forces and Moments:

The internal forces of the column can be defined as follows:

$$F_{ex} = \frac{M_{ex}}{L_{ex}} \text{ with } M_{ex} = A_{s.ex} f_y \left(D_{ex} - \frac{a}{2} \right) \qquad \text{(For the test data)}$$

$$F_{\text{mod}} = \frac{M_{\text{mod}}}{L_{\text{mod}}} \text{ with } M_{\text{mod}} = A_{s.\text{mod}} f_y \left(D_{\text{mod}} - \frac{a}{2} \right) \qquad \text{(For the model data)}$$

Therefore to scale the forces, the moments must be scaled. The first term is the steel reinforcement area, which can be scaled as follows:

$$A_{s.\text{mod}} = \left(\frac{D_{\text{mod}}}{D_{ex}} \right)^2 \cdot A_{s.ex}$$

The steel yield strength (f_y) is identical for each column in the scaling process. The second term is a function of the column diameter and the distance to the neutral axis. To be as exact as possible in the scaling process, two moment-curvature analyses were run. Since the steel reinforcement area and yield strength of both the specimen and the bridge column are known, a plot of $\left(D_{ex} - \frac{a}{2} \right)$ vs. $\left(D_{\text{mod}} - \frac{a}{2} \right)$ was drawn.

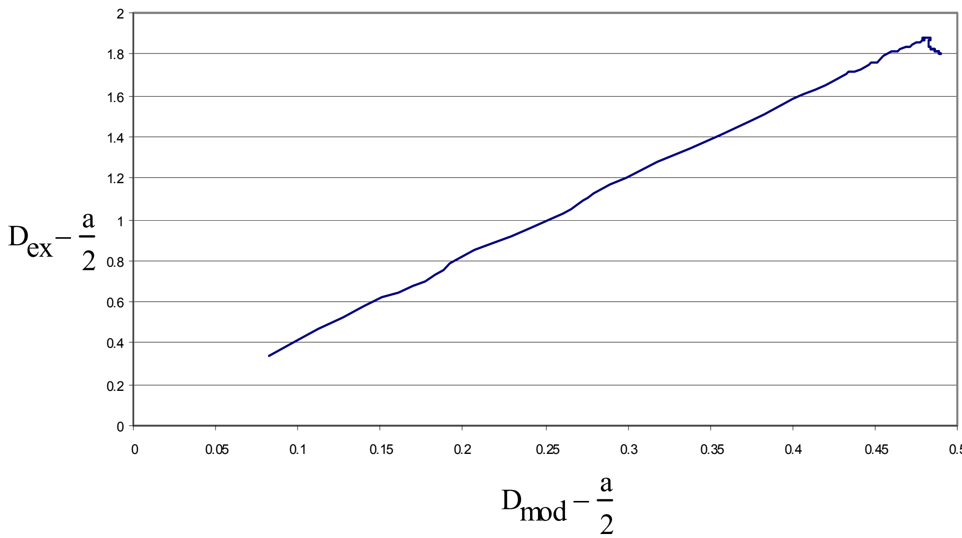

Figure 3.2.2-1 Relationship Between "D-a/2" Experimental and Model

The graph clearly shows that both quantities vary linearly with a slope of 0.259. The ratio of column diameters in this case is: $\frac{D_{ex}}{D_{mod}} = \frac{10}{36} = 0.278$

Therefore, the last term in the moment equation can be scaled as such:

$$D_{mod} - \frac{a}{2} = \frac{D_{mod}}{D_{ex}} \cdot \left(D_{ex} - \frac{a}{2} \right)$$

Using the two previous equations, the moment at the base of the model column can be expressed as a function of the moment at the base of the specimen.

$$M_{mod} = \left(\frac{D_{mod}}{D_{ex}} \right)^3 \cdot M_{ex}$$

The same factor can be used to scale the forces, taking the column lengths into account:

$$F_{mod} = \left(\frac{D_{mod}}{D_{ex}} \right)^3 \cdot \frac{L_{ex}}{L_{mod}} \cdot F_{ex}$$

Therefore the moment varies with the diameter cubed and the force varies with the diameter cubed times the ratio of lengths.

- <u>Scaling the Displacements</u>

For the displacements, the following equations were used:

$$\Delta_{y.ex} = \frac{\phi_{y.ex} \cdot L_{ex}^2}{6} \text{ with } \phi_{y.ex} = 2.25 \frac{\varepsilon_y}{D_{ex}}$$

$$\Delta_{y.\mathrm{mod}} = \frac{\phi_{y.\mathrm{mod}} \cdot L_{\mathrm{mod}}^2}{6} \text{ with } \phi_{y.\mathrm{mod}} = 2.25 \frac{\varepsilon_y}{D_{\mathrm{mod}}}$$

These equations can be combined to express the model displacements as a function of the specimen displacements. The curvature will vary with the inverse of the diameter and the displacement will vary with the length squared.

$$\Delta_{y.\mathrm{mod}} = \frac{D_{ex}}{D_{\mathrm{mod}}} \left(\frac{L_{\mathrm{mod}}^2}{L_{ex}^2} \right) \cdot \Delta_{y.ex}$$

However, for a displacement larger than the yield displacement, the equations differ. There is an additional term, Δ_p which can be calculated using the following equation:

$$\Delta_p = \left(\frac{M_u}{M_n} - 1 \right) \cdot \Delta_y + L_p \cdot (\phi_u - \phi_y) \cdot \left(L - \frac{L_p}{2} \right)$$

Where, M_u is the ultimate moment, M_n the moment at yield, Φ_u the ultimate curvature and L_p the plastic hinge length of the column :

In US units: $L_p = 0.08 \cdot \frac{L}{2} + 0.15 \cdot f_y \cdot d_b$

In metric units: $L_p = 0.08 \cdot \frac{L}{2} + 0.22 \cdot f_y \cdot d_b$

The deck is assumed to be infinitely rigid which makes the column react as if it were fixed at the base and constrained with a roller at the free end, making it behave in double bending. This is why half the length of the column is used to compute L_p.

Δ_y has already been factored. For the second term of the equation, the factored term is the following:

$$\boxed{\frac{L_{p.\mathrm{mod}} \cdot (\phi_u - \phi_y)_{\mathrm{mod}} \cdot \left(L_{\mathrm{mod}} - \frac{L_{p.ex}}{2}\right)}{L_{p.ex} \cdot (\phi_u - \phi_y)_{ex} \cdot \left(L_{ex} - \frac{L_{p.\mathrm{mod}}}{2}\right)}}$$

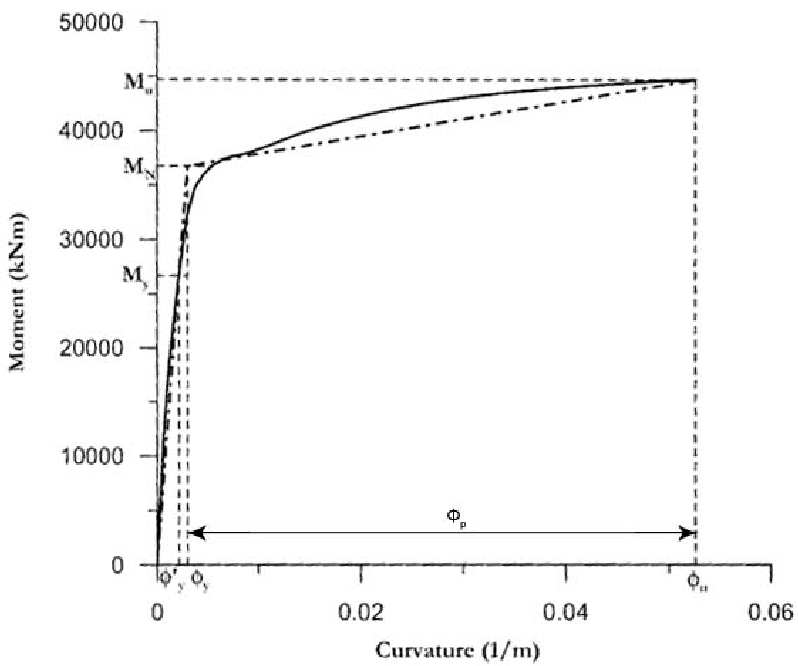

Figure 3.2.2-2 Bilinear Relationship Between Moment and Curvature

To correctly determine how to scale Φ_u - Φ_y, a moment-curvature analysis was run, identical to the one used to determine the scaling factors for the moment values.

Moment-curvature scaling

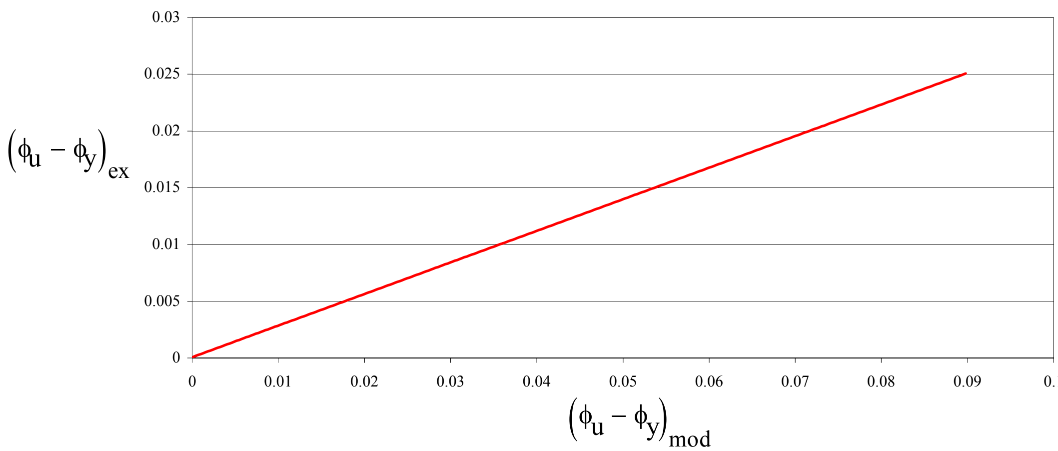

Figure 3.2.2-3 Linear Relationship Between Φ_u - Φ_y Factor

The plot illustrates the linear relationship between both plastic curvatures. The slope in this case is of 3.593, which is comparable to a scaling factor of: $\frac{D_{\mathrm{mod}}}{D_{ex}} = \frac{36}{10} = 3.6$

Therefore, to correctly scale up the displacements these are the equations used:

For $\Delta \leq \Delta_y$ use $\Delta_{\mathrm{mod}} = \frac{D_{ex}}{D_{\mathrm{mod}}} \cdot \left(\frac{L_{\mathrm{mod}}^2}{L_{ex}^2}\right) \cdot \Delta_{ex}$

For $\Delta \geq \Delta_y$ use $\Delta_{\mathrm{mod}} = \frac{D_{ex}}{D_{\mathrm{mod}}} \cdot \left(\frac{L_{\mathrm{mod}}^2}{L_{ex}^2}\right) \cdot \Delta_{ex} + \frac{L_{p.\mathrm{mod}} \cdot D_{ex} \cdot \left(L_{\mathrm{mod}} - \frac{L_{p.ex}}{2}\right)}{L_{p.ex} \cdot D_{\mathrm{mod}} \cdot \left(L_{ex} - \frac{L_{p.\mathrm{mod}}}{2}\right)} \cdot \left(\Delta_{ex} - \Delta_{y.ex}\right)$

The last component to factor is the axial load. The axial load varies with the cross-section of the column, therefore with the diameter squared:

$$P_{\mathrm{mod}} = \left(\frac{D_{\mathrm{mod}}}{D_{ex}}\right)^2 \cdot P_{ex}$$

See Appendix A-1 for an example of the scaling up of the center column of the center bent of Bridge 5/227 fitted column to Jaradat T2 specimen scaled up.

3.2.3 Modeling

In order to determine the properties of the columns, a moment/curvature analysis was run to determine the values at actual yield, idealized yield and at failure.

With the values obtained the effective moment of inertia of the column can be determined: $I_{eff} = \frac{M_n}{E_c \Phi_y}$ where Mn is the moment at idealized yield and ϕ_y is the curvature at idealized yield.

However, this inertia value doesn't represent the inertia of the actual bridge columns. Longitudinal reinforcement of the column penetrates into the footing and in the deck as detailed in figure 3.2.3-3 below.

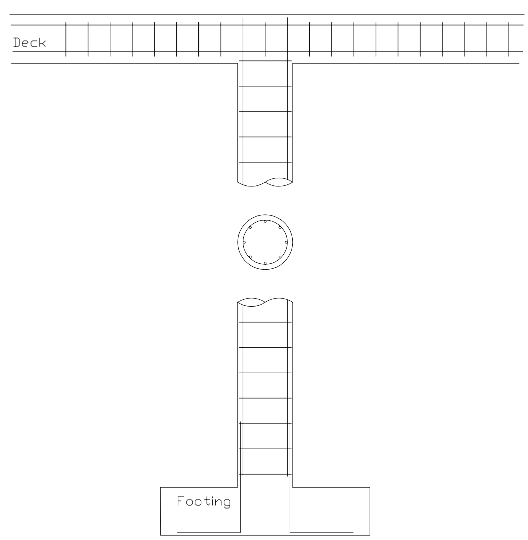

Figure 3.2.3-1 Column Reinforcement Pattern

The effect of the reinforcement penetration can be added to the clear height of the column: $L' = L + 2 \cdot L_{sp}$

Where L is the clear height, the strain penetration term is defined by $L_{sp} = 0.15 \cdot f_y \cdot d_b$, f_y is the reinforcing steel yield strength and d_b, the diameter of the longitudinal bars.

Running a pushover analysis with these two different lengths shows how the strain penetration affects the yield force and the inertia of the column:

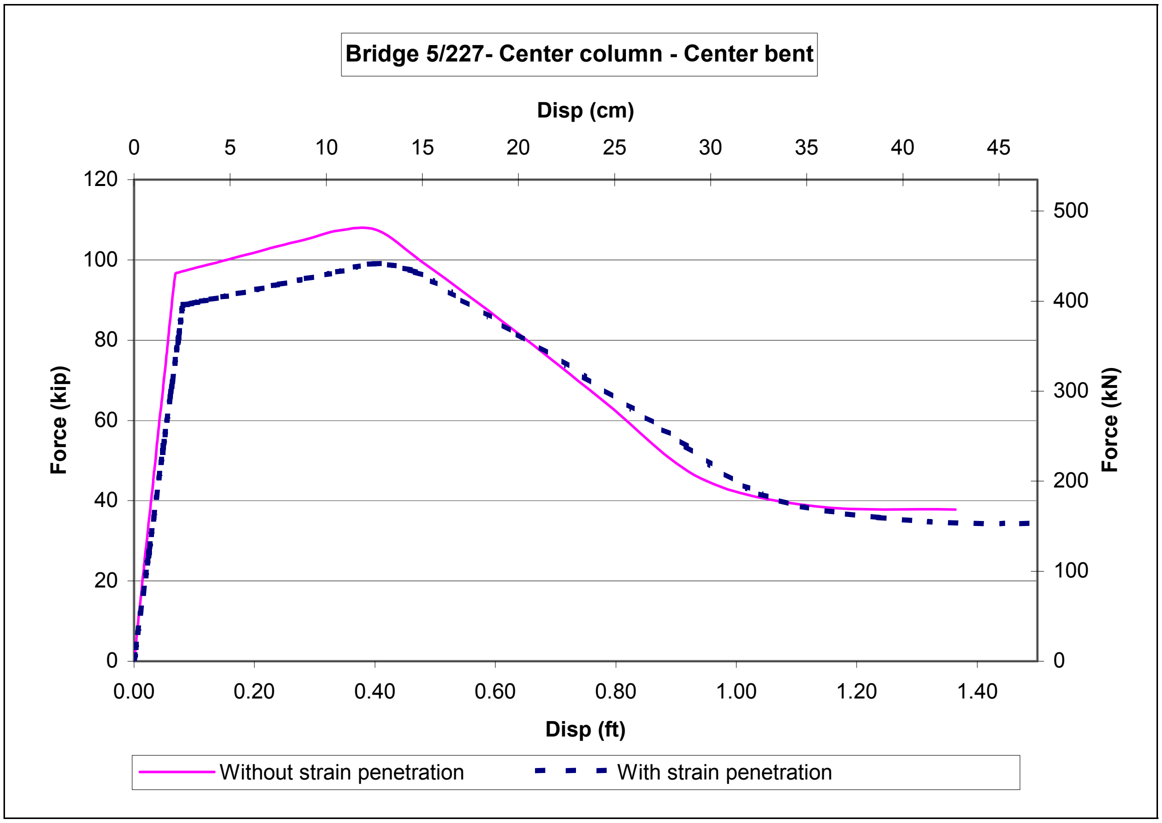

Figure 3.2.3-2 Comparison Between Force-Displacement Curves with Strain Penetration and Without

The stiffness of the column, k, can be found using the following equation:

$$k = 12 \cdot E_c \cdot \frac{I}{L^3}.$$

To match the test data, the model column and the scaled test column must have approximately the same stiffness. Therefore, the final moment of inertia of the column can be calculated as follows: $I = k_{test} \cdot \dfrac{L'^3}{12 \cdot E_c}$

See Appendix A-2 for a plot of a fitted column to Jaradat T2 specimen scaled up and the input files for each bridge.

- <u>Calculating the Spring Values</u>

The existing soil properties of each bridge are unknown. However, a previous WSU graduate student, Cody Cox (2005), has done an extensive study of the possible soil conditions in the Olympia region. The spring stiffness values for bridges 227, 512 and 649 were determined after comparison with Cody's bridges.

The soil properties for Bridge 5/227 have already been calculated by Cody using several different programs.

Bridge 5/649 presented similarities with bridge 826. They both had timber pile footings and the abutments were approximately the same height, however, the overall width of the bridges differed. Soil properties depend mainly on soil pressure surrounding the footing. Soil pressure varies in a non-linear manner with the depth of the footing but is assumed to be constant throughout the width of the footing. Therefore the assumption that the soil stiffness values at the abutments varied linearly with the width of the abutment was made.

Bridge 512/19 presented similarities with bridge 518. Both bridges were built on spread footings, however the abutment height and overall width of the bridges varied. As for Bridge 5/649, the spring values at the abutments were scaled linearly with the width of the bridge. Regarding the abutment height, it is known that the deeper the footing, the stiffer the spring model should be. However, this relationship is not linear, nor does it follow any type of mathematical equation. Looking through Cody's work on abutment stiffness, the relationship was dependant on several factors: the dimensions of the spread footings, the material properties of the bridge as well as two factors alpha and beta different for each spring direction. These two factors varied with the ratio length by width of the footings.

Table 3.2.3-1 Calculation Factors for Estimating Soil Spring Stiffness

	Translation X Direction		Translation Y Direction		Translation Z Direction		Rocking about X Dir.		Rocking about Y Dir.		Rotation about Z Dir.	
L/B	alpha	beta	alpha	beta	alpha	beta	alpha	beta	alpha	beta	alpha	beta
0.194	1.025	1.420	1.025	1.420	1.035	1.125	1.050	1.700	1.050	1.150	1.050	1.150
1.263	1.030	1.480	1.030	1.480	1.035	1.100	1.050	1.700	1.050	1.750	1.050	1.750
1.412	1.040	1.500	1.025	1.500	1.040	1.100	1.060	1.700	1.060	1.750	1.060	2.100
1.600	1.050	1.520	1.060	1.520	1.060	1.110	1.060	1.740	1.060	1.760	1.060	2.200
1.667	1.055	1.480	1.060	1.480	1.060	1.100	1.060	1.700	1.060	1.750	1.060	1.900
0.600	1.025	1.450	1.025	1.450	1.035	1.100	1.050	1.700	1.050	1.380	1.050	1.380

With these values were calculated the spring stiffness at each abutment in all six directions. Since the spring values were calculated with approximate soil properties, a range of soil elastic modulus were used to model each bridge. These values are presented below in metric units (for US units see Appendix A-3) .

Table 3.2.3-2 Spring Values for Each Bridge

Bridge 512/19	Es (MN/m2)	Translational Springs			Rotational Springs		
		K11 (Trans) MN/m	K22 (Long.) MN/m	K33 (Vert.) MN/m	K44 (Trans.) MN/m/rad	K55 (Long.) MN/m/rad	K66 (Vert.) MN/m/rad
North Abut	47.88	2.0427E+03	2.0427E+03	2.1346E+03	5.9570E+04	1.6292E+05	1.2418E+05
	287.28	1.2256E+04	1.2256E+04	1.2807E+04	3.5742E+05	9.7754E+05	7.4510E+05
	861.84	3.6768E+04	3.6768E+04	3.8422E+04	1.0723E+06	2.9326E+06	2.2353E+06
North Pier	47.88	2.3082E+02	2.3082E+02	2.3851E+02	1.0903E+04	6.6909E+03	1.1950E+04
	287.28	1.3849E+03	1.3849E+03	1.4311E+03	6.5417E+04	4.0145E+04	7.1701E+04
	861.84	4.1547E+03	4.1547E+03	4.2932E+03	1.9625E+05	1.2044E+05	2.1510E+05
Center Pier	47.88	2.3845E+02	2.3845E+02	2.5094E+02	1.1739E+04	8.5124E+03	1.1385E+04
	287.28	1.4307E+03	1.4307E+03	1.5056E+03	7.0437E+04	5.1074E+04	6.8312E+04
	861.84	4.2920E+03	4.2920E+03	4.5169E+03	2.1131E+05	1.5322E+05	2.0494E+05
South Pier	47.88	2.2182E+02	2.2182E+02	2.3043E+02	1.0159E+04	5.0775E+03	1.0759E+04
	287.28	1.3309E+03	1.3309E+03	1.3826E+03	6.0957E+04	3.0465E+04	6.4554E+04
	861.84	3.9927E+03	3.9927E+03	4.1477E+03	1.8287E+05	9.1395E+04	1.9366E+05
South Abut	47.88	8.2237E+02	8.2237E+02	8.5937E+02	2.3983E+04	6.5593E+04	4.9996E+04
	287.28	4.9342E+03	4.9342E+03	5.1562E+03	1.4390E+05	3.9356E+05	2.9998E+05
	861.84	1.4803E+04	1.4803E+04	1.5469E+04	4.3169E+05	1.1807E+06	8.9993E+05

Bridge 5/227	Es (MN/m2)	Translational Springs			Rotational Springs		
West Abut	0.24	1.1485E+03	1.2372E+03	4.6675E+03	2.0087E+05	2.0096E+05	4.5472E+02
	47.88	2.0784E+03	2.1598E+03	5.6232E+03	2.5356E+05	2.7206E+05	9.0945E+04
	287.28	6.7512E+03	6.7961E+03	1.0426E+04	5.1836E+05	6.2934E+05	5.4567E+05
	861.84	1.7966E+04	1.7923E+04	2.1952E+04	1.1539E+06	1.4868E+06	1.6370E+06
West Pier	0.24	2.8936E+02	2.8936E+02	1.3613E+03	7.7936E+03	7.7740E+03	6.4175E+01
	47.88	5.3621E+02	5.3621E+02	1.6247E+03	1.9522E+04	1.5598E+04	1.2835E+04
	287.28	1.7766E+03	1.7766E+03	2.9486E+03	7.8461E+04	5.4912E+04	7.7010E+04
	861.84	4.7536E+03	4.7536E+03	6.1259E+03	2.1991E+05	1.4927E+05	2.3103E+05
Center Pier	0.24	2.8936E+02	2.8936E+02	1.3613E+03	7.7936E+03	7.7740E+03	6.4175E+01
	47.88	5.3621E+02	5.3621E+02	1.6247E+03	1.9522E+04	1.5598E+04	1.2835E+04
	287.28	1.7766E+03	1.7766E+03	2.9486E+03	7.8461E+04	5.4912E+04	7.7010E+04
	861.84	4.7536E+03	4.7536E+03	6.1259E+03	2.1991E+05	1.4927E+05	2.3103E+05
East Pier	0.24	2.8936E+02	2.8936E+02	1.3613E+03	7.7936E+03	7.7740E+03	6.4175E+01
	47.88	5.3621E+02	5.3621E+02	1.6247E+03	1.9522E+04	1.5598E+04	1.2835E+04
	287.28	1.7766E+03	1.7766E+03	2.9486E+03	7.8461E+04	5.4912E+04	7.7010E+04
	861.84	4.7536E+03	4.7536E+03	6.1259E+03	2.1991E+05	1.4927E+05	2.3103E+05
East Abut	0.24	1.1485E+03	1.2373E+03	4.6677E+03	2.0087E+05	2.0096E+05	4.5472E+02
	47.88	2.0784E+03	2.1598E+03	5.6232E+03	2.5356E+05	2.7206E+05	9.0945E+04
	287.28	6.7512E+03	6.7961E+03	1.0426E+04	5.1836E+05	6.2934E+05	5.4567E+05
	861.84	1.7966E+04	1.7923E+04	2.1952E+04	1.1539E+06	1.4868E+06	1.6370E+06

Bridge 5/649	Es (MN/m2)	Translational Springs			Rotational Springs		
South Abut	47.88	1.0839E+03	1.1804E+03	2.6482E+03	8.9691E+03	1.4740E+05	1.1481E+05
	287.28	2.7672E+03	2.8637E+03	4.6792E+03	5.1353E+04	8.8195E+05	6.8887E+05
	861.84	6.8071E+03	6.9036E+03	9.5536E+03	1.5308E+05	2.6449E+06	2.0666E+06
South Pier	47.88	4.9103E+02	4.9103E+02	9.2741E+02	1.7840E+04	1.7840E+04	2.4969E+04
	287.28	1.9461E+03	1.9461E+03	2.4257E+03	1.0666E+05	1.0666E+05	1.4981E+05
	861.84	5.4383E+03	5.4383E+03	6.0216E+03	3.1984E+05	3.1984E+05	4.4944E+05
North Pier	47.88	3.0897E+02	3.0897E+02	9.2741E+02	1.7808E+04	1.7808E+04	2.4969E+04
	287.28	1.7641E+03	1.7641E+03	2.4257E+03	1.0663E+05	1.0663E+05	1.4981E+05
	861.84	5.2563E+03	5.2563E+03	6.0216E+03	3.1980E+05	3.1980E+05	4.4944E+05
North Abut	47.88	1.2430E+03	1.3395E+03	2.8724E+03	9.0303E+03	1.4746E+05	1.1481E+05
	287.28	2.9263E+03	3.0228E+03	4.9034E+03	5.1415E+04	8.8201E+05	6.8887E+05
	861.84	6.9662E+03	7.0627E+03	9.7778E+03	1.5314E+05	2.6449E+06	2.0666E+06

CHAPTER FOUR

SEISMIC ANALYSIS

4.1 SEISMIC EXCITATIONS

Ten seismic excitations were used to assess the bridges: four short-duration and six long-duration motions. The short-duration motions were the Olympia and Kobe excitations, with the Kobe excitation being also a near-fault motion. The long-duration motions were the Mexico, Peru and Chile excitations. Figures 4.1-1 to 4.1-10 show the time histories for the longitudinal and transverse directions of these earthquakes. The Peru and Chile earthquake time histories were generated by modifying the ground motions from South American, inter-plate, subduction zone earthquakes to fit a target acceleration spectrum for the Seattle area. The spectrum was derived from the Atkinson and Boore (2003) relationship which includes several terms including soil classification and a near-source saturation term.

The other six earthquakes (Olympia, Mexico and Kobe, both 475 and 975-year return periods), were provided by WSDOT. These three time histories were modified by PanGeo Inc., a geotechnical subconsultant of WSDOT for The Aurora Avenue bridge retrofit project in Seattle. Probalistic and deterministic approaches were used to develop the ground motion. They relied on several design requirement criteria (The current WSDOT (500-yr return period), CalTrans (1000 year), UBC (1000 year) and the 2000 IBC (2500 year)) for the probalistic approach.

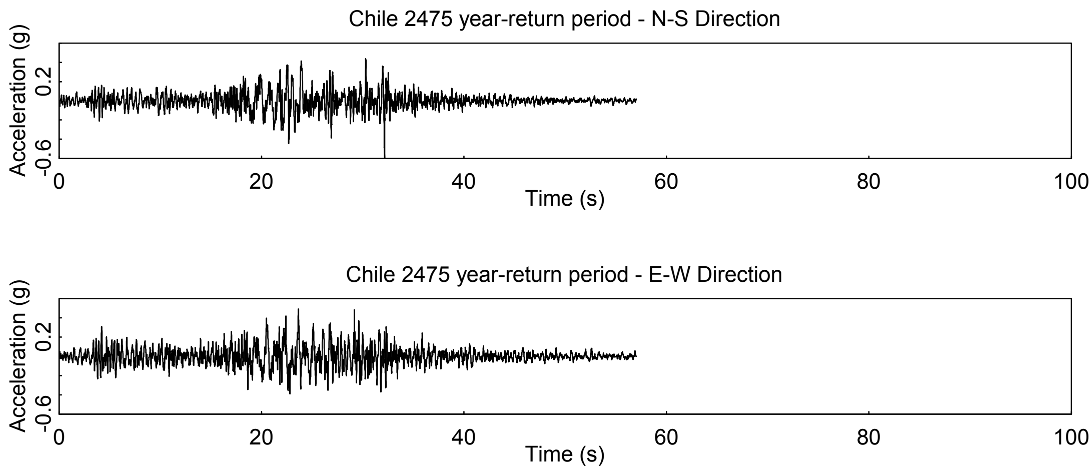

Figures 4.1-1 Time Histories for the Large Return Period Earthquakes: Chile 2475

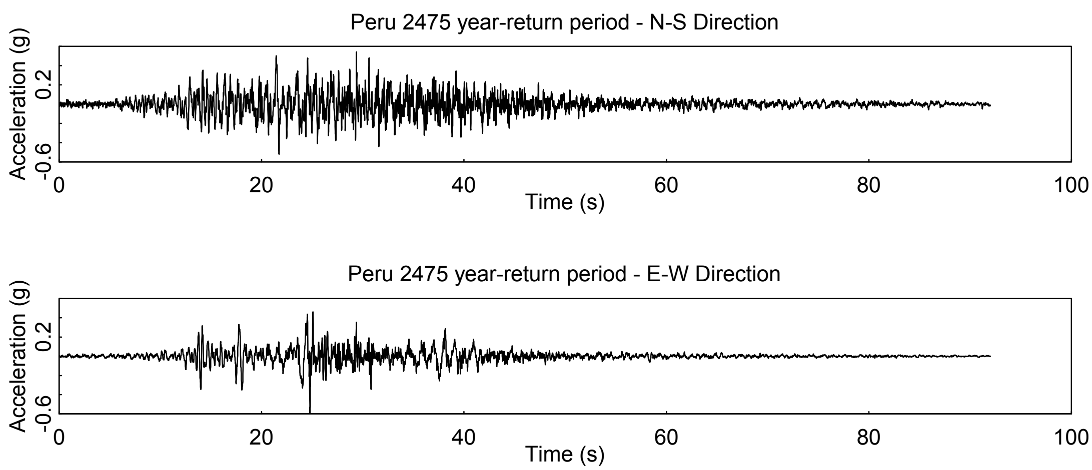

Figures 4.1-2 Time Histories for the Large Return Period Earthquakes: Peru 2475

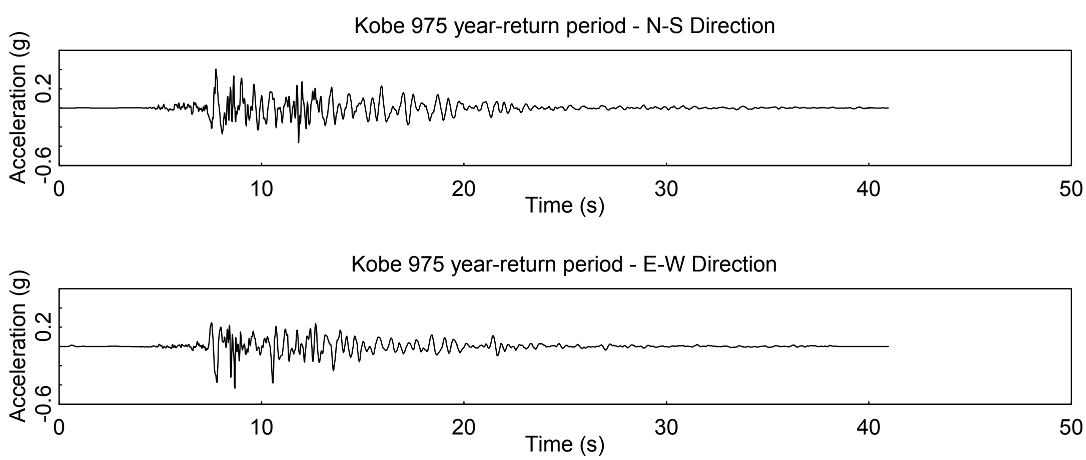

Figures 4.1-3 Time Histories for the Large Return Period Earthquakes: Kobe 975

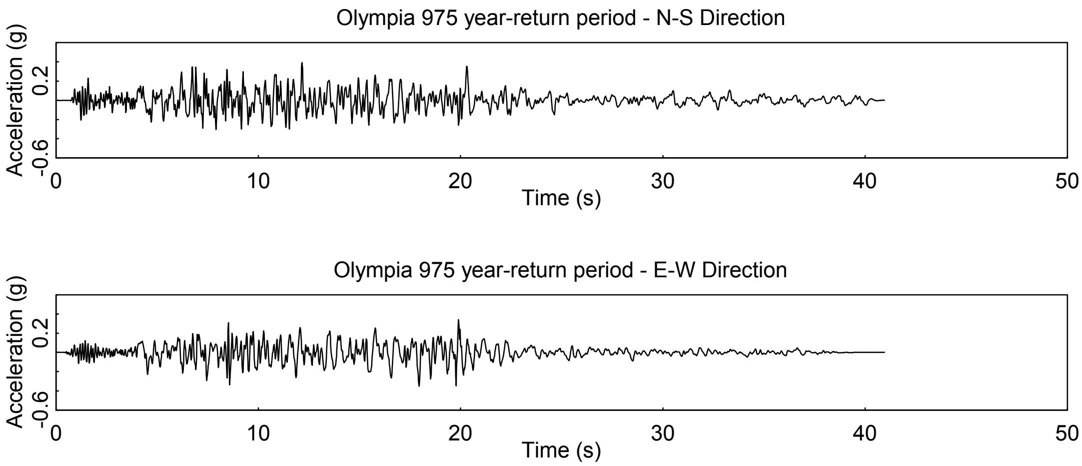

Figures 4.1-4 Time Histories for the Large Return Period Earthquakes: Olympia 975

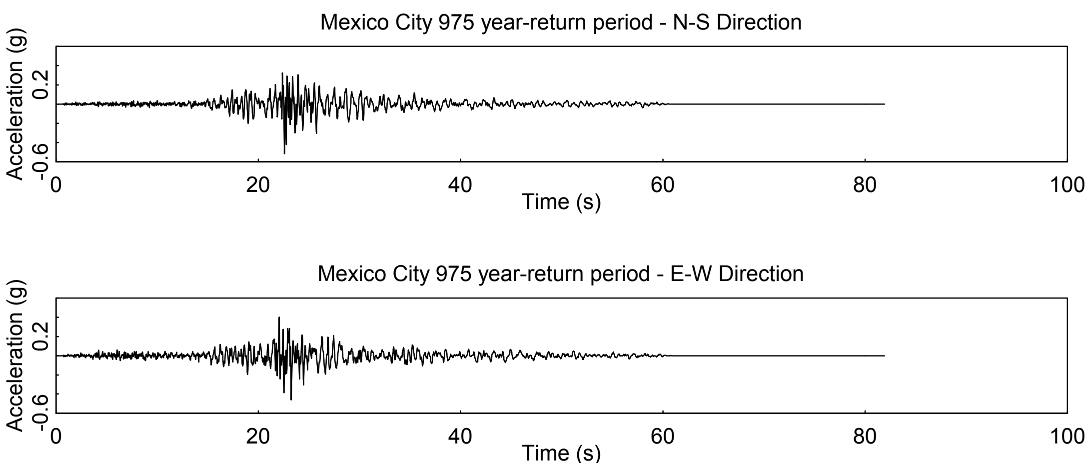

Figures 4.1-5 Time Histories for the Large Return Period Earthquakes: Mexico City 975

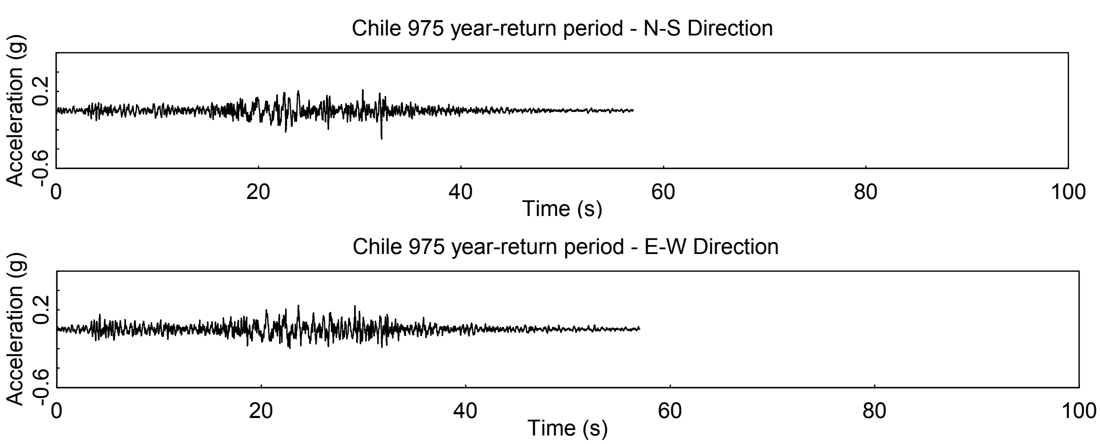

Figures 4.1-6 Time Histories for the Small Return Period Earthquakes: Chile 975

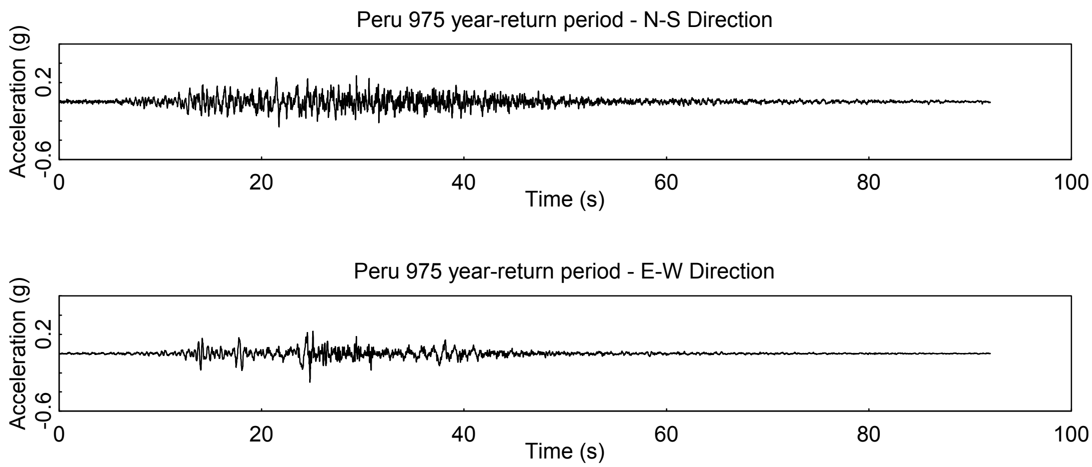

Figures 4.1-7 Time Histories for the Small Return Period Earthquakes: Peru 975

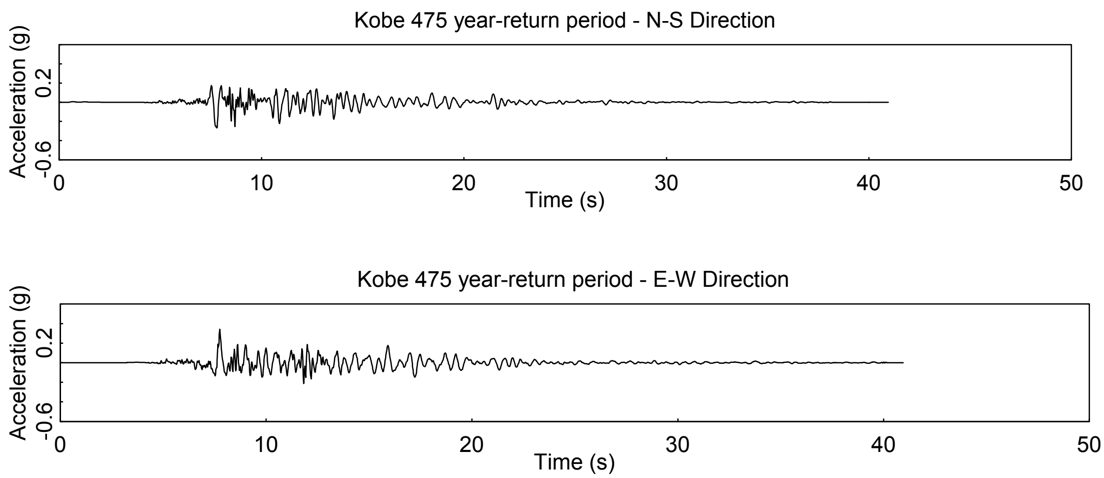

Figures 4.1-8 Time Histories for the Small Return Period Earthquakes: Kobe 475

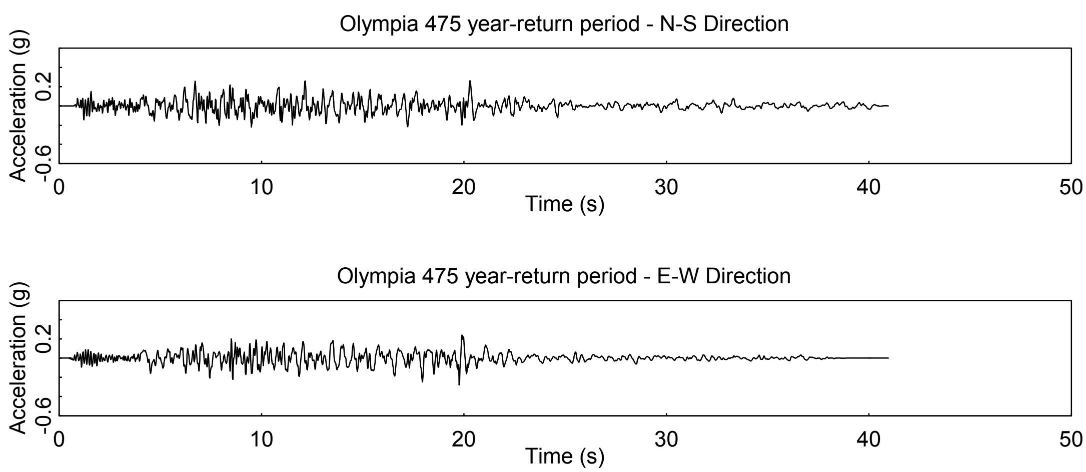

Figures 4.1-9 Time Histories for the Small Return Period Earthquakes: Olympia 475

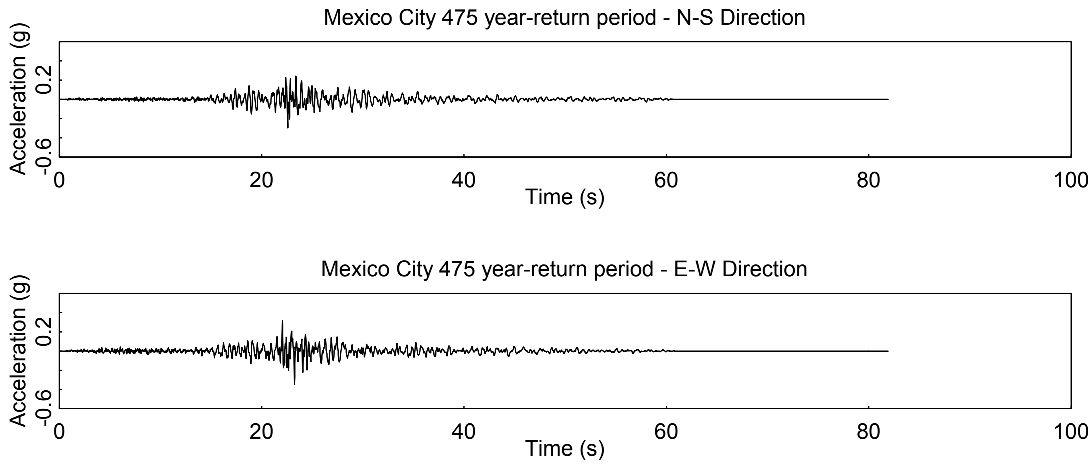

Figures 4.1-10 Time Histories for the Small Return Period Earthquakes: Mexico City 475

A typical way of characterizing a bridge's response under seismic loading is to use acceleration and displacement spectra, which in this case were created using the software SPECTRA (Carr, 2004). The vertical excitation being a linear scaled version of the highest between the transverse and the longitudinal directions, it would be redundant to display it. Figures 4.1-11 to 4.1-16 show the acceleration and displacement spectra for each earthquake.

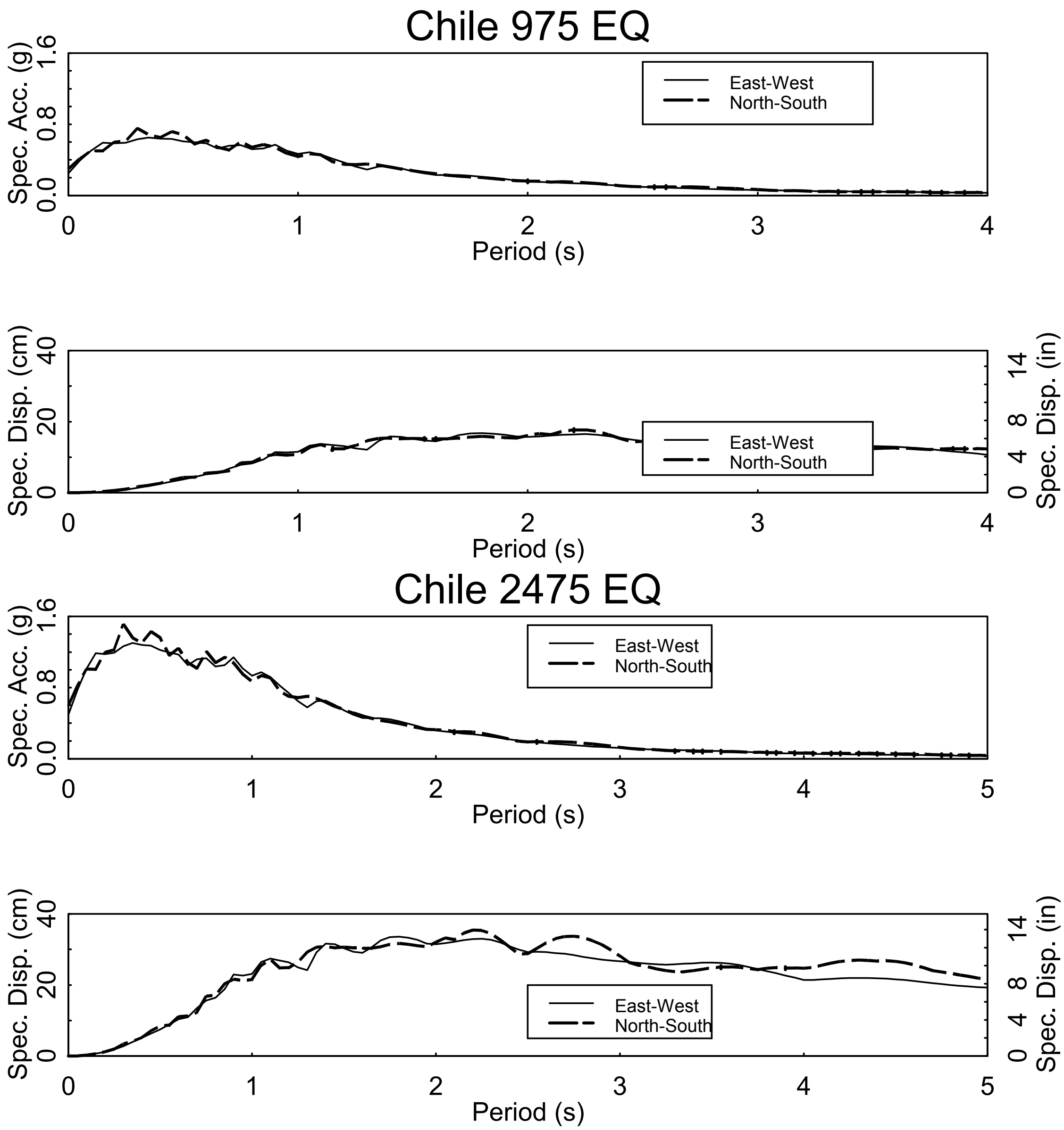

Figure 4.1-11 ARS and DRS for Chile 975 and 2475 Earthquakes

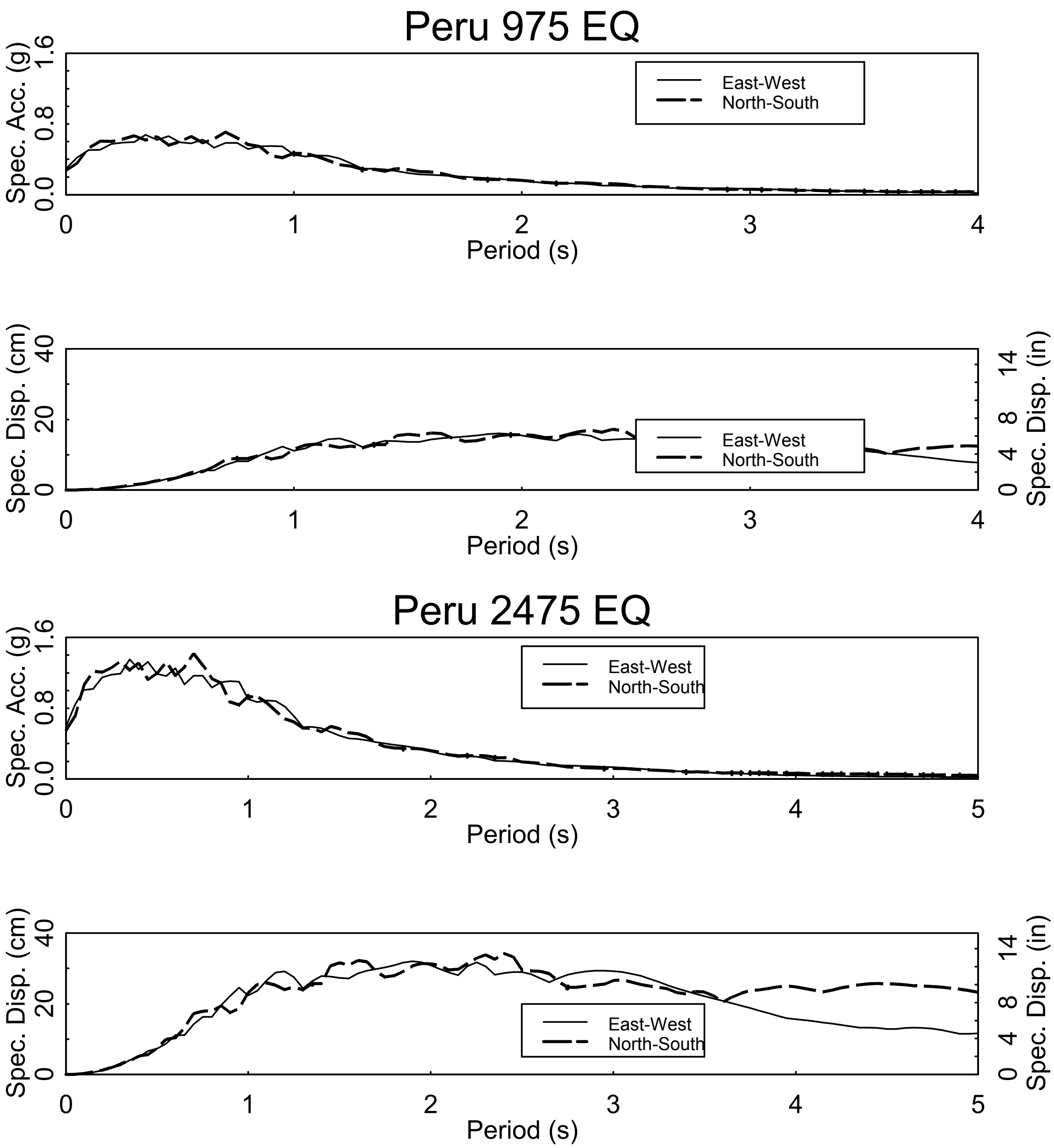

Figure 4.1-12 ARS and DRS for Peru 975 and 2475 Earthquakes

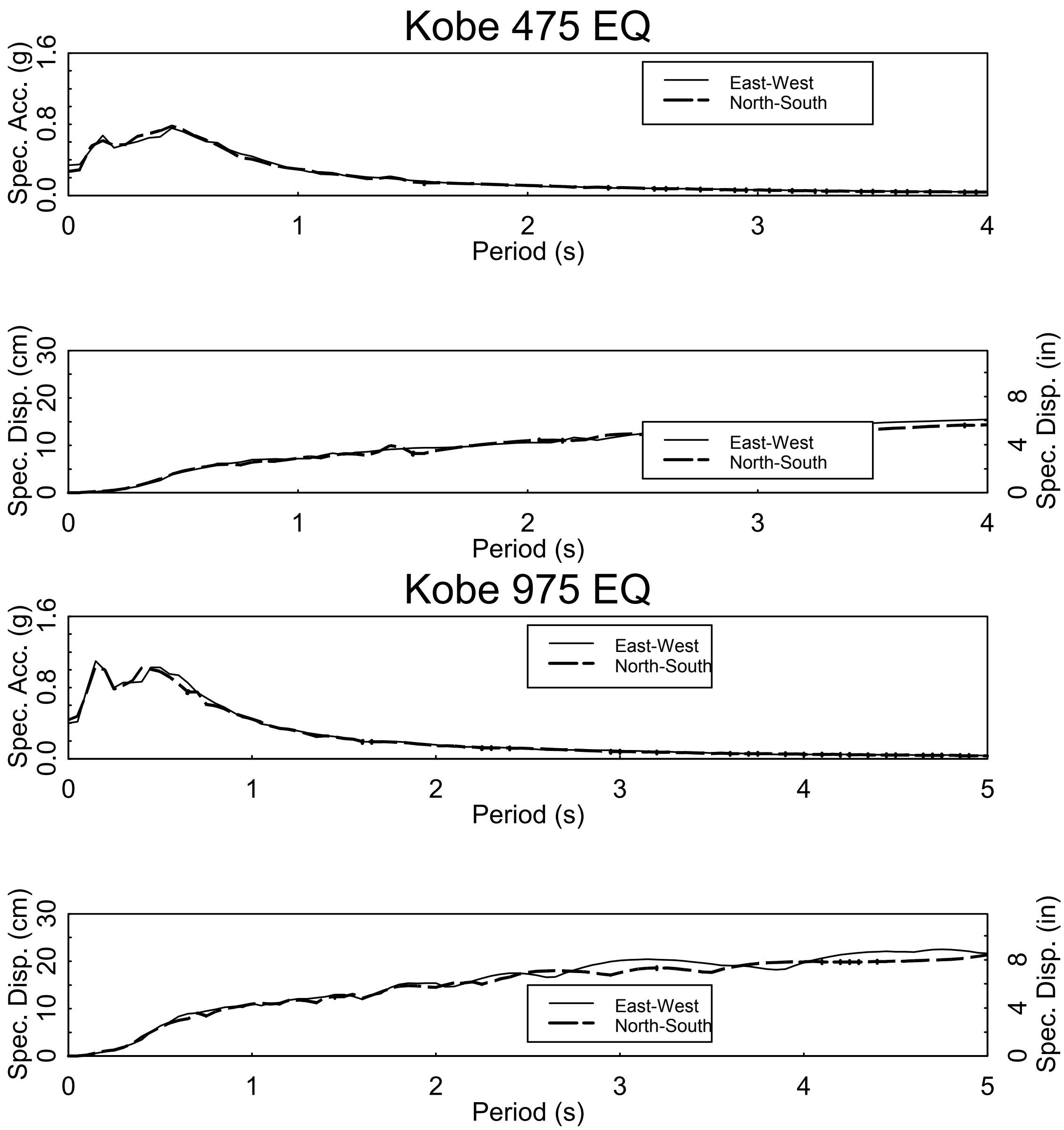

Figure 4.1-13 ARS and DRS for Kobe 475 and 975 Earthquakes

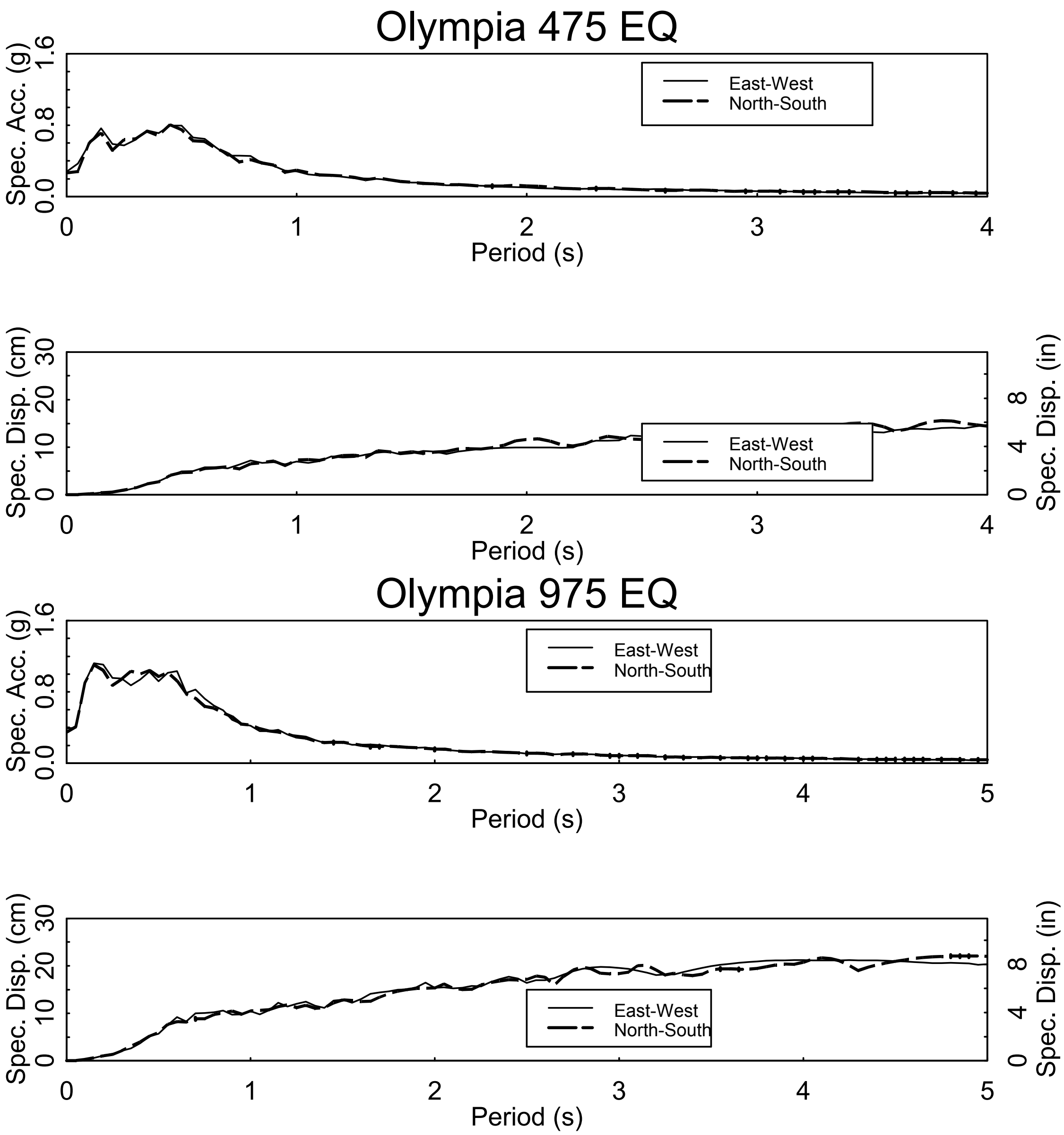

Figure 4.1-14 ARS and DRS for Olympia 475 and 975 Earthquakes

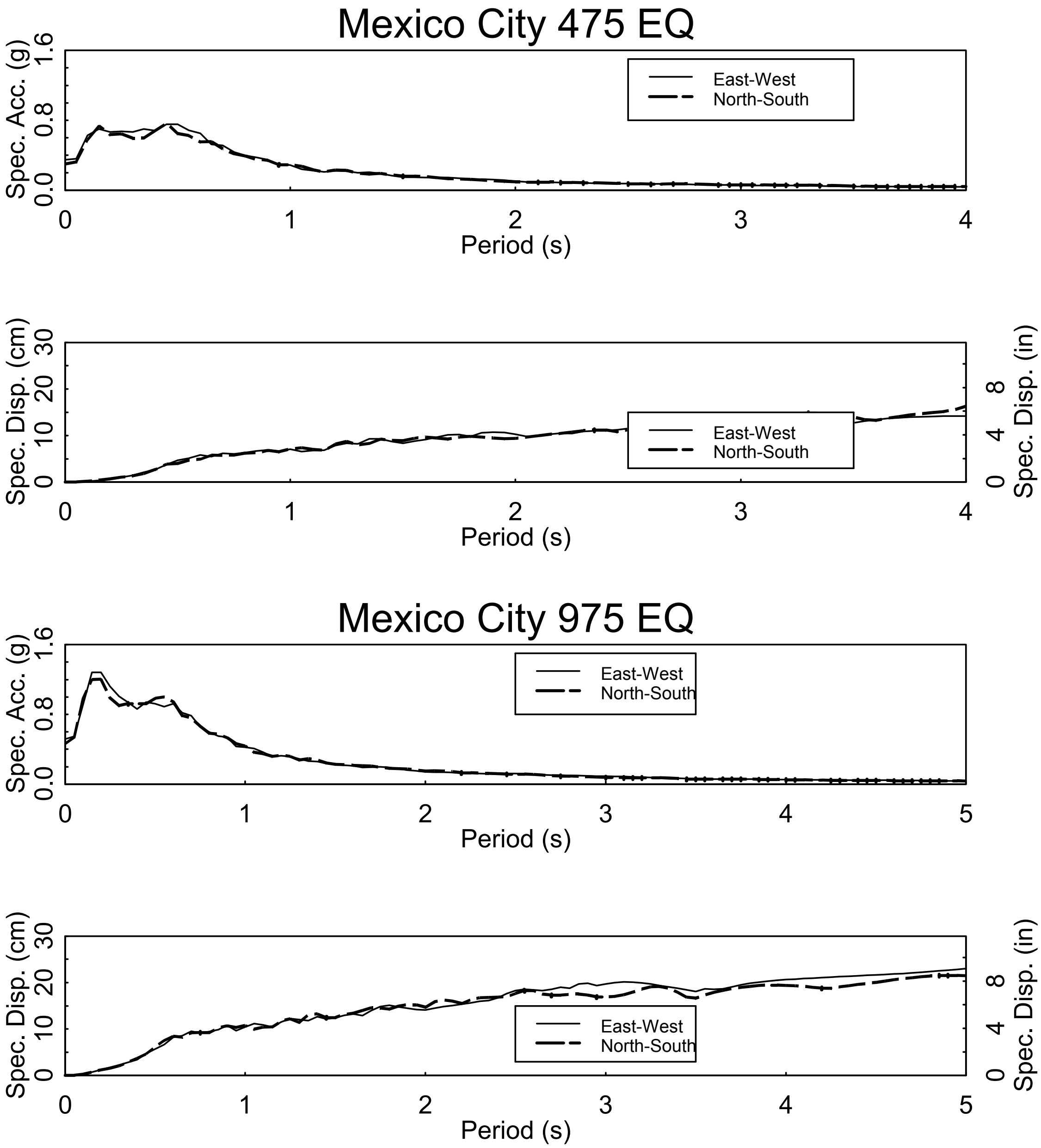

Figure 4.1-15 ARS and DRS for Mexico City 475 and 975 Earthquakes

It is interesting to note that the displacement spectra for the Olympia, Kobe and Mexico earthquake have a displacement that increases with the period. However, the Chile and Peru earthquakes reach a peak displacement at around 1.5 to 2.5 second periods and then displacement is reduced as the period increases.

Table 4.1-1 Bridge Periods, Spectral Accelerations and Spectral Displacement Values

Bridge model	Es (ksf - MPa)	Lg Dir. Period (s)	Tr Dir. Period (s)	Longitudinal Dir. Mean period (s)	Longitudinal Dir. Earthquake	Longitudinal Dir. S_A (g)	Longitudinal Dir. S_D (cm)	Transverse Dir. Mean period (s)	Transverse Dir. Earthquake	Transverse Dir. S_A (g)	Transverse Dir. S_D (cm)
5/227				East-West Dir.				North-South Dir.			
	6000 - 287.3	0.33	0.39	0.37	Kobe 475	0.65	1.98	0.40	Kobe 475	0.73	2.90
					Kobe 975	0.86	2.74		Kobe 975	1.02	3.96
					Mexico 475	0.69	2.29		Mexico 475	0.68	2.74
	18000 - 861.8	0.33	0.39		Mexico 975	0.90	3.05		Mexico 975	0.92	3.51
					Olympia 475	0.73	2.29		Olympia 475	0.68	2.59
					Olympia 975	0.90	3.05		Olympia 975	1.00	3.96
	Fixed / Roller	0.53	0.38		Peru 975	0.65	4.88		Peru 975	0.66	5.49
					Peru 2475	1.30	4.27		Peru 2475	1.31	4.88
					Chile 975	0.65	1.83		Chile 975	0.65	2.44
					Chile 2475	1.30	4.27		Chile 2475	1.29	4.88
512/19				North-South Dir.				East-West Dir.			
	6000 - 287.3	0.53	0.27	0.58	Kobe 475	0.62	5.05	0.39	Kobe 475	0.66	2.59
					Kobe 975	0.84	7.47		Kobe 975	0.87	2.88
					Mexico 475	0.55	4.92		Mexico 475	0.68	2.69
	18000 - 861.8	0.53	0.27		Mexico 975	0.95	8.41		Mexico 975	0.86	3.66
					Olympia 475	0.62	4.88		Olympia 475	0.71	2.71
					Olympia 975	0.95	8.23		Olympia 975	0.94	3.72
	Fixed	0.69	0.62		Peru 975	0.63	4.93		Peru 975	0.62	2.59
					Peru 2475	1.22	10.42		Peru 2475	1.24	4.91
					Chile 975	0.62	5.52		Chile 975	0.65	2.59
					Chile 2475	1.20	10.40		Chile 2475	1.28	5.01
5/649 - without skew				North-South Dir.				East-West Dir.			
	6000 - 287.3	0.53	0.62	0.60	Kobe 475	0.62	5.49	0.62	Kobe 475	0.58	5.79
					Kobe 975	0.83	7.32		Kobe 975	0.89	8.53
					Mexico 475	0.55	4.72		Mexico 475	0.58	5.49
	18000 - 861.8	0.53	0.61		Mexico 975	0.92	8.23		Mexico 975	0.87	8.23
					Olympia 475	0.61	5.49		Olympia 475	0.60	5.79
					Olympia 975	0.92	8.23		Olympia 975	0.90	8.53
	Fixed / Roller	0.81	0.62		Peru 975	0.59	4.88		Peru 975	0.58	5.49
					Peru 2475	1.17	10.97		Peru 2475	1.15	10.67
					Chile 975	0.62	5.49		Chile 975	0.57	4.88
					Chile 2475	1.24	10.67		Chile 2475	1.13	10.36
5/649 - with skew				North-South Dir.				East-West Dir.			
	6000 - 287.3	0.61	0.62	0.68	Kobe 475	0.49	6.40	0.62	Kobe 475	0.60	5.79
					Kobe 975	0.75	8.99		Kobe 975	0.94	8.53
					Mexico 475	0.47	5.79		Mexico 475	0.65	5.49
	18000 - 861.8	0.61	0.61		Mexico 975	0.75	8.53		Mexico 975	0.92	8.23
					Olympia 475	0.48	5.79		Olympia 475	0.65	5.79
					Olympia 975	0.73	8.53		Olympia 975	1.03	8.53
	Fixed / Roller	0.81	0.62		Peru 975	0.71	7.92		Peru 975	0.63	5.49
					Peru 2475	1.42	15.24		Peru 2475	1.25	10.67
					Chile 975	0.51	5.94		Chile 975	0.59	4.88
					Chile 2475	1.02	11.89		Chile 2475	1.17	10.36

Table 4.1-1 shows the spectral accelerations for all four bridge models for a mean period. Since the bridges are not oriented the same way, the east-west direction earthquakes correspond to the longitudinal direction for Bridge 5/227, and transverse

direction for Bridges 512/19 and 5/649. Similarly, the north-south direction earthquakes correspond to the transverse direction for Bridge 5/227 and longitudinal direction for Bridges 512/19 and 5/649. It can be seen that the Peru 2475 earthquake will pose the largest demand for all bridge models.

The Nisqually earthquake of 2001 had a moment magnitude of 6.8. Figure 4.1-16 shows the acceleration response spectra (ARS) for the Nisqually earthquake at two different locations as well as the acceleration spectra for the Peru 2475 and the Olympia 975 earthquakes. The Olympia DNR building was the location where the highest peak ground acceleration was recorded (374.4 cm/s^2). The SeaTac fire station is a better location for an estimate of the ground motions that loaded the three bridges modeled in this study. Based on the target acceleration spectra for the Seattle area, the Nisqually earthquake at the SeaTac fire station has a return period that can be estimated at approximately 475 years depending on the location and based on a structure with a period of 0.5 seconds. The ground motion recorded at the Olympia DNR building has a return period of approximately 975 years (based on the USGS target acceleration spectra for the Seattle and Olympia regions, 2003).

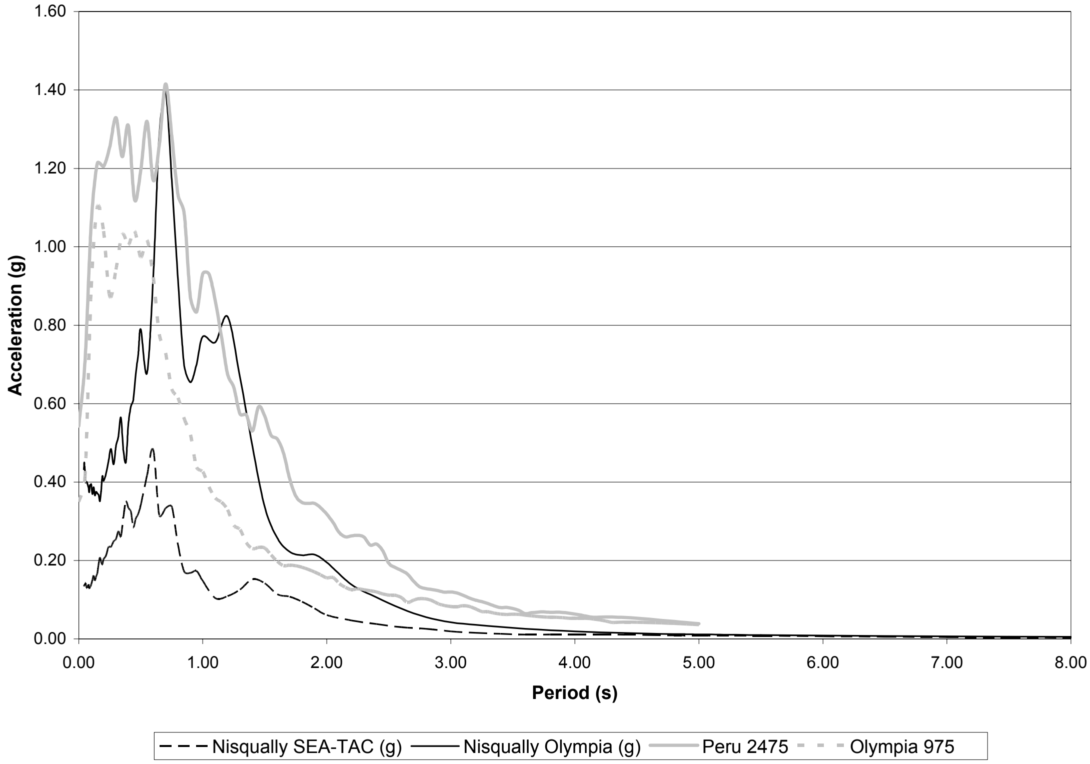

Figure 4.1-16 ARS for the 2001 Nisqually, Peru 2475 and Olympia 975 Earthquakes

CHAPTER FIVE

BRIDGE 5/649 SKEW COMPARISON

5.1 BRIDGE 5/649 SKEW OR STRAIGHT MODEL

Modeling a structure requires that simplifications be made in describing the elements. Cox (2005) compared the response of a spine bridge model and a grillage bridge model. He concluded that although the global bridge response varied between the two models, the changes were not significant when the deck was modeled as a spine versus a grillage. A similar study was conducted in this research to determine if the skew of a bridge deck significantly influenced the overall response of the bridge. Bridge 5/649 was modeled in two different ways as illustrated below. The existing bridge was built with a 45º skew. Dimensions were taken parallel to the skew so that the length of the bents in both models was identical.

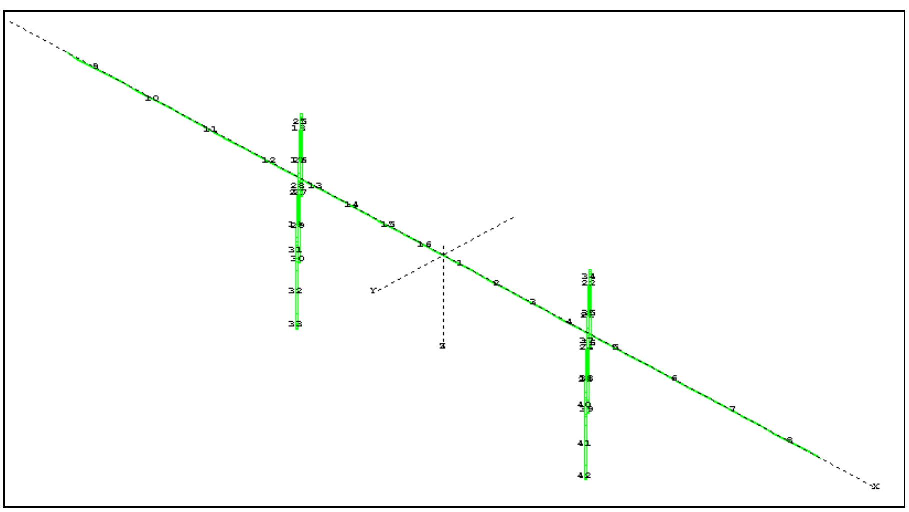

Figure 5.1-1 5/649 Bridge Spine Model with Skew

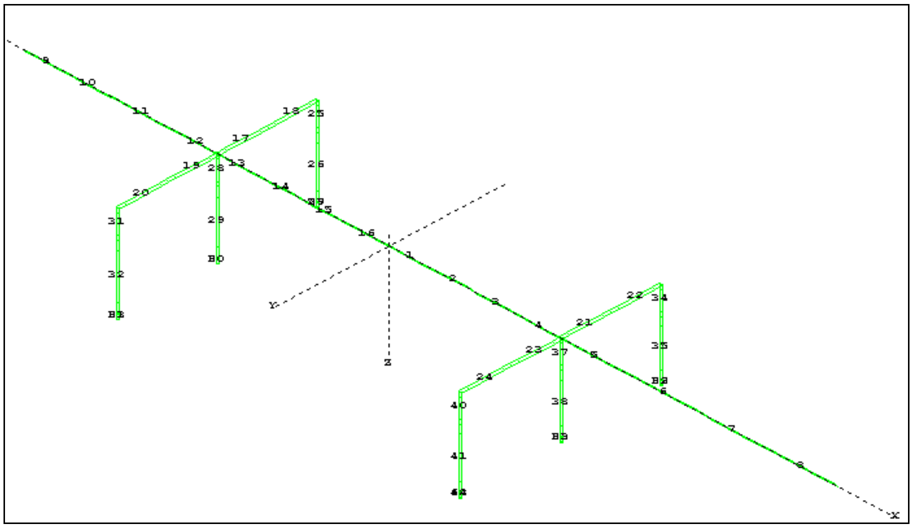

Figure 5.1-2 5/649 Bridge Spine Model without Skew

5.1.1 <u>Maximum Demands</u>

To evaluate the difference in behaviors of the models, several parameters were studied: the maximum total shear in the columns (V), the maximum relative displacement at the top of the columns (Δ), the maximum moments at the top and at the bottom of he columns (M) and the maximum curvature at the top of the columns (Φ). Both models were run under two earthquakes, Olympia 975 and Peru 2475, for this comparison. Two different boundary conditions were used in the models: the spring values for an elastic modulus of 287.3 MPa (6000 ksf) and 861.9 MPa (18000 ksf). Tables 5.1.1-1 and -2 present the results obtained.

Table 5.1.1-1 Bridge 5/649 Displacement and Shear Force Demands Due to the Olympia 975 Earthquake

With skew			
Bent	**649 - O - 283.7**	**649 - O - 861.9**	**649 - O - fixed**
Max Δ (cm)			
North - East	8.24	8.92	8.02
North - Center	7.38	7.49	8.02
North - West	7.33	7.35	8.02
South - East	8.28	8.55	10.05
South - Center	8.27	8.27	10.05
South - West	8.26	8.17	10.06
Max V (kN)			
North - East	271	272	331
North - Center	200	205	245
North - West	323	455	404
South - East	282	298	333
South - Center	170	225	263
South - West	315	316	402

Without skew			
Bent	**649 - O - 283.7**	**649 - O - 861.9**	**649 - O - fixed**
Max Δ (cm)			
North - East	7.88	7.79	8.67
North - Center	7.46	7.45	8.10
North - West	7.08	7.15	7.56
South - East	8.08	8.73	11.06
South - Center	8.09	8.73	10.59
South - West	8.09	8.74	10.15
Max V (kN)			
North - East	282	282	353
North - Center	203	200	257
North - West	309	318	374
South - East	287	294	359
South - Center	183	188	267
South - West	311	327	403

The maximum variation in displacement demands between the skewed and the straight model occurred for the fixed model, at the east column of the south bent (9%).

The shear demands varied by 43% for the 861.9 MPa elastic soil modulus value model, between the skewed and the straight model at the west column of the north bent.

Table 5.1.1-2 Bridge 5/649 Displacement and Shear Force Demands Due to the Peru 2475 Earthquake

With skew			
Bent	**649 - P - 283.7**	**649 - P - 861.9**	**649 - P - fixed**
Max Δ (cm)			
North - East	17.70	18.48	20.17
North - Center	17.54	17.37	20.08
North - West	17.41	16.61	19.99
South - East	16.46	17.14	22.32
South - Center	17.32	16.58	22.25
South - West	18.22	17.11	22.20
Max V (kN)			
North - East	522	537	715
North - Center	455	552	755
North - West	584	634	836
South - East	389	421	584
South - Center	377	420	613
South - West	509	487	759

Without skew			
Bent	**649 - P - 283.7**	**649 - P - 861.9**	**649 - P - fixed**
Max Δ (cm)			
North - East	17.11	18.13	23.13
North - Center	17.00	18.13	19.78
North - West	16.89	18.13	16.63
South - East	17.19	18.16	22.40
South - Center	17.00	17.61	21.39
South - West	17.10	17.27	20.39
Max V (kN)			
North - East	474	519	747
North - Center	453	568	699
North - West	568	640	773
South - East	428	458	622
South - Center	433	420	564
South - West	532	464	657

The variation in demands was larger for the Peru 2475 earthquake. There was an increase of 20%, approximately 3.3 cm (1.3 in), in displacement demands for the west column of the north bent, between the skew and straight models. There was a 15% increase, approximately 102 kN (23 kips), in the shear force demands between the skewed and straight fixed column base/roller abutment models at the south bent, west column.

5.1.2 Hysteresis Curves

Another way to compare the effect of the skew on the response of the bridge is to study the force versus displacement hysteresis curves for both models. Below are displayed the hysteresis curves for the bridge with two different soil types and two earthquakes. The column with the highest demand is displayed, the center column of the south bent.

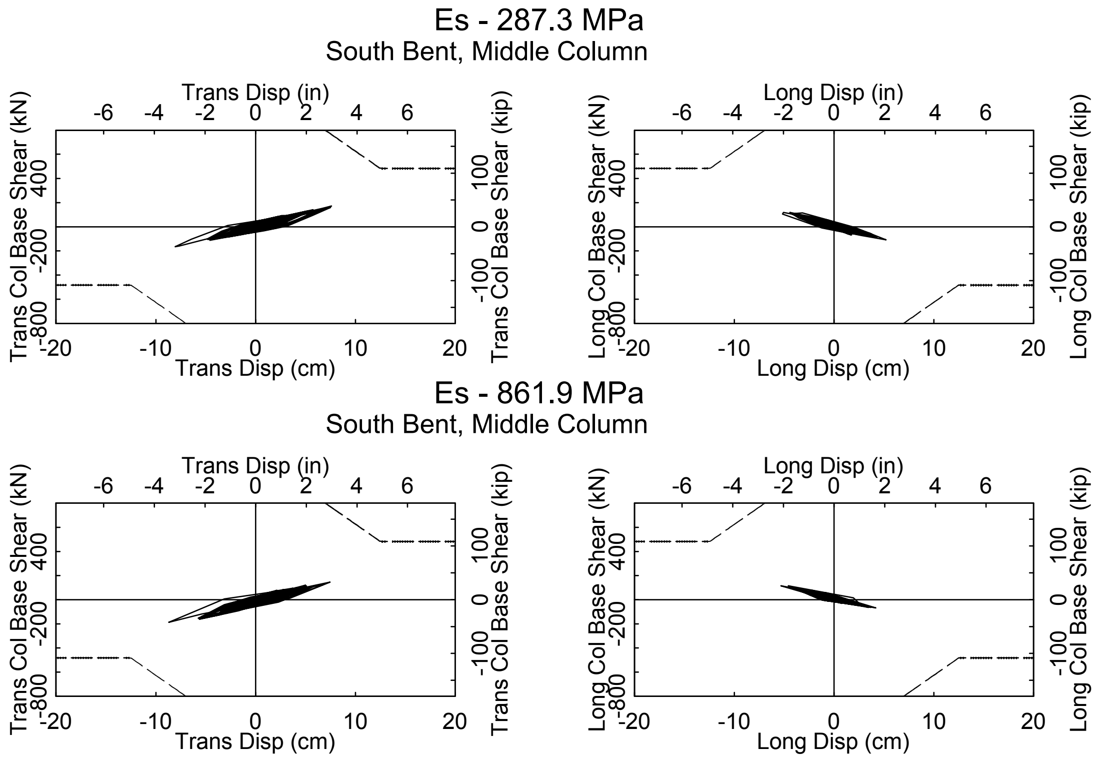

Figure 5.1.2-1 South Bent, Center Column: Hysteresis Curves for Bridge 5/649 – Without Skew; Olympia 975 EQ; Es=47.9 MPa (1000ksf); 861.9 MPa (18000 ksf)

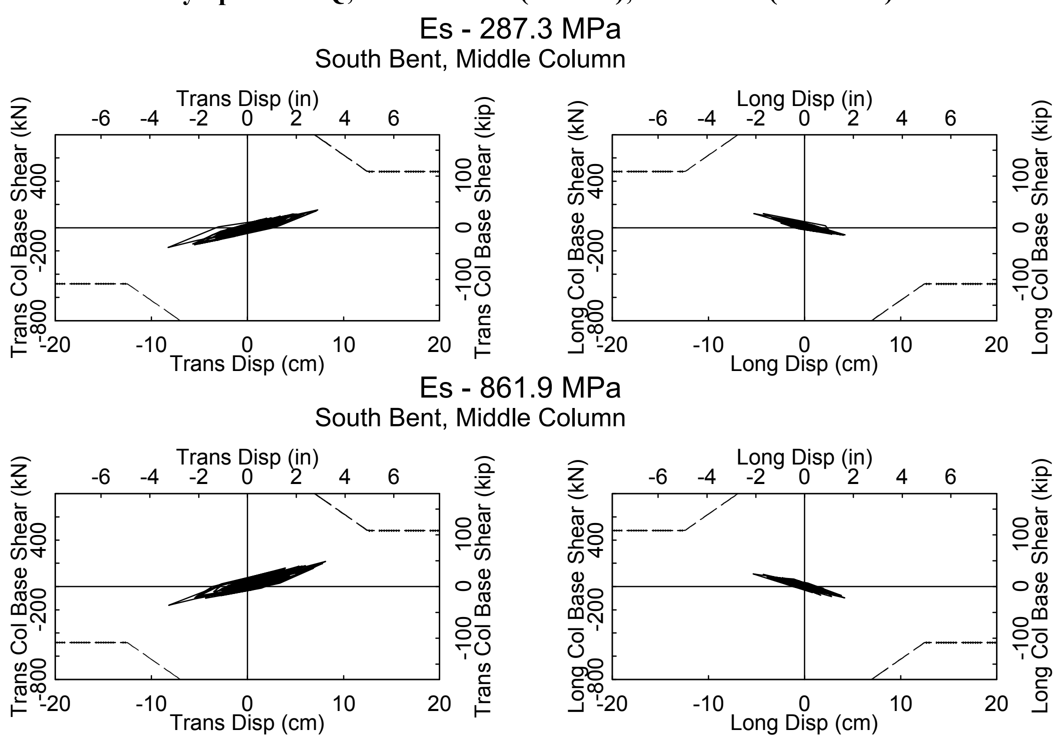

Figure 5.1.2-2 South Bent, Center Column: Hysteresis Curves for Bridge 5/649 - With Skew; Olympia 975 EQ; Es=287.3 MPa (6000 ksf); 861.9 MPa (18000 ksf)

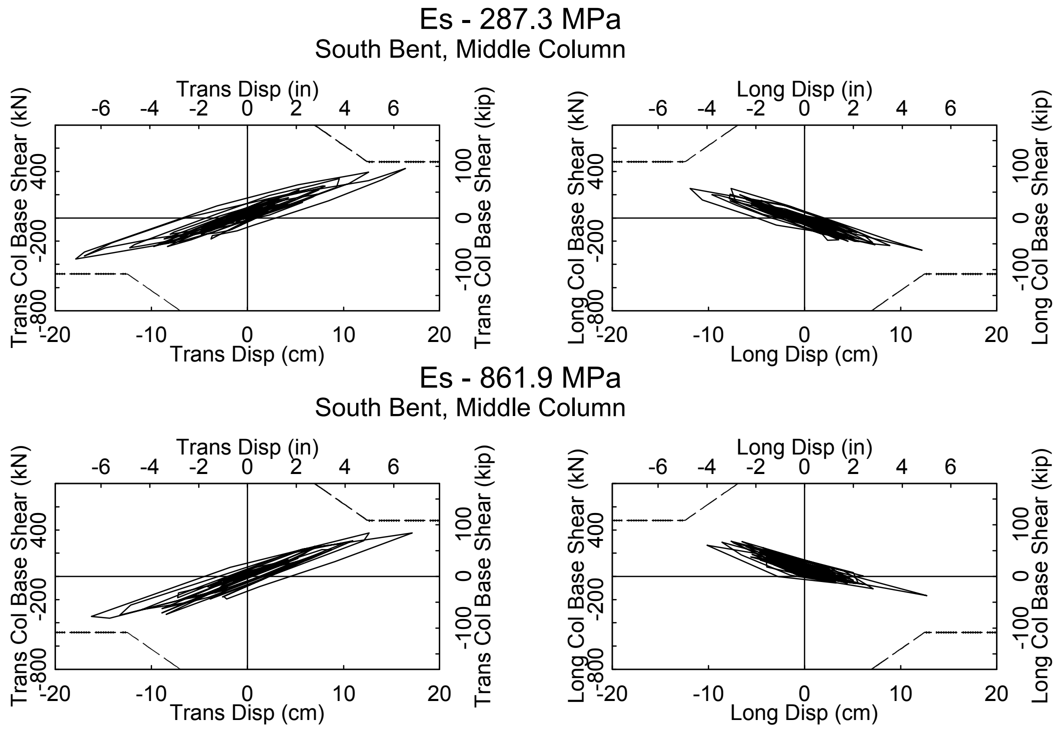

Figure 5.1.2-3 South Bent, Center Column: Hysteresis Curves for Bridge 5/649 - Without Skew; Peru 2475 EQ; Es=47.9 MPa (1000ksf); 861.9 MPa (18000 ksf)

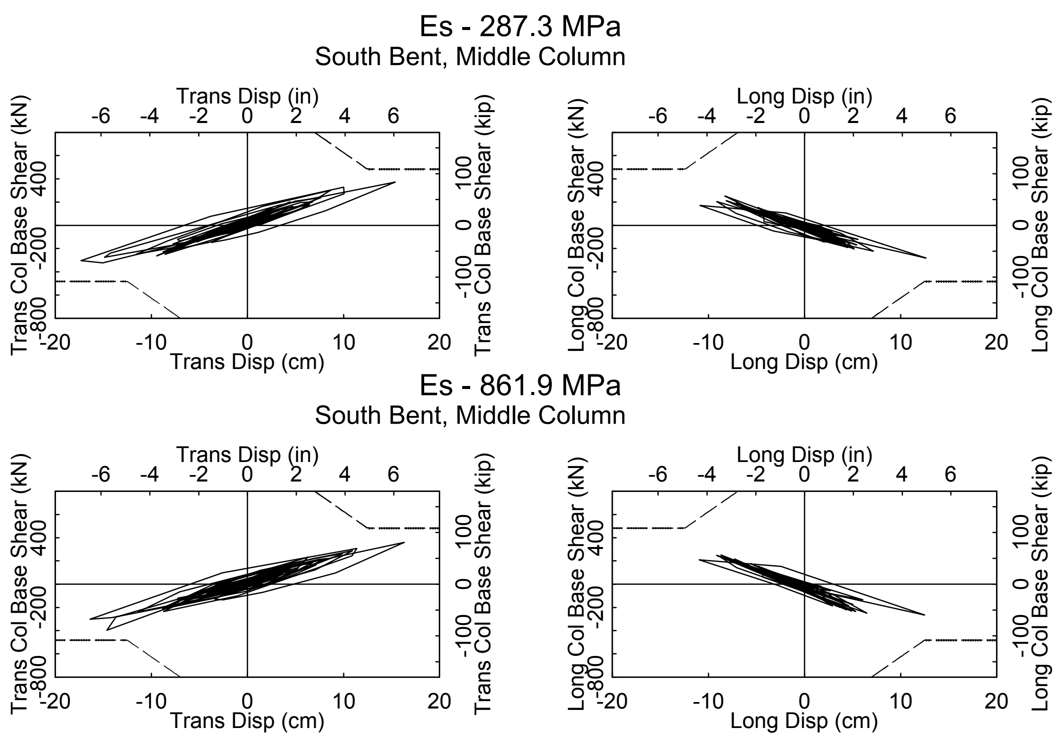

Figure 5.1.2-4 South Bent, Center Column: Hysteresis Curves for Bridge 5/649 - With Skew; Peru 2475 EQ; Es=287.3 MPa (6000 ksf); 861.9 MPa (18000 ksf)

The general shape of the hysteresis curves is the same for both models.

5.1.3 Time History Comparison

Another way to compare the response of a bridge under earthquake loading is to investigate the relative displacement between the column tops and column bottoms versus time. Below are plotted the relative displacement versus time for the Olympia 975 and Peru 2475 earthquakes, for the middle column of the south bent, for the two soil spring elastic modulus values of 287.3 MPa and 861.9 MPa.

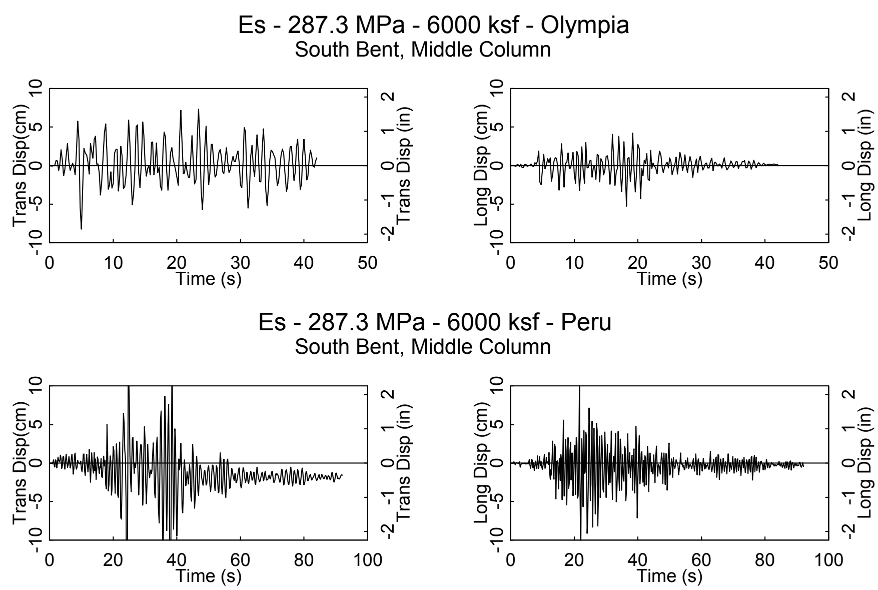

Figure 5.1.3-1 Displacement Versus Time for the Olympia 975 and Peru 2475 Earthquakes, 287.3 MPa Spring Models With Skew

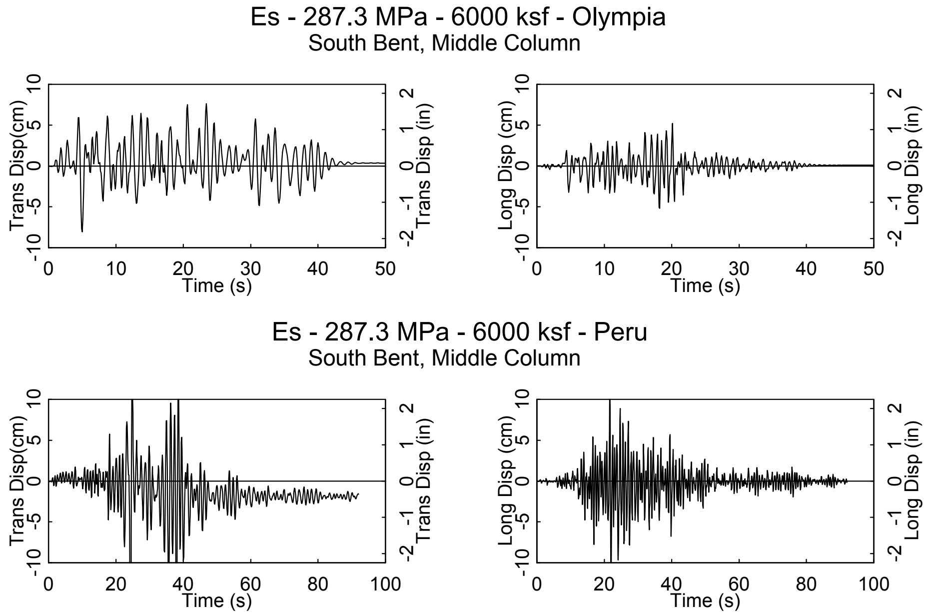

Figure 5.1.3-2 Displacement Versus Time for the Olympia 975 and Peru 2475 Earthquakes, 287.3 MPa Spring Models Without Skew

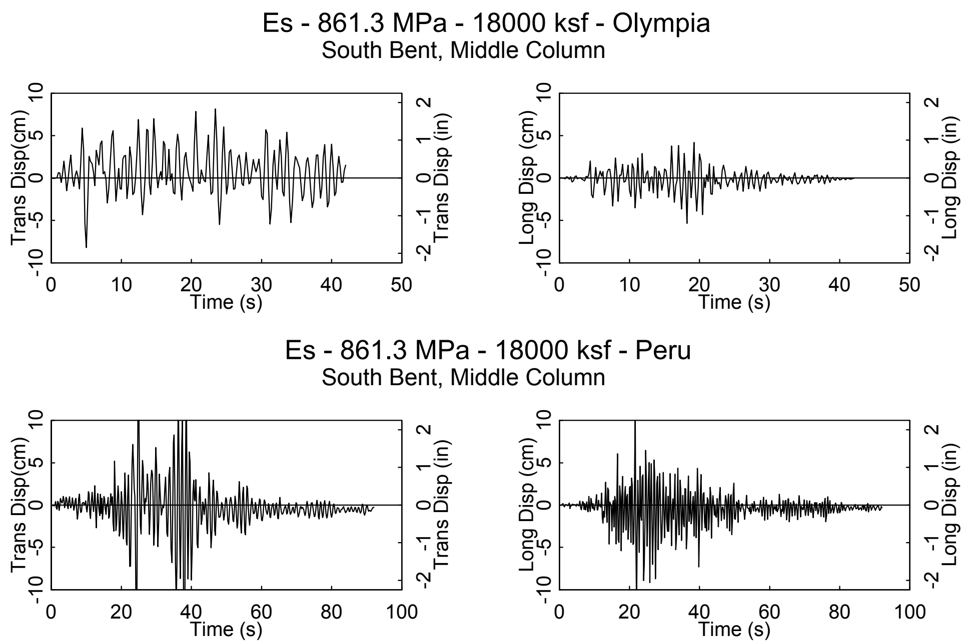

Figure 5.1.3-3 Displacement Versus Time for the Olympia 975 and Peru 2475 Earthquakes, 861.9 MPa Spring Models With Skew

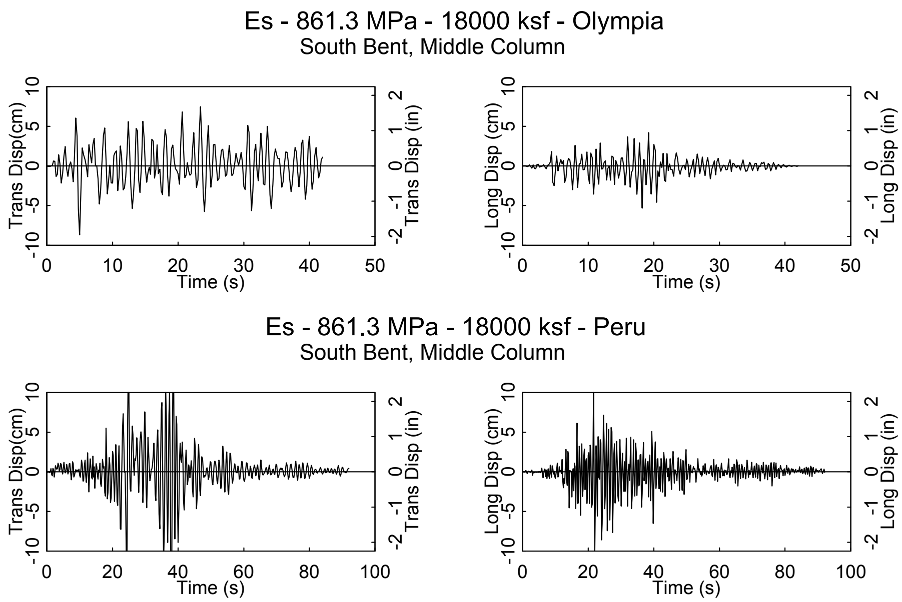

Figure 5.1.3-4 Displacement Versus Time for the Olympia 975 and Peru 2475 Earthquakes, 861.9 MPa Spring Models Without Skew

The plots of transverse and longitudinal displacement versus time show that the differences between the skew model and the non-skew model of Bridge 5/649 are not significant. However, the maximum displacement and shear demands are significant, approximately 20% and 40% variation respectively. For Bridge 5/649, the skew affected the bridge response enough that modeling the skew is necessary to assess successfully the seismic response of the bridge. In addition, further investigations are needed to draw a general conclusion as to how important an existing bridge skew is to the overall behavior of the bridge.

CHAPTER SIX

BRIDGE RESPONSE

The main goal of this research was to assess the response of multicolumn bent prestressed concrete bridges subject to long-duration earthquake excitations. Ten earthquake records were used to evaluate the bridge response (see Chapter four). To avoid numerous pages of data, selected results will be displayed. However, conclusions will be drawn based on all the analyses. The maximum demands obtained and the force-displacement hysteresis curves are presented below. The following notations are used in the tables and figures in this chapter: Δ (cm) represents the relative displacement between the top and bottom of the column, V (kN) is the shear in the column, M top (kN-m) is the moment at the top of the column, M bot (kN-m) is the moment at the bottom of the column, and Φ top (1/m) is the curvature at the top of the column. When comparing analyses, the percentile indicates the variation between the considered model and the model with the lowest soil spring stiffnesses.

6.1 BRIDGE 5/227

Bridge 5/227 has three bents with three columns per bent, a non-monolithic deck and spread footings resting on concrete piles. In an effort to assess the bridge's seismic vulnerability, the maximum demands obtained during the analysis of Bridge 5/227 under the Olympia 975 earthquake and the Peru 2475 earthquake are presented in tables 6.1-1 and 6.1-3 for soil springs based on a soil modulus of elasticity of 287.3 MPa (6000 ksf), 861.9 MPa (18000 ksf) and fixed-column/roller-abutment boundary condition.

Table 6.1-1 Maximum Earthquake Demands for Bridge 5/227 Subject to the Olympia 975 Loading

Bent	227 - O - 283.7	227 - O - 861.9	227 - O - fixed
Max Δ (cm)			
West - South	3.07	6.23	11.01
West - Center	2.70	5.99	10.88
West - North	2.38	5.79	10.80
Center - South	5.37	7.59	7.79
Center - Center	4.24	7.59	5.41
Center - North	3.92	7.59	7.73
East - South	1.72	5.06	3.00
East - Center	2.10	5.06	3.00
East - North	2.10	5.06	3.00
Max V (kN)			
West - South	378	307	652
West - Center	388	251	686
West - North	378	307	669
Center - South	391	321	628
Center - Center	412	274	685
Center - North	391	321	538
East - South	308	280	456
East - Center	334	291	496
East - North	308	280	456

The bridge displacements increased as the soil spring stiffness increased. There was a 144% (approximately 3.41 cm, 1.34 in) increase in the displacement demands between the two spring models at the west bent. Similarly, a 355% increase in displacement in the east bent occurred between the 287.3 MPa model and the fixed condition model, which corresponds to an increase of approximately 6.5 cm (2.6 in). There was approximately a 20% variation in the shear demands between both spring models and a 60% variation between the 861.9 MPa spring model and the fixed column base model.

The bearing pad displacements can be found in Table 6.1-2 below. Each gap between consecutive deck slabs at the intermediate bents is filled by a rubber bearing pad that was modeled as two springs with identical stiffnesses. Table 6.1-2 summarizes the relative displacements between the deck and the middle of the bearing pad for the intermediate bents and the relative displacement between the deck and the abutment. These results show a significant increase in the bearing pad displacement between the west bent and the west abutment (+215%) for the fixed model.

Table 6.1-2 Maximum Bearing Pad Displacements for Bridge 5/227 Subject to the Olympia 975 Earthquake

Bearing Pad disp (cm)			
	227 - O - 283.7	**227 - O - 861.9**	**227 - O - fixed**
West Abut	2.38	2.91	5.66
West bent west pad	1.28	1.15	1.79
West bent east pad	1.94	1.36	1.17
Center bent west pad	1.21	1.57	1.62
Center bent east pad	1.02	1.11	1.46
East bent west pad	2.16	1.76	1.40
East bent east pad	0.77	1.26	1.71
East Abut	1.93	2.33	5.47

Failure in the bearing pads was defined by a bearing pad displacement greater than 3.66 cm (1.44 in.) (Cox, 2005). Bridge 5/227 bearing pads failed at the abutments under the Olympia 975 earthquake for the fixed column base boundary conditions.

Table 6.1-3 Maximum Earthquake demands for Bridge 5/227 Subject to the Peru 2475 Loading

Bent	227 - P - 283.7	227 - P - 861.9	227 - P - fixed
Max Δ (cm)			
West - South	9.58	7.53	16.07
West - Center	9.58	7.53	13.95
West - North	9.58	7.53	13.88
Center - South	11.87	13.66	13.57
Center - Center	11.96	13.66	13.61
Center - North	12.06	13.66	14.72
East - South	8.13	4.43	12.85
East - Center	8.13	4.41	12.68
East - North	8.13	4.48	12.50
Max V (kN)			
West - South	364	355	431
West - Center	425	347	452
West - North	364	355	425
Center - South	403	380	436
Center - Center	422	414	476
Center - North	403	380	432
East - South	429	341	425
East - Center	422	481	440
East - North	429	369	431

The Peru 2475 earthquake is a larger magnitude and longer duration earthquake than Olympia 975. The displacements obtained during the analysis, were highest in the center bent. The displacements in the center bent increased by 45% (+ 3.5 cm, 1.4 in) between the two spring models and by 55% (+ 4.4 cm, 1.7 in) between the lowest spring value and the fixed column base model. The base shear demands varied by approximately 15% between the two spring models, and 8% between the lowest spring model and fixed column base model.

Table 6.1-4 Maximum Bearing Pad Displacements for Bridge 5/227 Subject to the Peru 2475 Earthquake

Bearing Pad disp (cm)			
	227 - P - 287.3	227 - P - 861.9	227 - P - fixed
West Abut	3.07	3.81	15.01
West bent west pad	1.67	1.33	2.44
West bent east pad	2.87	2.59	1.76
Center bent west pad	2.07	1.63	2.53
Center bent east pad	2.12	1.86	1.81
East bent west pad	2.66	2.30	2.68
East bent east pad	1.62	1.15	2.45
East Abut	3.01	2.57	15.10

The bearing pad displacements were similar for both spring models and there was a slight increase in the displacements at the abutments versus the displacements at the bents. Failure occurs at the west abutment under Peru loading for the highest soil spring stiffness model. However in the fixed model, the displacements at the abutments increased by 400% (+12.5 cm) between the bent bearing pad and the abutment bearing pad. This jump in values at the abutments for the fixed models indicates that there is failure of the bearing pad in the abutment and possibly pounding of the deck into the abutment. Below is the summary of the pounding of the deck for all three models under the Peru 2475 earthquake. The difference in displacement between the west side and the east side of each bearing pad was compared to the width of the bearing to determine if pounding occurred or not. Below is a table summarizing these results:

Table 6.1-5 Pounding in the Deck and Abutments for Bridge 5/227 with the 287.3 MPa Soil Values

Bent	disp end 1 (ft)	disp end 2 (ft)	time	max disp (ft)	max disp (cm)
West abt	-2.67E-03	-8.63E-02	15.2	0.08632	2.6310336
	-3.74E-03	-1.17E-01	17.8	0.1169	3.563112
West bent	-4.46E-02	-1.53E-01	18.4	0.1525	4.6482
Center bent	no pounding				
East bent	1.14E-01	3.25E-02	14.4	0.1135	3.45948
East abt	9.68E-02	2.73E-03	18.6	0.09678	2.9498544

Table 6.1-6 Pounding in the Deck and Abutments for Bridge 5/227 with the 861.9 MPa Soil Values

Bent	disp end 1 (ft)	disp end 2 (ft)	time	max disp (ft)	max disp (cm)
West abt	-3.11E-04	-8.29E-02	15.2	0.08291	2.5270968
	-3.66E-04	-9.43E-02	17.8	0.09429	2.8739592
West bent	no pounding				
Center bent	no pounding				
East bent	1.22E-01	3.46E-02	14.4	0.1224	3.730752
East abt	no pounding				

Table 6.1-7 Pounding in the Deck and Abutments for Bridge 5/227 with Fixed Column Base Boundary Conditions

Bent	times	disp end 1 (ft)	disp end 2 (ft)	time	max disp (ft)	max disp (cm)
West abt	12 times	0.00E+00	-4.32E-01	24.6	0.4324	13.179552
West bent		no pounding				
Center bent		no pounding				
East bent		no pounding				
East abt	43 times	3.76E-01	0.00E+00	25	3.76E-01	11.472672

For the spring models, pounding occurred only once or twice and at the outer bents and abutments. The maximum displacements reached by those two models were 4.65 cm (1.8 in) for the lowest spring value at the west bent, and 3.73 cm (1.5 in) at the east bent for the 861.9 MPa soil elastic modulus value. However, the fixed boundary condition model did result in numerous poundings in both abutments, the maximum displacements being 13.2 cm (5.2 in) for the west abutment and 11.5 cm (4.5 in) at the east abutment.

Figures 6.1-1 to 6.1-7 represent the force-displacement hysteresis curves for the column with the largest demands, the center column of the center bent, under different earthquake loadings. The dotted line located in the corners of the graphs represents the column shear capacity envelope. The capacity envelopes were calculated using equations developed by Kowalsky and Priestley (2000).

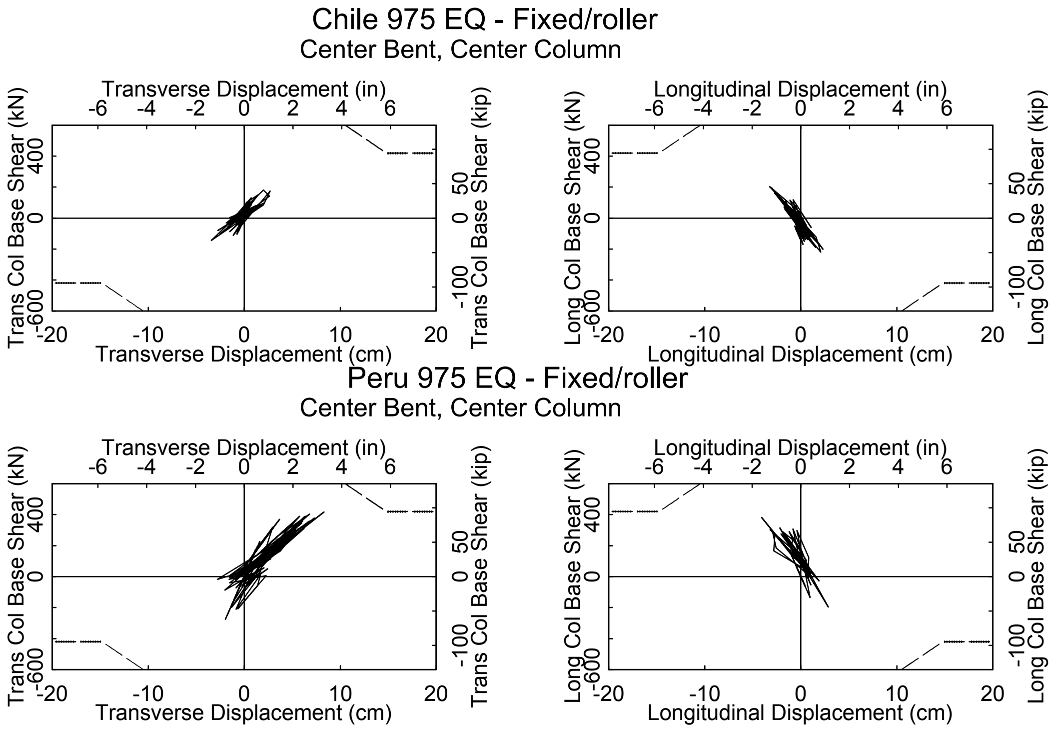

Figure 6.1-1 Center Bent, Center Column: Hysteresis Curves for Bridge 5/227; Chile 975 and Peru 975 EQ; Fixed Column Bases/Roller Abutment Boundary Conditions

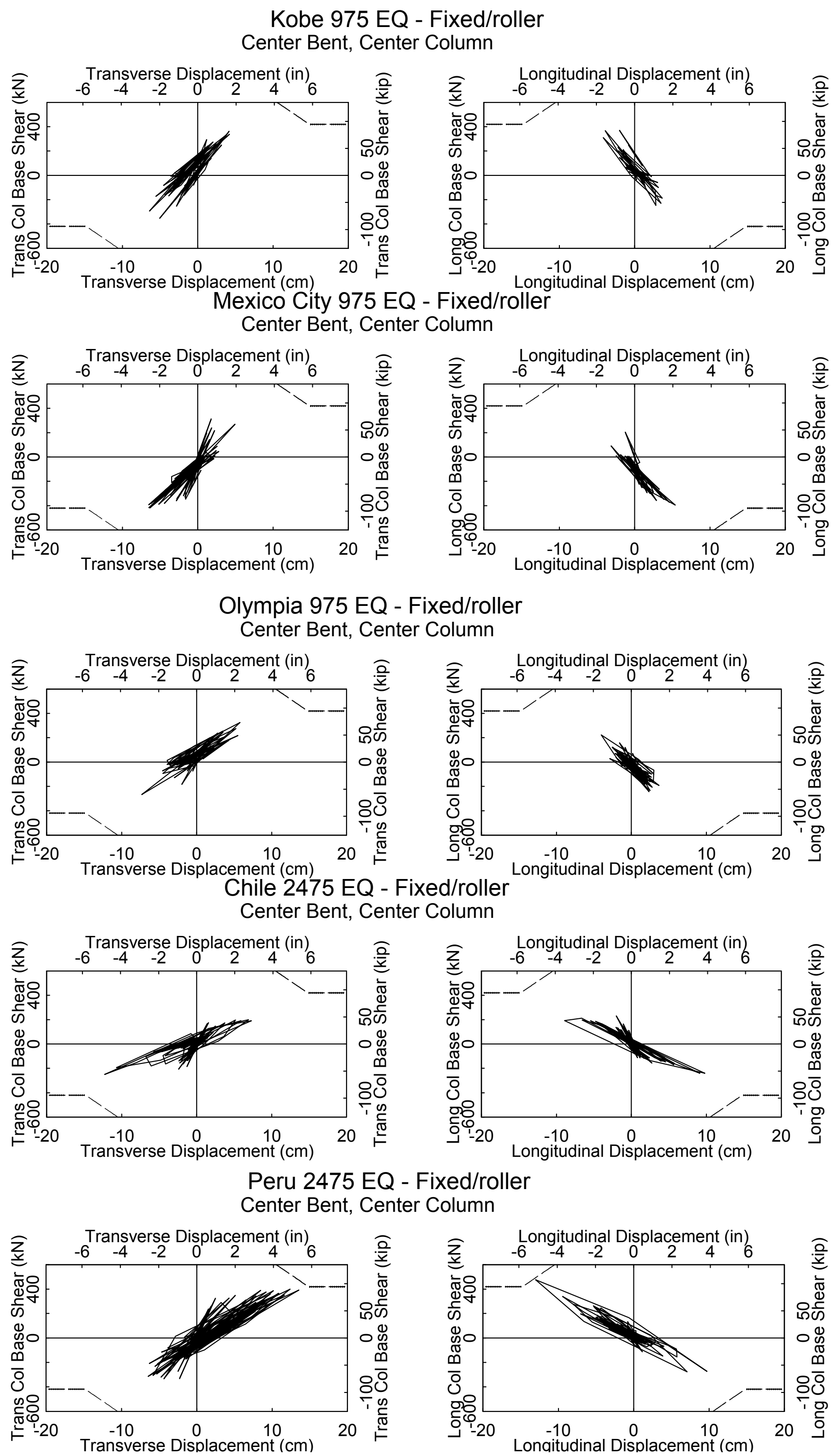

Figure 6.1-2 Center Bent, Center Column: Hysteresis Curves for Bridge 5/227; Kobe 975 EQ, Mexico City 975 EQ; Olympia 975 EQ; Chile 2475 EQ and Peru 2475 EQ; Fixed Column Bases/Roller Abutment Boundary Conditions

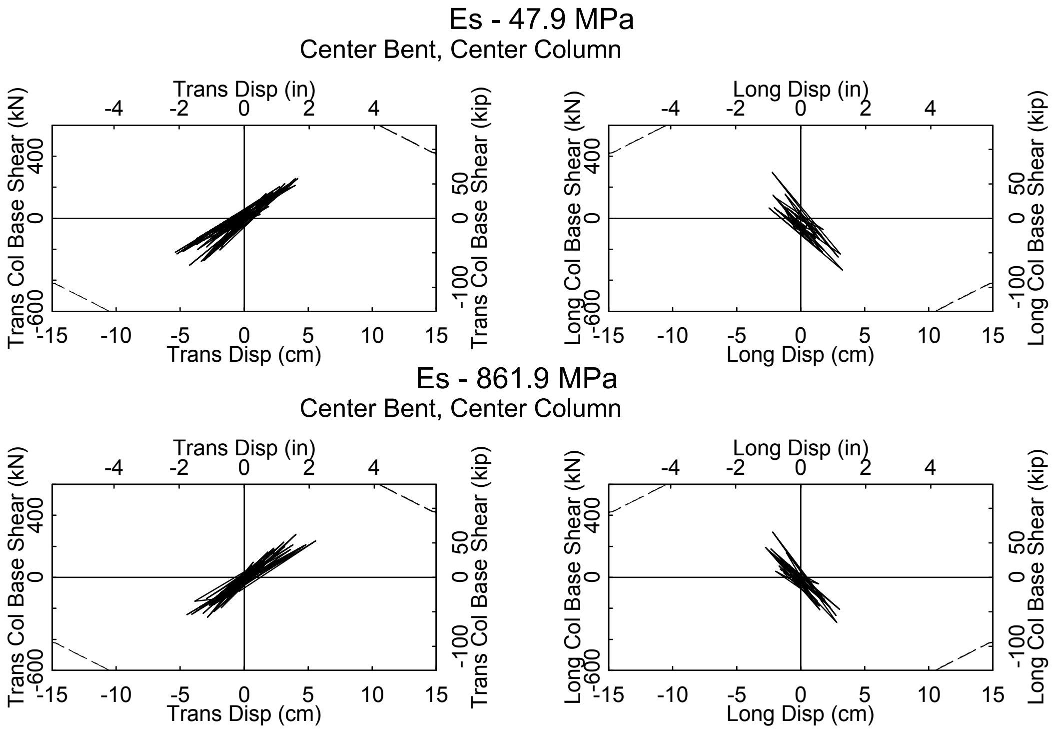

Figure 6.1-3 Center Bent, Center Column: Hysteresis Curves for Bridge 5/227; Kobe 975 EQ; Es=47.9 MPa (1000ksf); 861.9 MPa (18000 ksf)

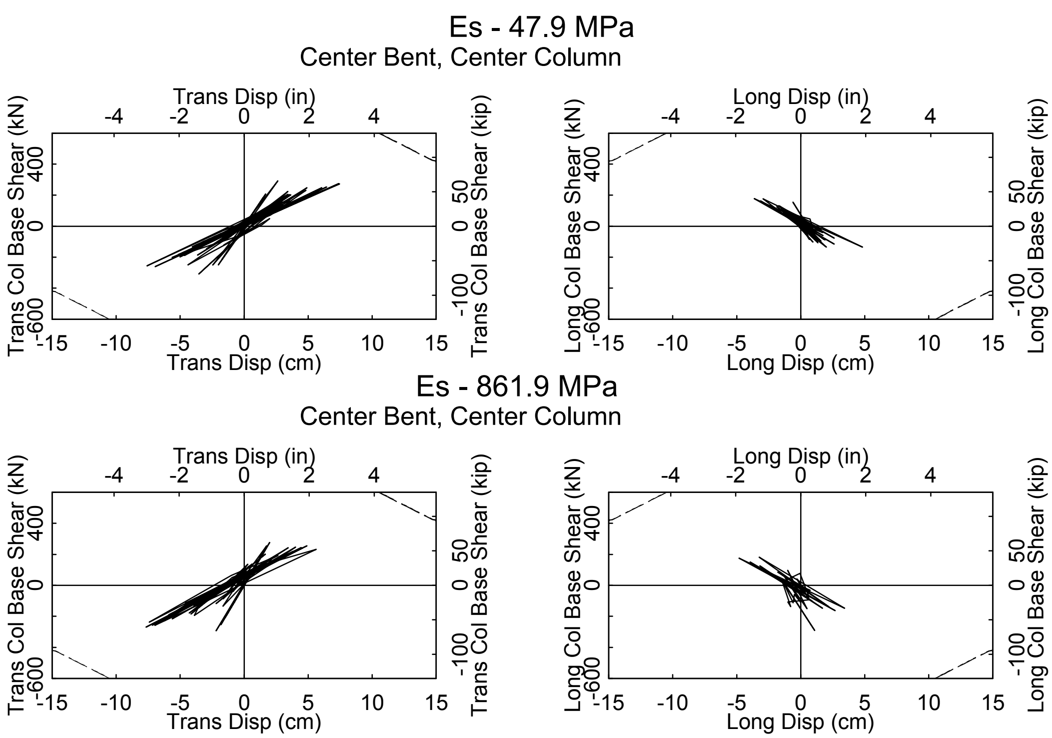

Figure 6.1-4 Center Bent, Center Column: Hysteresis Curves for Bridge 5/227; Mexico City 975 EQ; Es= 47.9 MPa (1000ksf); 861.9 MPa (18000 ksf)

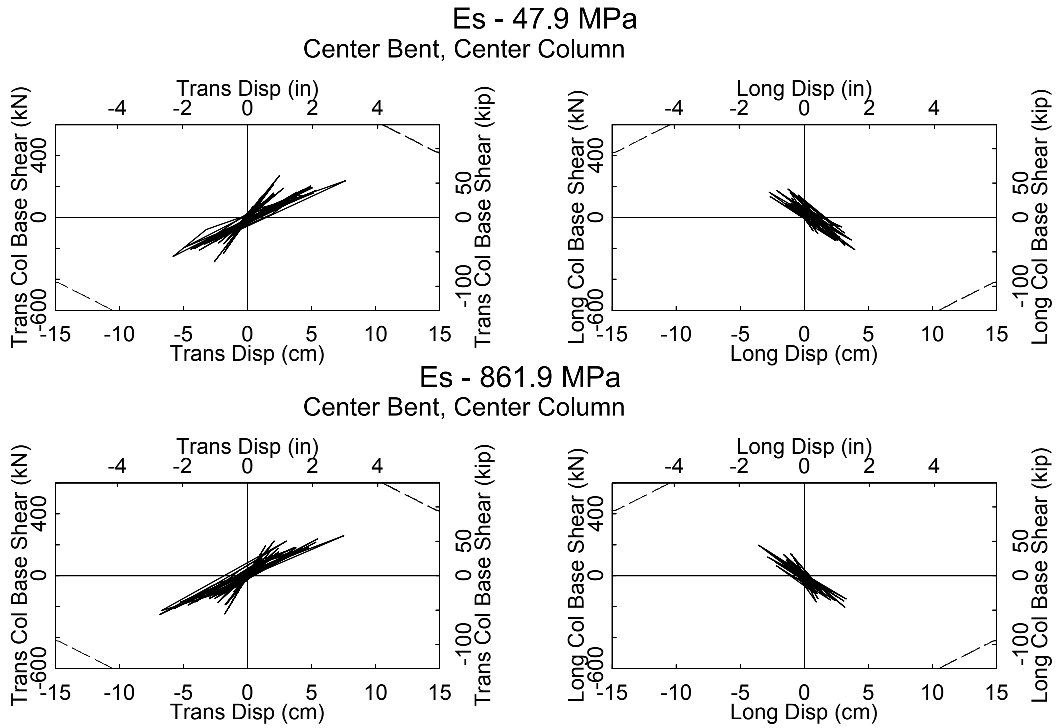

Figure 6.1-5 Center Bent, Center Column: Hysteresis Curves for Bridge 5/227; Olympia 975 EQ; Es=47.9 MPa (1000ksf); 861.9 MPa (18000 ksf)

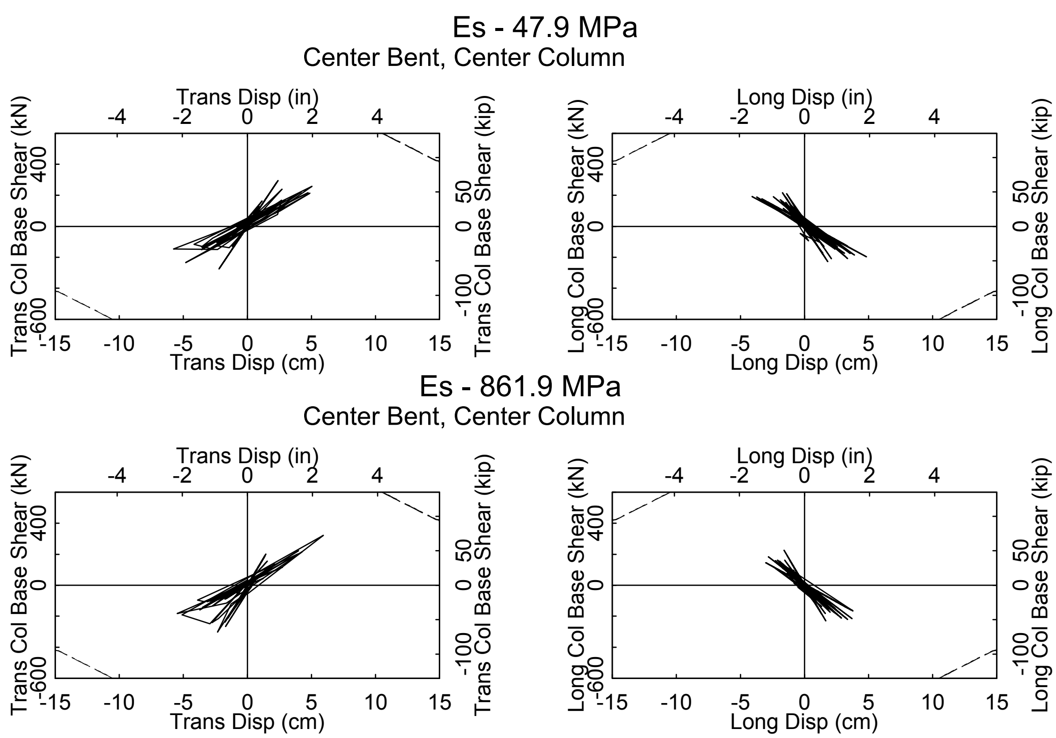

Figure 6.1-6 Center Bent, Center Column: Hysteresis Curves for Bridge 5/227; Chile 2475 EQ; Es=47.9 MPa (1000ksf); 861.9 MPa (18000 ksf)

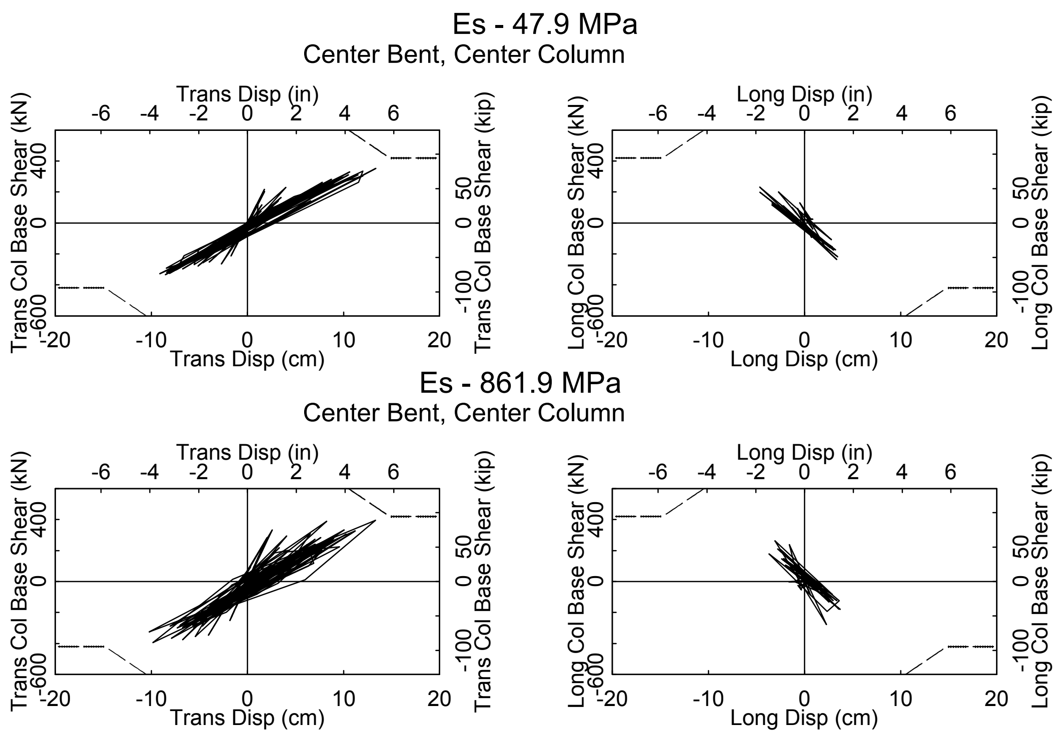

Figure 6.1-7 Center Bent, Center Column: Hysteresis Curves for Bridge 5/227; Peru 2475 EQ; Es=47.9 MPa (1000ksf); 861.9 MPa (18000 ksf)

The overall shape of the hysteresis curves did not vary significantly with the foundation spring stiffness values. The transverse direction of the bridge experienced a higher demand than that of the longitudinal, largely due to the non-monolithic deck. Yielding of the columns tended to occur at a smaller displacement for the fixed-column base/roller-abutment models than for the soil spring models for all excitations. This was due to the spring flexibility at the column base absorbing some of the rotational demand of the column for a given relative displacement demand.

Both the Peru 975 and 2475 earthquakes produce high demands in the center column of the center bent with fixed-column base/roller-abutment boundary conditions, coming relatively close to failing the column. The column almost fails under all three boundary conditions when the bridge is subject to Peru 2475, and comes close to failing for the fixed-base column model, subject to Peru 975.

To estimate the potential damage in the columns, the number of cycles reaching a given ductility was determined and compared to test results obtained by Jaradat (1996). The maximum displacement demands were predicted for the center column of the center bent under the Peru 2475 earthquake. Figures 6.1-8 and 6.1-9 show the displacement time histories for this column with the soil spring boundary conditions.

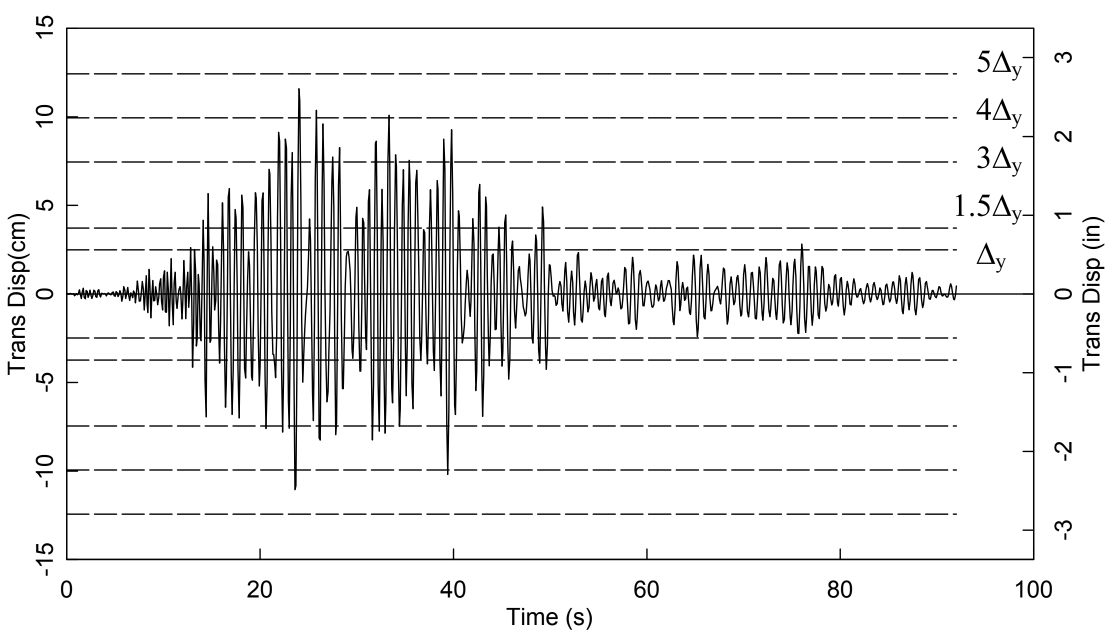

Figure 6.1-8 Center Bent, Center Column: Displacement Time History for Bridge 5/227; Peru 2475 EQ; Es=287.3 MPa

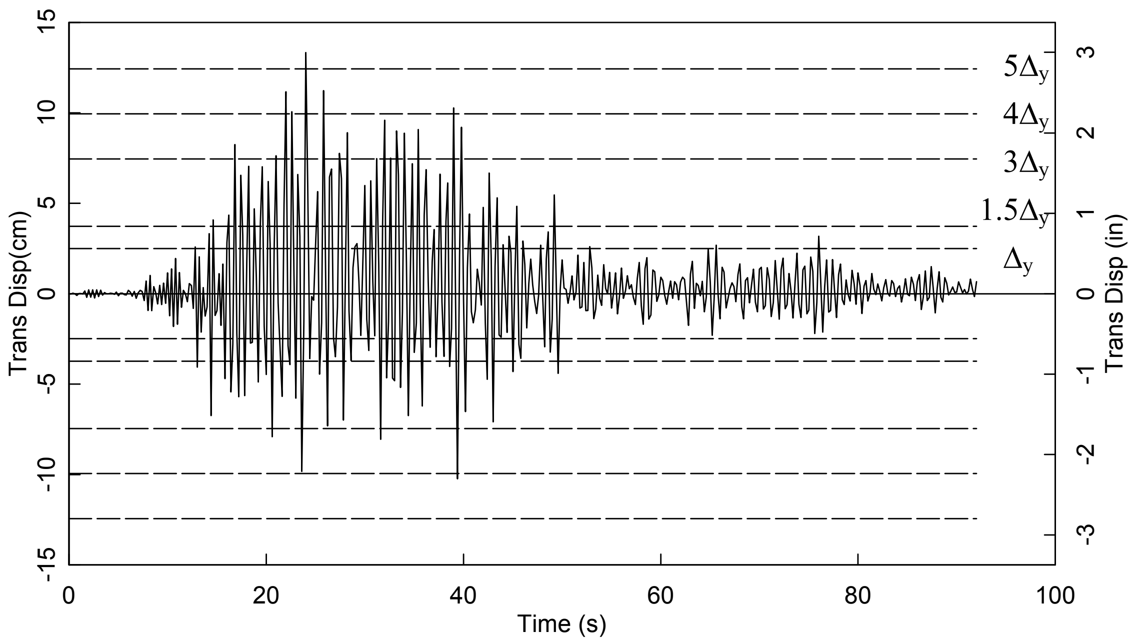

Figure 6.1-9 Center Bent, Center Column: Displacement Time History for Bridge 5/227; Peru 2475 EQ; Es=861.9 MPa

The following damage was observed for Jaradat's test column. At a ductility level of 3 Δ_y, six half-cycles occurred. Vertical cracks in the bottom splice region and circumferential cracks in the top hinging region appeared. After six half-cycles at a ductility level of 4 Δ_y, spalling in both top and bottom hinging regions was observed and after six half-cycles at 5 Δ_y, longitudinal bar buckling in the top hinging region occurred.

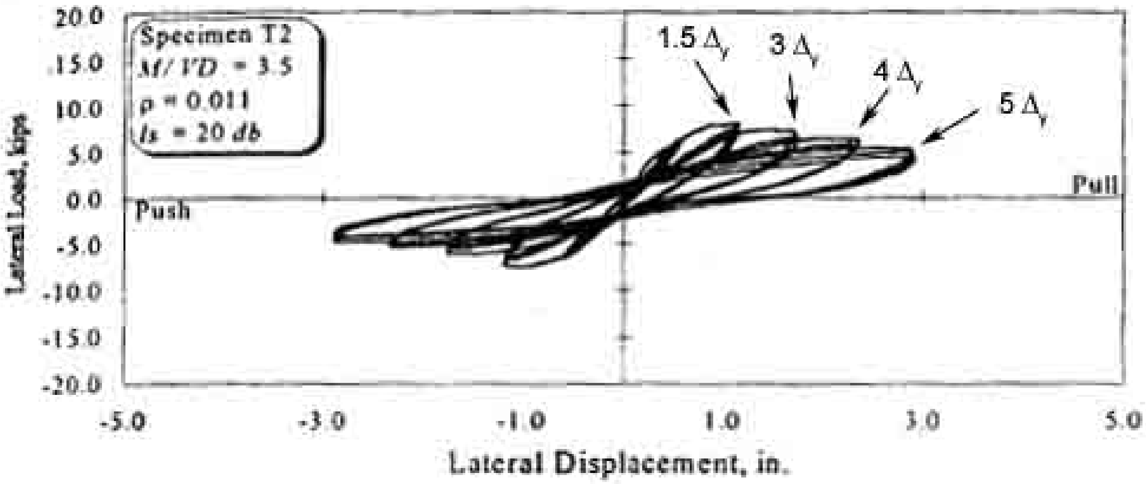

Figure 6.1-10 Specimen T2 Lateral Load-Displacement Hysteresis Curve

Figure 6.1-11 Spalling of the Concrete (Stapelton, 2004)

Figure 6.1-12 Vertical Cracks at Tension Face (Stapelton, 2004)

For the center column of Bridge 5/227, approximately 20 half-cycles occurred at a ductility level of 3 $\Delta_{y,}$ therefore damage in this column can be expected to include large vertical cracks in the bottom splice region and circumferential cracks in the top hinging region. 5 half-cycles at a ductility level of 4 Δ_y would produce moderate spalling in both top and bottom hinging regions. Due to the numerous cycles at 3 Δ_y coupled with the cycles at 4 Δ_y, failure of Bridge 5/227 columns is likely under the Peru 2475 earthquake. Similar damage was predicted for the 861.9 MPa soil elastic modulus model.

The shear force demand in the girders at the abutments was also investigated. Bridge 5/227 has two girder stops at each bent and abutment, resisting displacements in the transverse direction. Due to previous problems with bridge girders, a check was made to determine if the shear forces coming into the girder stops would cause a shear failure in the web of the prestressed I-girders supporting the deck. The results indicated that the shear capacity of the girder webs is approximately 1312 kN (295 kips) and the maximum shear force under Chile 2475 loading was approximately 338 kN (91 kips) in the west abutment for the lowest spring stiffness (Es = 47.9 MPa). The shear force calculations can be found in Appendix 4.

The shear force demand/capacity ratio in the column footings was also investigated. The shear forces in the footing act as a combination of longitudinal and transverse forces, creating a resultant force acting at a given angle depending on the magnitudes of the forces. The shear force demand was studied independently for both directions in this research. The maximum shear demands in the footings for both the longitudinal and transverse directions were extracted from the analyses and can be found in Appendix 4. Longitudinal shear force demands for Bridge 5/227 in the column footings were of 476 kN (107 kips). The footing capacity is 2185 kN (492 kips) or four times higher than the demands. Transverse shear force demands were maximum for a value 417 kN (94 kips) and the capacity in the transverse direction for the footing was 1641 kN (369 kips), sufficient to support the shear forces. However, studies have shown that the joint shear strength was often a cause of brittle failure in the column/footing connection (McLean, 1999). Due to the significantly low shear forces in the column footings, this failure mode was not investigated in this research but should however be taken into consideration as a potential governing failure mode for future studies.

6.2 BRIDGE 512/19

Bridge 512/19 is the largest of all three bridges. It is made of three bents of four columns each, a 77ft long monolithic deck, and it rests on spread footings without piles. The analysis showed that the two center columns were subjected to the most demands, the results will therefore concentrate on those two columns. Table 6.2-1 presents the maximum values obtained in the analysis:

Table 6.2-1 Maximum Earthquake demands for Bridge 512/19 Subject to the Olympia 975 Loading

Bent	512 - O - 283.7	512 - O - 861.9	512 - O - fixed
Max Δ (cm)			
North - East	8.06	8.01	9.60
North - Middle East	6.61	6.53	7.91
North - Middle West	6.09	6.14	8.14
North - West	7.26	7.09	9.65
Center - East	9.10	9.43	9.87
Center - Middle East	9.13	9.42	9.84
Center - Middle West	9.16	9.41	9.81
Center - West	9.20	9.40	9.78
South - East	7.26	7.13	9.57
South - Middle East	6.08	6.16	8.07
South - Middle West	6.22	6.49	7.92
South - West	7.74	8.05	9.70
Max V (kN)			
North - East	219	230	253
North - Middle East	198	230	305
North - Middle West	219	215	397
North - West	222	372	257
Center - East	241	239	227
Center - Middle East	238	244	229
Center - Middle West	250	243	227
Center - West	239	235	228
South - East	234	331	268
South - Middle East	211	215	253
South - Middle West	205	211	352
South - West	212	265	253

The maximum displacements were found at the center bent, center columns. The displacements were similar for the two spring models and increased for the fixed column base model (maximum increase of 30%). There was a slight increase in shear force demands between the 287.3 MPa soil modulus model and the fixed column base/roller abutment model, for the south bent, middle-east column.

Table 6.2-2 Maximum Earthquake Demands for Bridge 512/19 Subject to the Peru 2475 Loading

Bent	512 - P - 283.7	512 - P - 861.9	512 - P - fixed
Max Δ (cm)			
North - East	15.07	14.24	22.19
North - Middle East	14.04	12.51	19.73
North - Middle West	13.02	12.04	17.30
North - West	15.60	14.88	16.88
Center - East	19.19	18.59	20.50
Center - Middle East	19.17	18.58	20.53
Center - Middle West	19.15	18.58	20.56
Center - West	19.12	18.57	20.58
South - East	15.35	14.63	16.83
South - Middle East	12.95	11.70	17.23
South - Middle West	14.06	12.47	19.72
South - West	15.18	13.93	22.24
Max V (kN)			
North - East	359	334	450
North - Middle East	338	304	423
North - Middle West	352	334	370
North - West	409	375	350
Center - East	366	393	420
Center - Middle East	395	360	423
Center - Middle West	428	398	419
Center - West	418	372	421
South - East	416	305	352
South - Middle East	509	263	389
South - Middle West	400	306	419
South - West	380	322	434

Bridge 512/19 behaved similarly under Peru 2475 but with larger demands. Displacements were maximum in the center bent for all three models. The largest increase (approximately 45%) in displacement occurred at the north and south bents, between the 287.3 MPa model and the fixed columns base/roller abutment model. There was a moderate increase in the shear force demands (25%) between the lowest spring model and fixed column base model. Pounding of the deck at the abutments was not an issue for this bridge. The hysteresis curves for Bridge 512/19 spring and fixed column base models under Chile 975, Peru 975, Kobe 975, Mexico City 975, Olympia 975, Chile 2475 and Peru 2475 can be found in figures 6.2-2 through 6.2-10 .

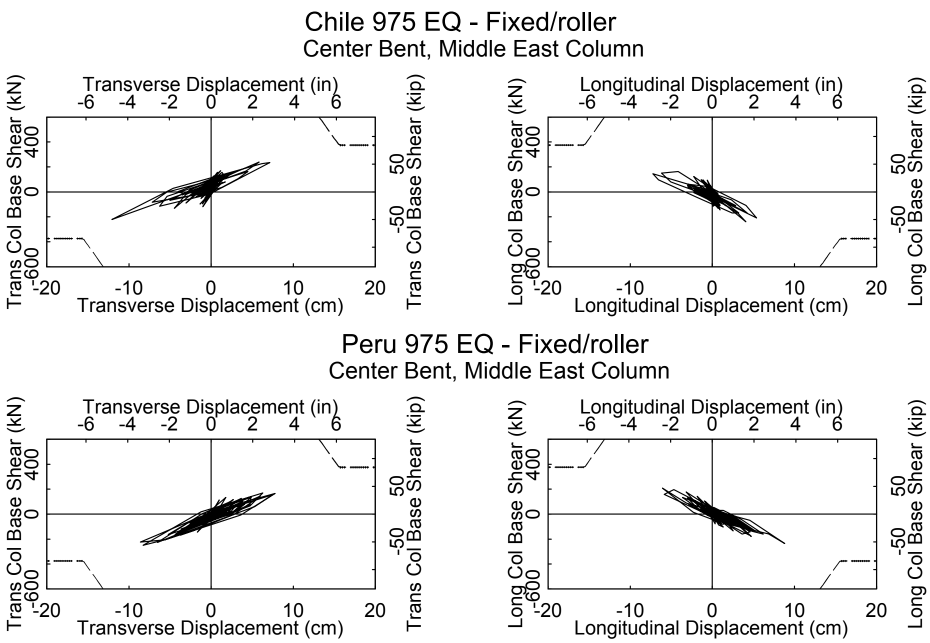

Figure 6.2-1 Center Bent, Middle East Column: Hysteresis Curves for Bridge 512/19; Chile 975 EQ and Peru 975 EQ; Fixed Column Base/Roller Abutment Boundary Conditions

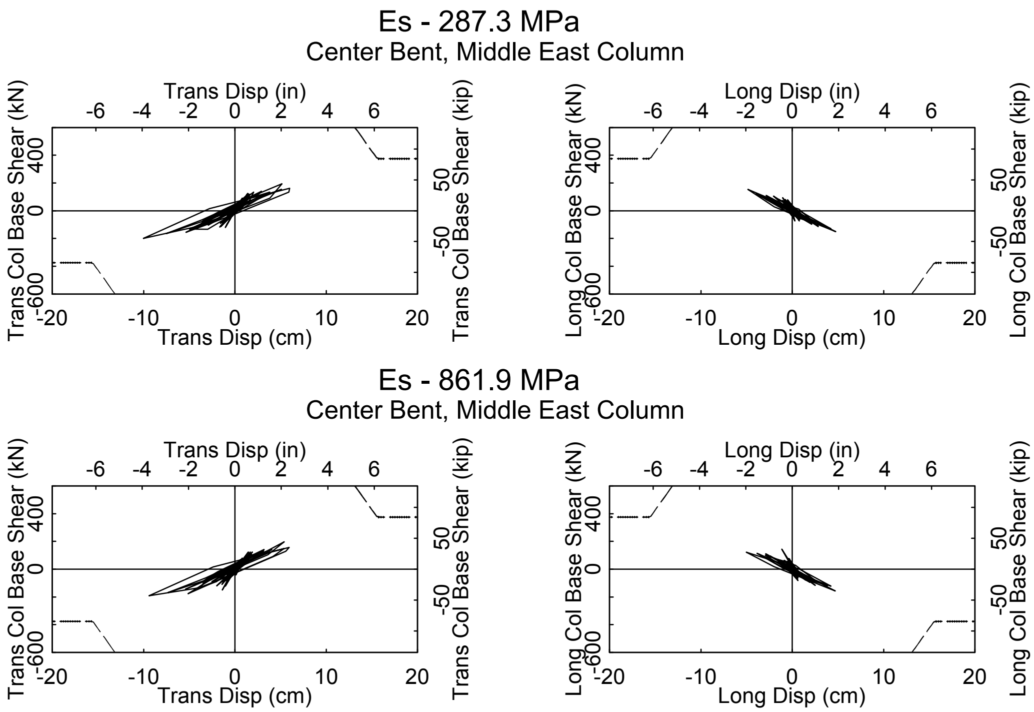

Figure 6.2-2 Center Bent, Middle East Column: Hysteresis Curves for Bridge 512/19; Chile 975 EQ; Es=47.9 MN/m^2 (1000ksf); 861.9 MN/m^2 (18000 ksf)

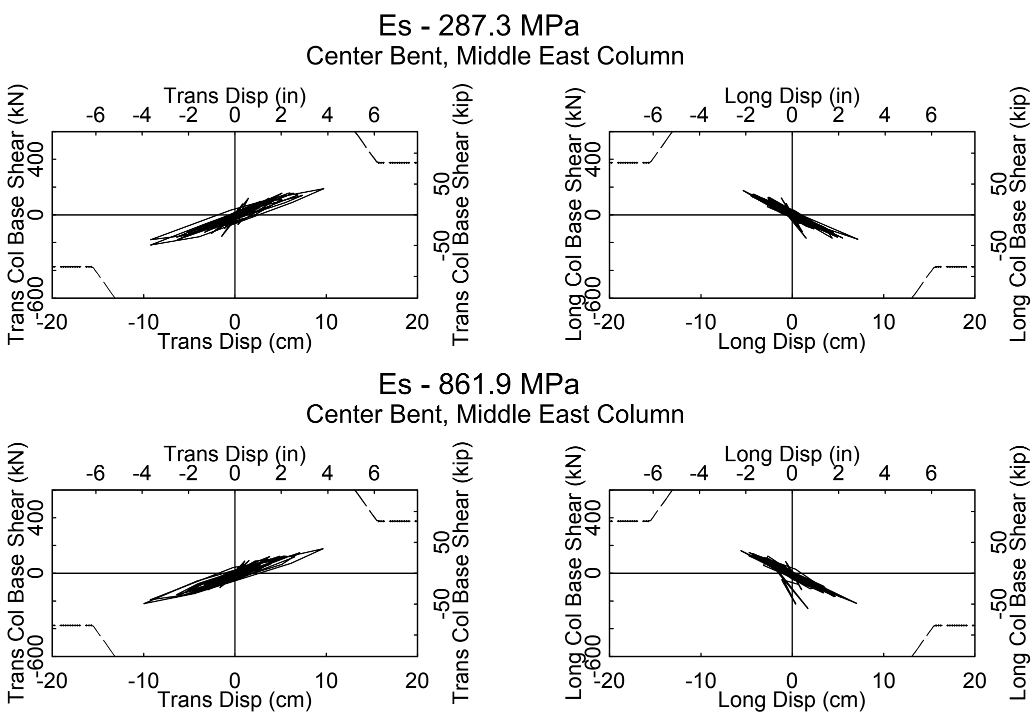

Figure 6.2-3 Center Bent, Middle East Column: Hysteresis Curves for Bridge 512/19; Peru 975 EQ; Es=47.9 MN/m^2 (1000ksf); 861.9 MN/m^2 (18000 ksf)

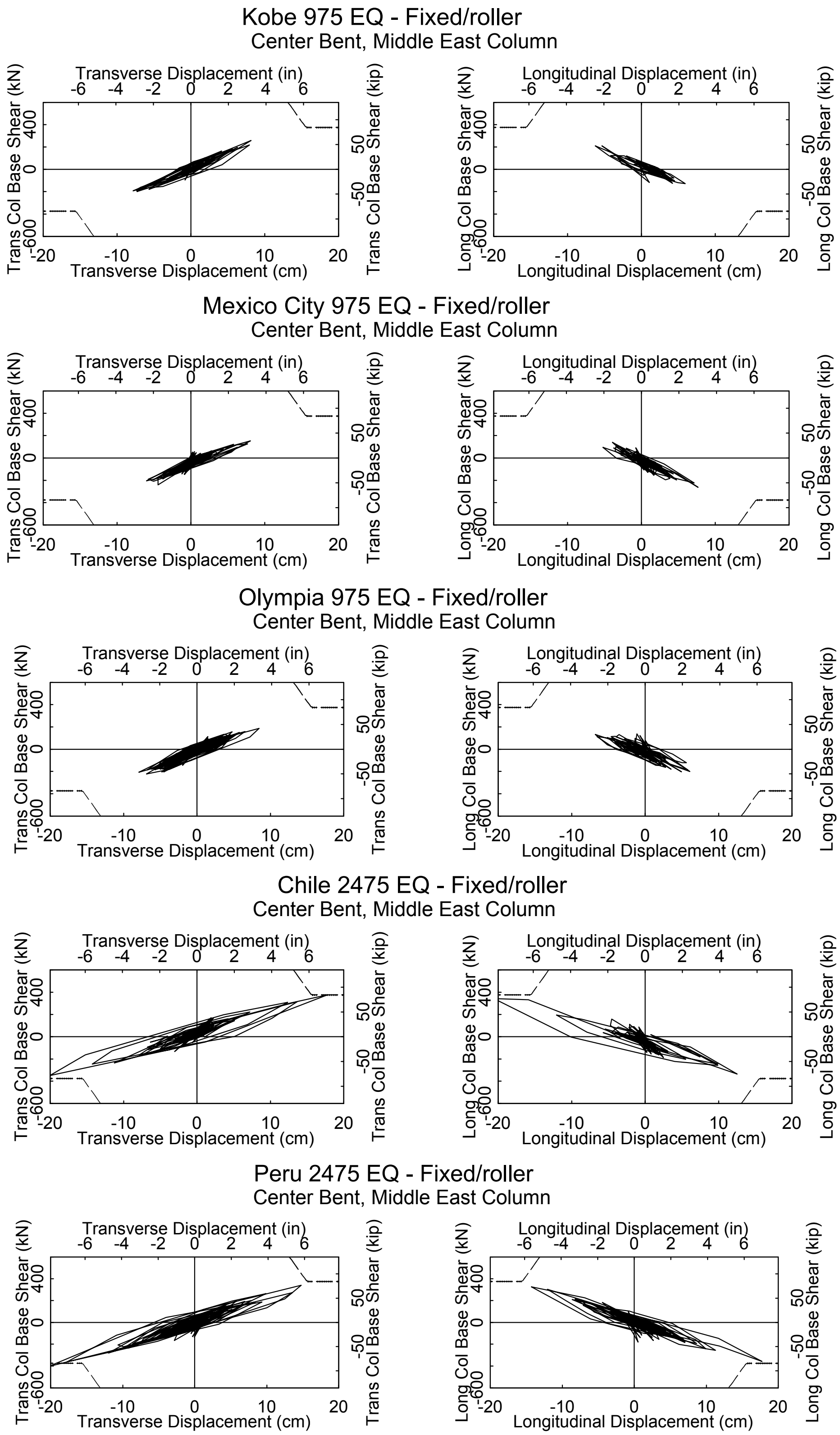

Figure 6.2-4 Center Bent, Middle East Column: Hysteresis Curves for Bridge 512/19; Kobe 975 EQ, Mexico City 975 EQ, Olympia 975 EQ, Chile 2475 EQ and Peru 2475 EQ; Fixed Column Base/Roller Abutment Boundary Conditions

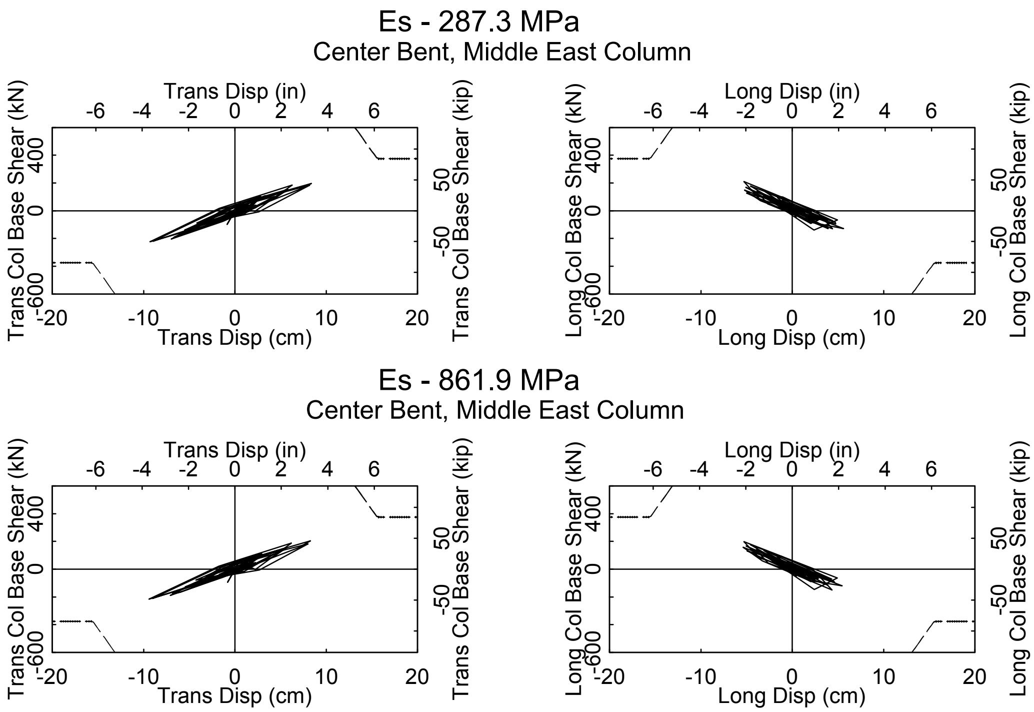

Figure 6.2-5 Center Bent, Middle East Column: Hysteresis Curves for Bridge 512/19; Kobe 975 EQ; Es=287.3 MN/m^2 (6000 ksf); 861.9 MN/m^2 (18000 ksf)

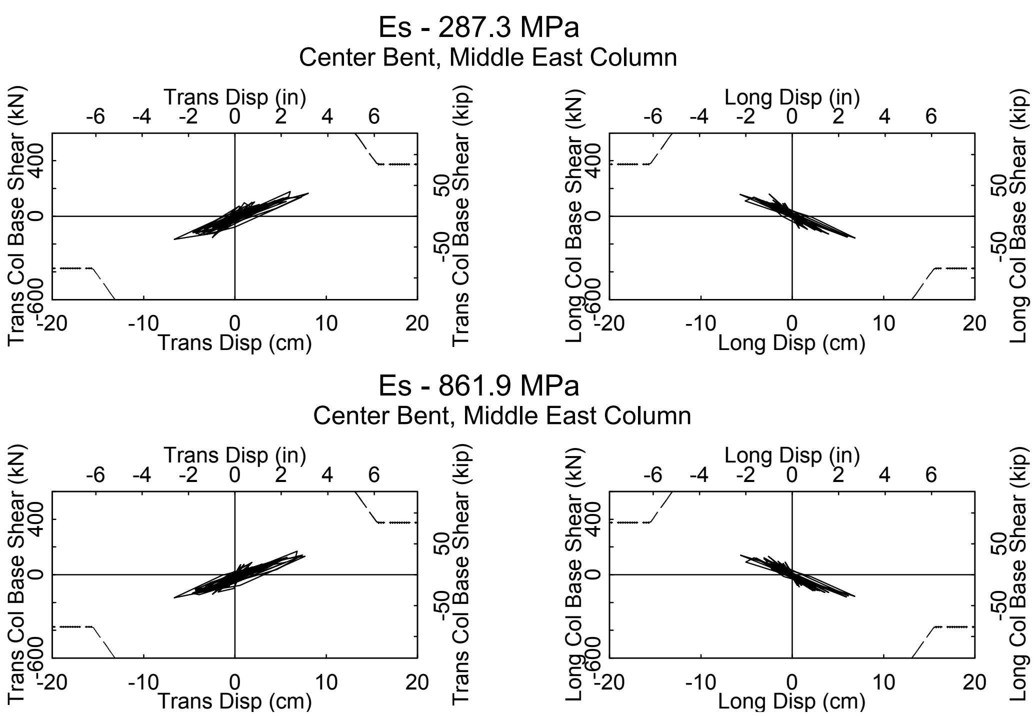

Figure 6.2-6 Center Bent, Middle East Column: Hysteresis Curves for Bridge 512/19; Mexico City 975 EQ; Es=287.3 MPa (6000 ksf); 861.9 MPa (18000 ksf)

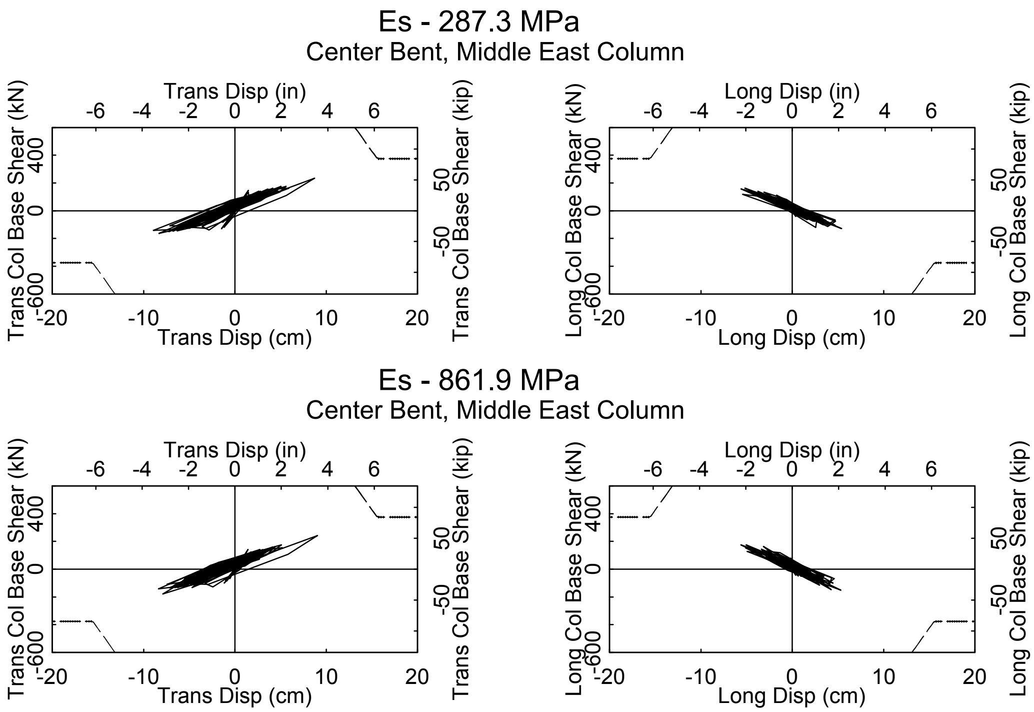

Figure 6.2-7 Center Bent, Middle East Column: Hysteresis Curves for Bridge 512/19; Olympia 975 EQ; Es=287.3 MN/m^2 (6000 ksf); 861.89 MN/m^2 (18000 ksf)

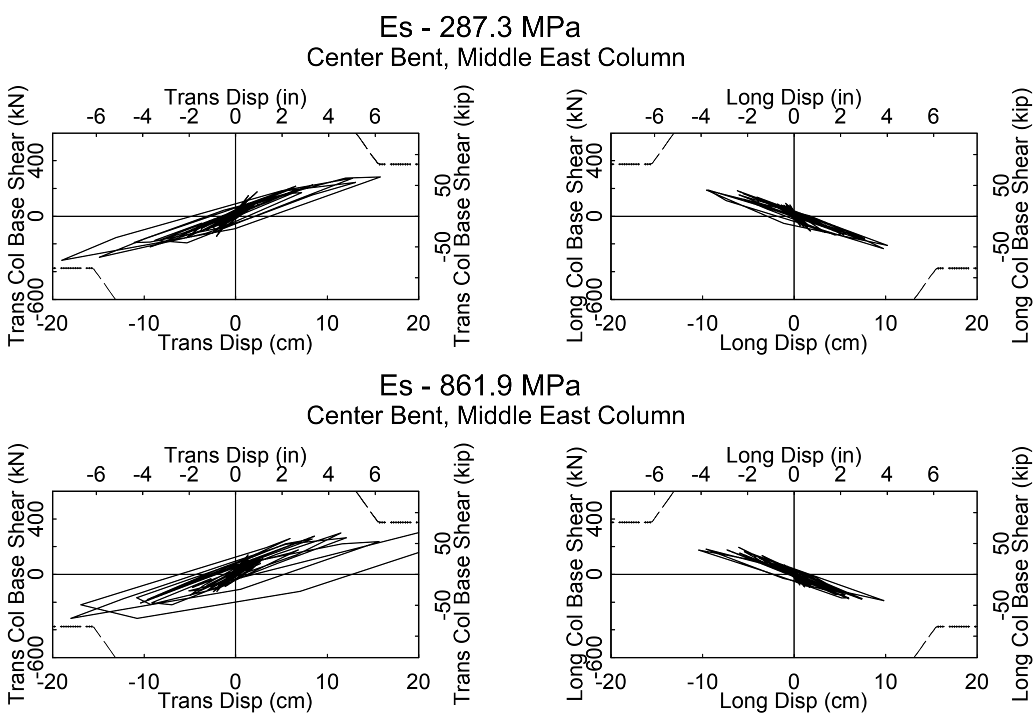

Figure 6.2-8 Center Bent, Middle East Column: Hysteresis Curves for Bridge 512/19; Chile 2475 EQ; Es=287.3 MN/m^2 (6000 ksf); 861.9 MN/m^2 (18000 ksf)

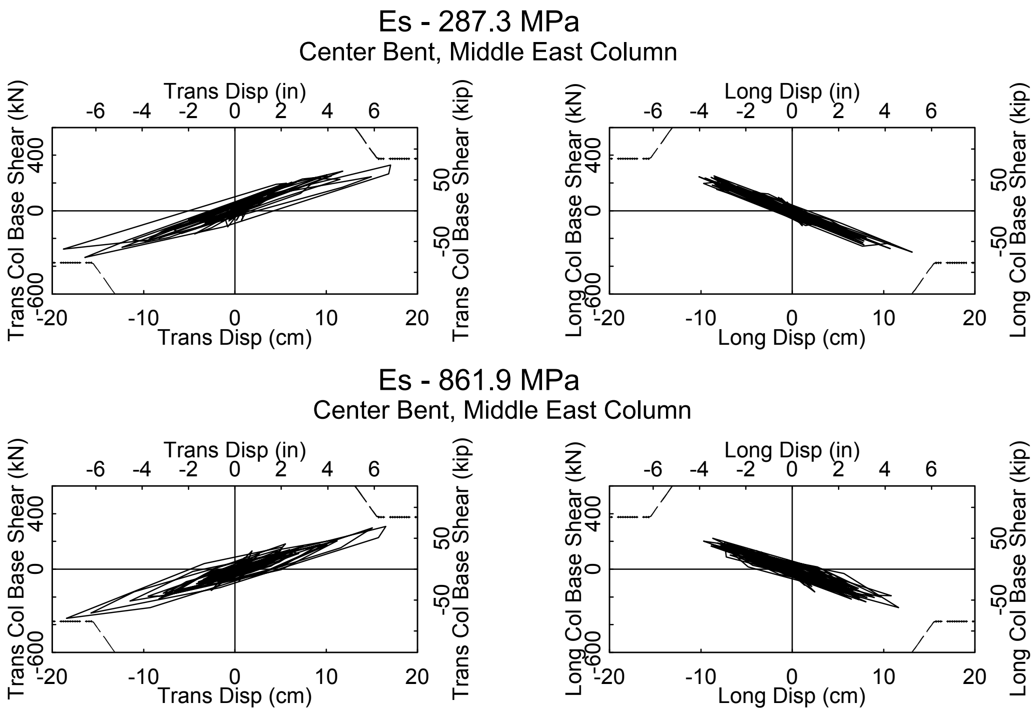

Figure 6.2-9 Center Bent, Middle East Column: Hysteresis Curves for Bridge 512/19; Peru 2475 EQ; Es=287.3 MN/m^2 (6000 ksf); 861.9 Pa (18000 ksf)

The column shear in the transverse direction comes very close to failure under Peru 2475 and Chile 2475 for all three stiffness values. The general shape of the hysteresis curves was not affected by the variation in spring values. Bridge 512/19's middle-east column of the center bent fails in shear under Peru 2475 and comes close to failing under Chile 2475 and Peru 975 for all boundary conditions.

As for Bridge 227, the damage in the columns was estimated based on Jaradat's (1996) test results. The maximum demands were predicted for the center bent, middle-east column under the Peru 2475 for all spring models. Below are presented the displacement time-histories for both soil spring boundary conditions under the Peru 2475 earthquake.

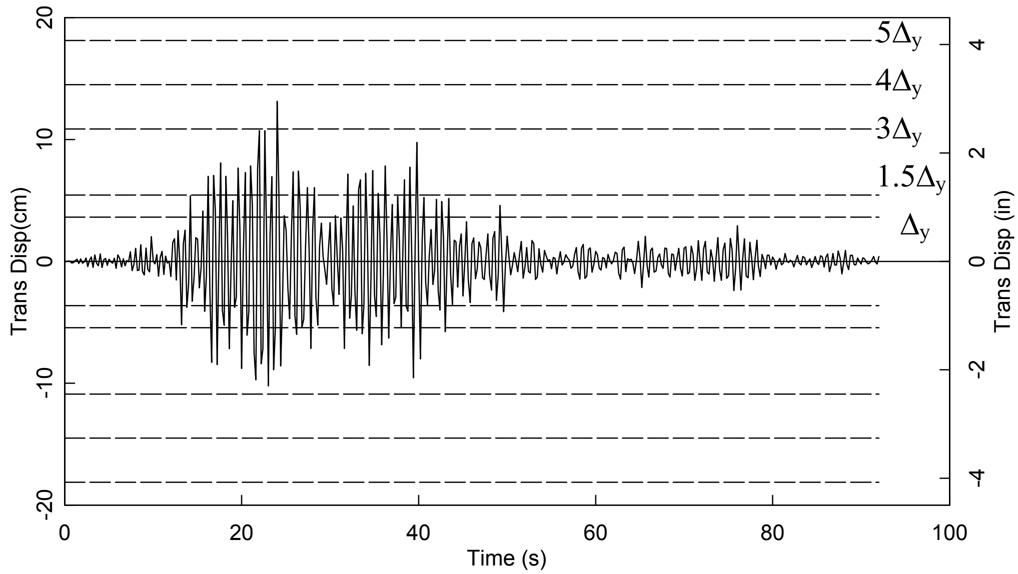

Figure 6.2-10 Center Bent, Middle East Column: Displacement Time History for Bridge 512/19; Peru 2475 EQ; Es=287.3 MPa

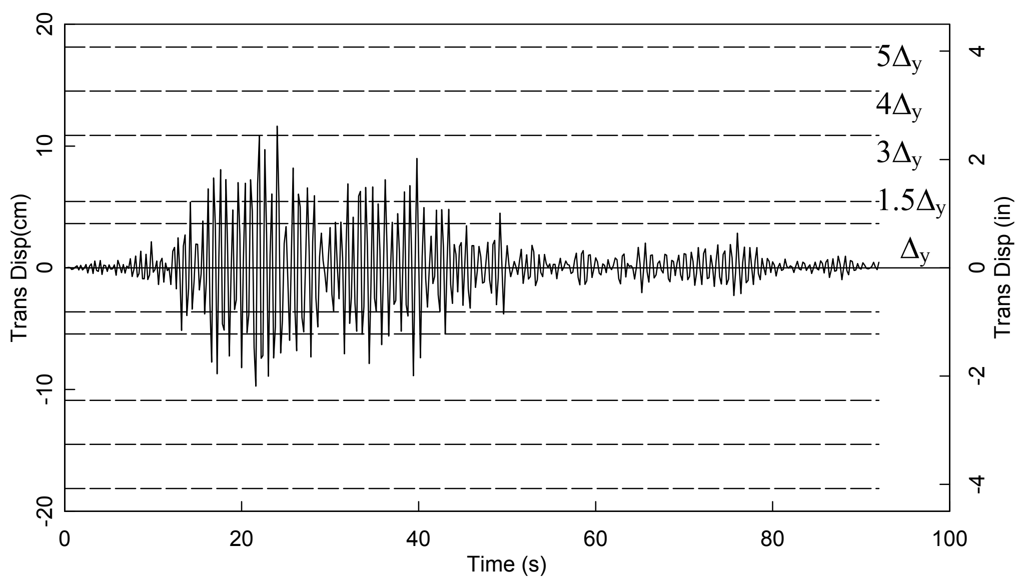

Figure 6.2-11 Center Bent, Middle East Column: Displacement Time History for Bridge 512/19; Peru 2475 EQ; Es=861.9 MPa

The soft soil spring model time history shows that one half-cycle nearly reaches a ductility level of 4 Δ_y, while a few half cycles nearly reach 3 Δ_y. Damage in the columns can be expected to include vertical cracks and spalling in the hinging regions. Due to the small number of high ductility demand cycles, damage can be expected to be lighter than for Bridge 227. However, the proximity of the force/displacement hysteresis curves to the column shear capacity envelope highlights the probability of column failure.

Shear in the prestressed I-girders was investigated for Bridge 512/19. Four girder stops were constructed on each abutment, two in each direction. The shear capacity of the girder webs was 2096 kN (451 kips). The maximum shear force was at the north abutment under the Peru 2475 earthquake loading and was 1372 kN (308 kips) per girder stop. The shear in the footings was the highest in the fixed condition model under the Peru 2475 earthquake loading. The maximum value was approximately 404 kN (91 kips) in the transverse direction and 365 kN (82 kips) in the longitudinal direction. The shear capacity of the footing was calculated at 972 kN (219 kips), more than twice the highest shear demand. Shear failure in the girder webs and at the column footings is not an issue for Bridge 512/19. The shear demand calculations are detailed in Appendix 4. As for Bridge 227, the shear force demands in the column footings were low enough that column/footing joint failure was not studied.

The previous analyses show that spring values have a significant effect on the displacements in the bridge. The fixed column base model creates the highest shear and displacements demands for all earthquake loadings. Under the Peru 2475 and Chile 2475 earthquakes, Bridge 512/19 column hysteresis demands come to close to or exceed the shear failure envelope for all three spring models. The three 975-year return earthquakes, Olympia, Kobe and Mexico City, produced similar hysteresis responses, with Mexico City having slightly lower displacement demands than the other two.

6.3 BRIDGE 5/649

Bridge 5/649 has a 74.7 m (245 ft) long non-monolithic deck, two bents with three columns per bent, resting on spread footings supported by timber piles. It was determined in chapter four that the skew had a significant effect on the behavior of the bridge and could not be neglected in the modeling process. The following maximum demands were obtained during the analysis of Bridge 5/649.

Table 6.3-1 Maximum Earthquake demands for Bridge 5/649 Subject to the Olympia 975 Loading

Bent	649 - O - 283.7	649 - O - 861.9	649 - O - fixed
Max Δ (cm)			
North - East	8.24	8.92	8.02
North - Center	7.38	7.49	8.02
North - West	7.33	7.35	8.02
South - East	8.28	8.55	10.05
South - Center	8.27	8.27	10.05
South - West	8.26	8.17	10.06
Max V (kN)			
North - East	271	272	331
North - Center	200	205	245
North - West	323	455	404
South - East	282	298	333
South - Center	170	225	263
South - West	315	316	402

The displacement demands slightly varied with the increase of stiffness, the highest variation occurring between the 287.3 MPa elastic modulus value model and the fixed model for the east column of the south bent (+22% or +1.8 cm, 0.71 in). The shear demands followed the same trend as the displacements. A significant 82 % increase was found in the longitudinal shear demands between the spring values for the east column of the south bent. However, in all other columns for all three models, the variation was not significant under the Olympia 975 earthquake.

Table 6.3-2 Maximum Earthquake demands for Bridge 5/649 Subject to the Peru 2475 Loading

Bent	649 - P - 283.7	649 - P - 861.9	649 - P - fixed
Max Δ (cm)			
North - East	17.70	18.48	20.17
North - Center	17.54	17.37	20.08
North - West	17.41	16.61	19.99
South - East	16.46	17.14	22.32
South - Center	17.32	16.58	22.25
South - West	18.22	17.11	22.20
Max V (kN)			
North - East	522	537	715
North - Center	455	552	755
North - West	584	634	836
South - East	389	421	584
South - Center	377	420	613
South - West	509	487	759

The displacement demands under the Peru 2475 loading follows the same trends as for the Olympia 975 loading. There were small variations between the two spring models. The displacements increased by a maximum of 35% between the lowest spring model and the fixed column base model at the south bent, east column. Shear forces were highest for the columns that were fixed at the base, with an average increase of 60% between the spring soil conditions and the fixed column base/roller abutment boundary condition models.

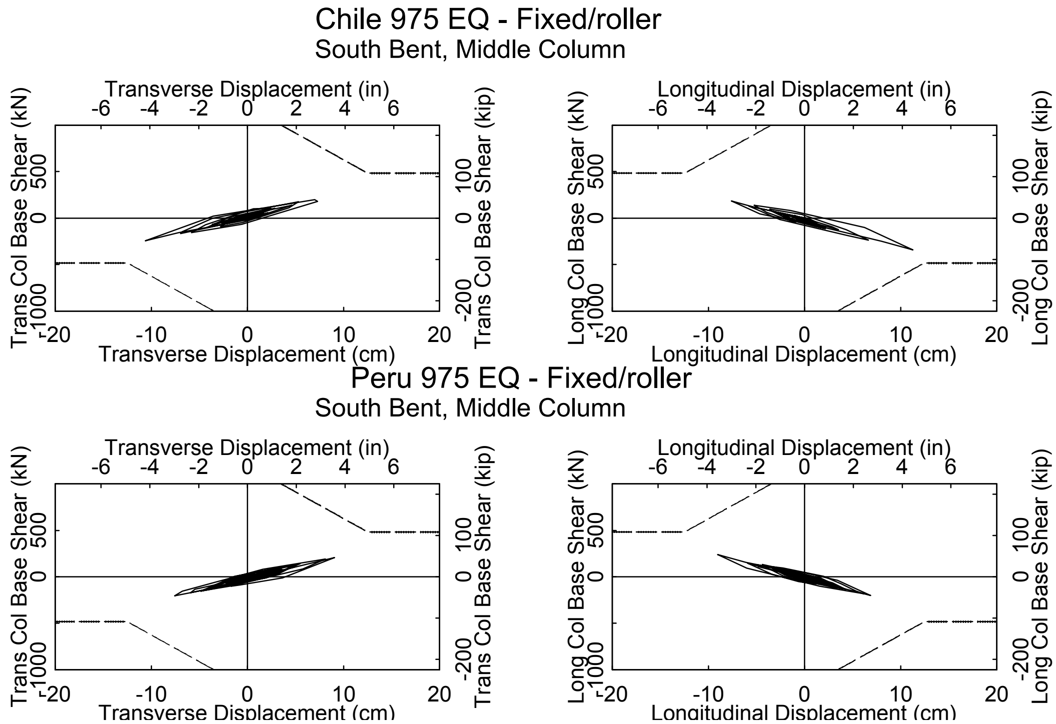

Figure 6.3-1 South Bent, Center Column: Hysteresis Curves for Bridge 5/649 E; Chile 975 EQ, Peru 975 EQ; Fixed Column Bases/Roller Abutment Boundary Conditions

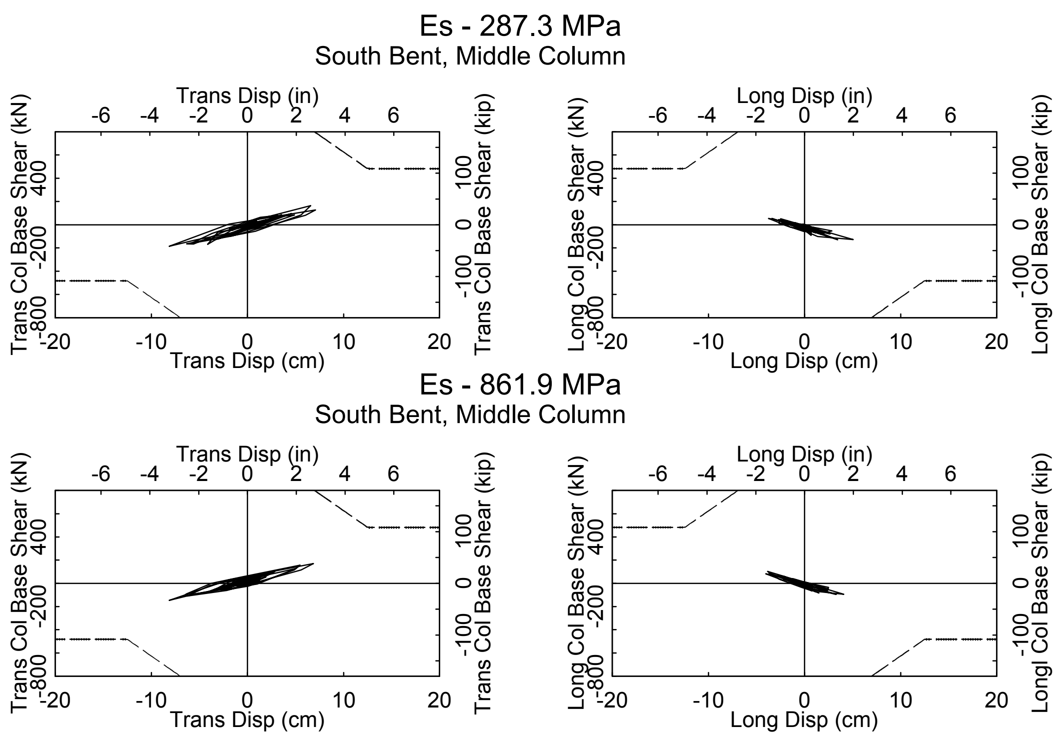

Figure 6.3-2 South Bent, Center Column: Hysteresis Curves for Bridge 5/649E; Chile 975 EQ; Es=287.3 MPa (6000 ksf); 861.9 MPa (18000 ksf)

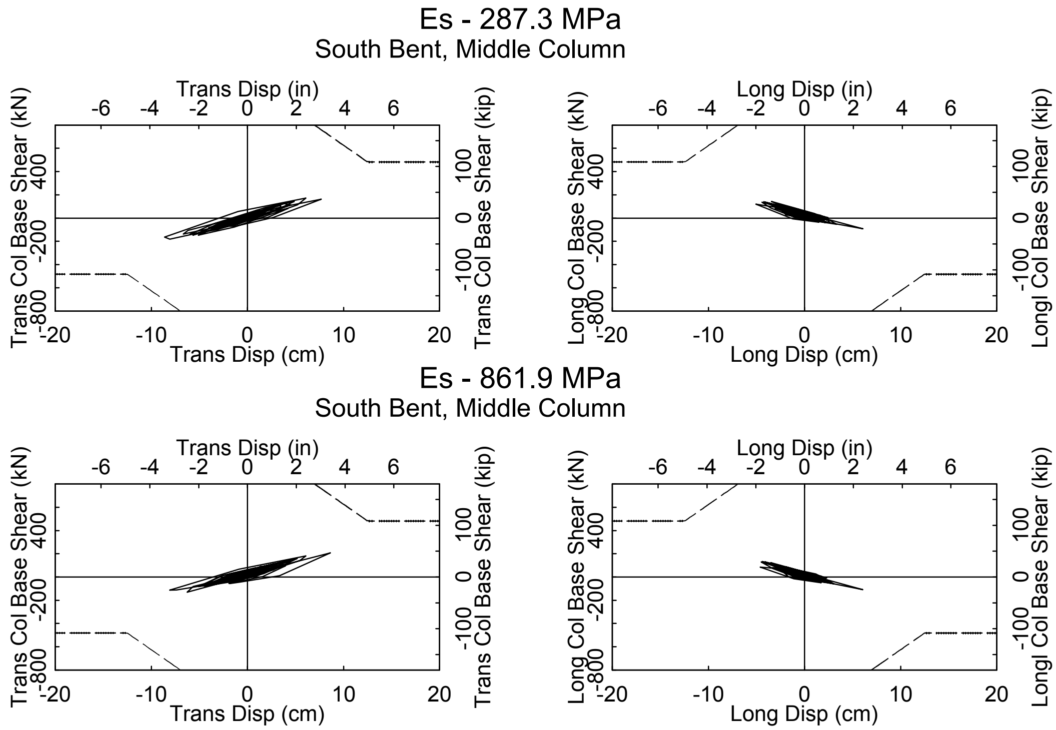

Figure 6.3-3 South Bent, Center Column: Hysteresis Curves for Bridge 5/649E; Peru 975 EQ; Es=287.3 MPa (6000 ksf); 861.9 MPa (18000 ksf)

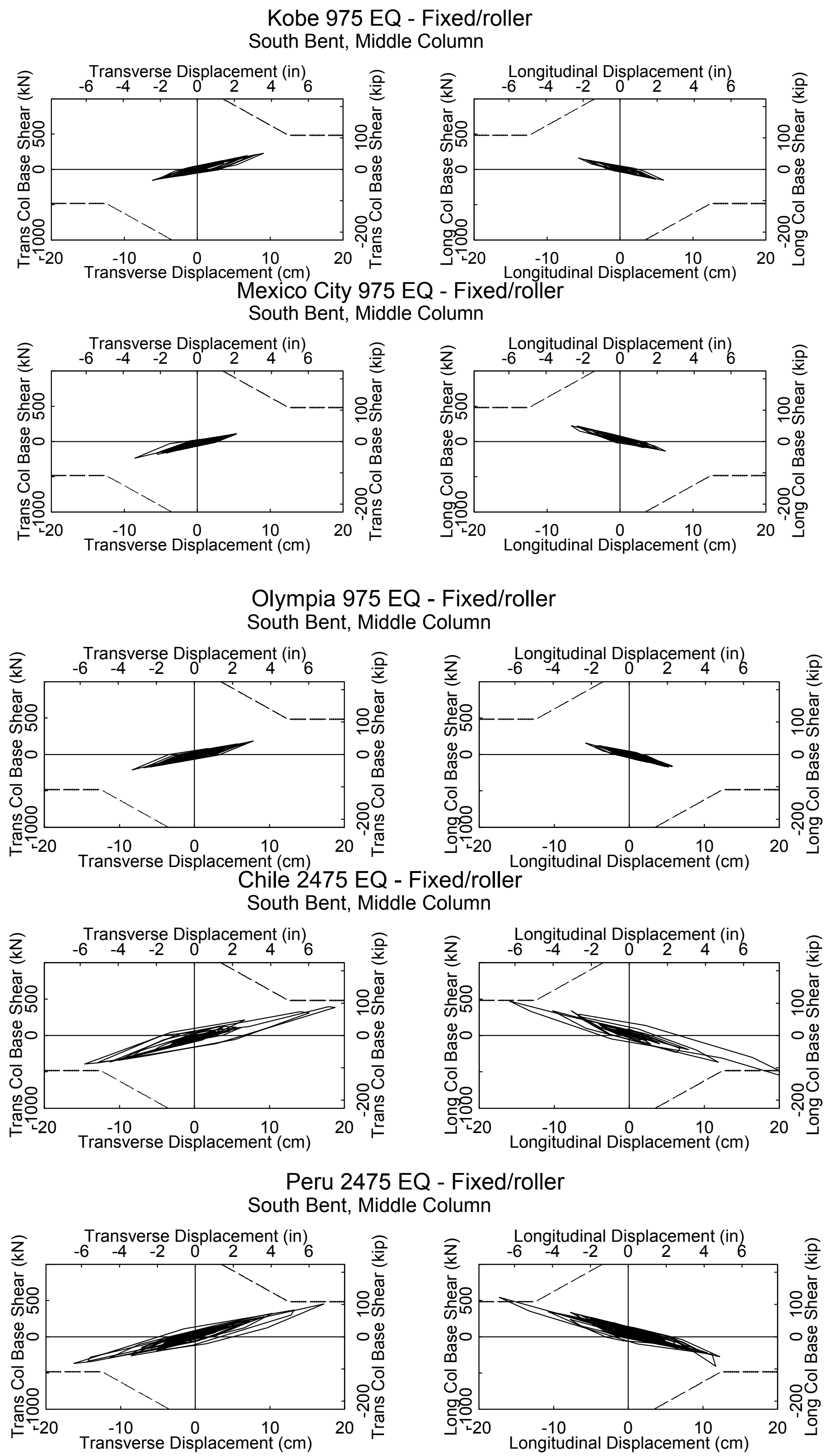

Figure 6.3-4 South Bent, Center Column: Hysteresis Curves for Bridge 5/649 E; Kobe 975 EQ, Mexico City 975 EQ, Olympia 975 EQ, Chile 2475 EQ and Peru 2475 EQ; Fixed Column Base/Roller Abutment Boundary Conditions

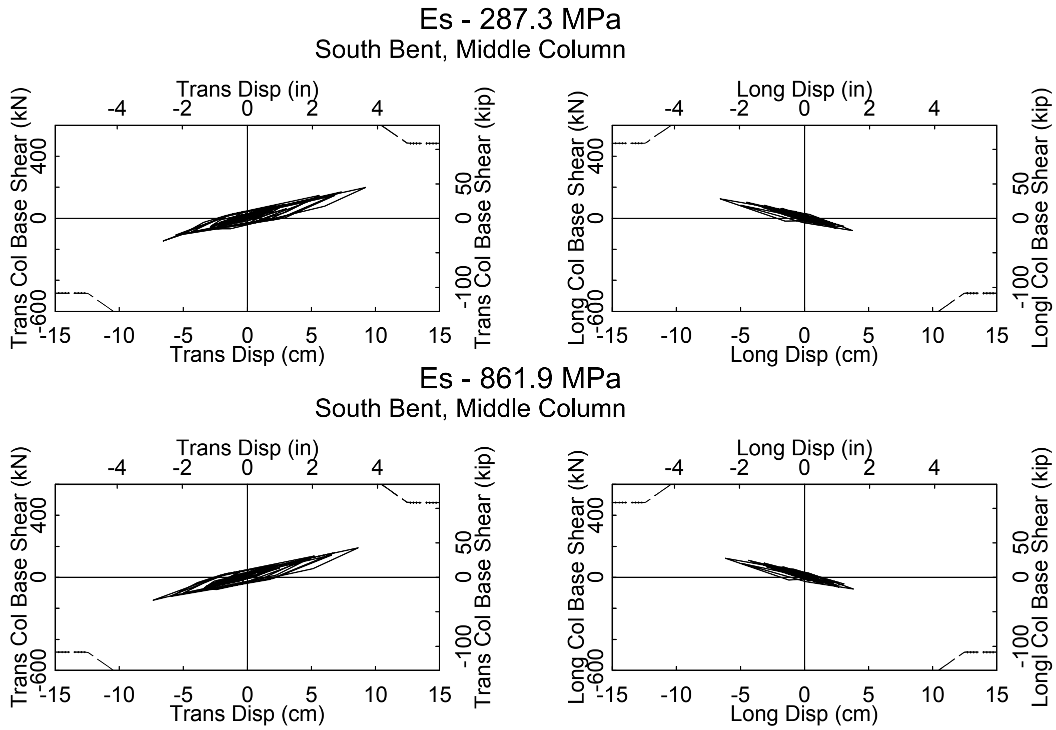

Figure 6.3-5 South Bent, Center Column: Hysteresis Curves for Bridge 5/649E; Kobe 975 EQ; Es=287.3 MPa (6000 ksf); 861.9 MPa (18000 ksf)

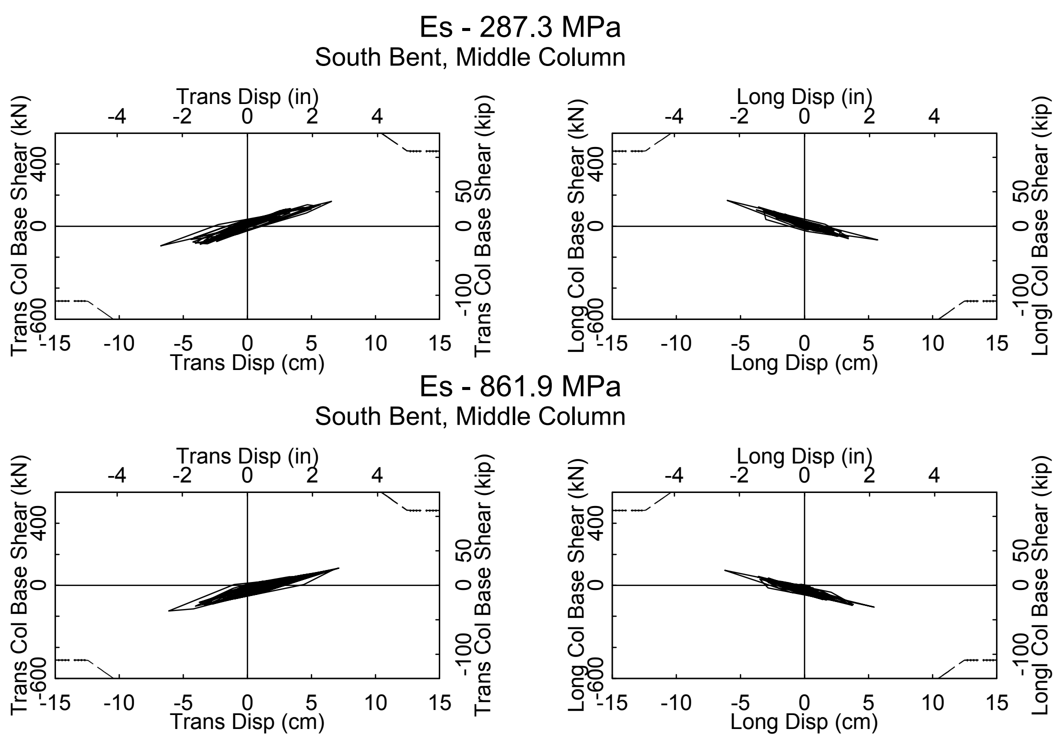

Figure 6.3-6 South Bent, Center Column: Hysteresis Curves for Bridge 5/649E; Mexico City 975 EQ; Es=287.3 MPa (6000 ksf); 861.9 MPa (18000 ksf)

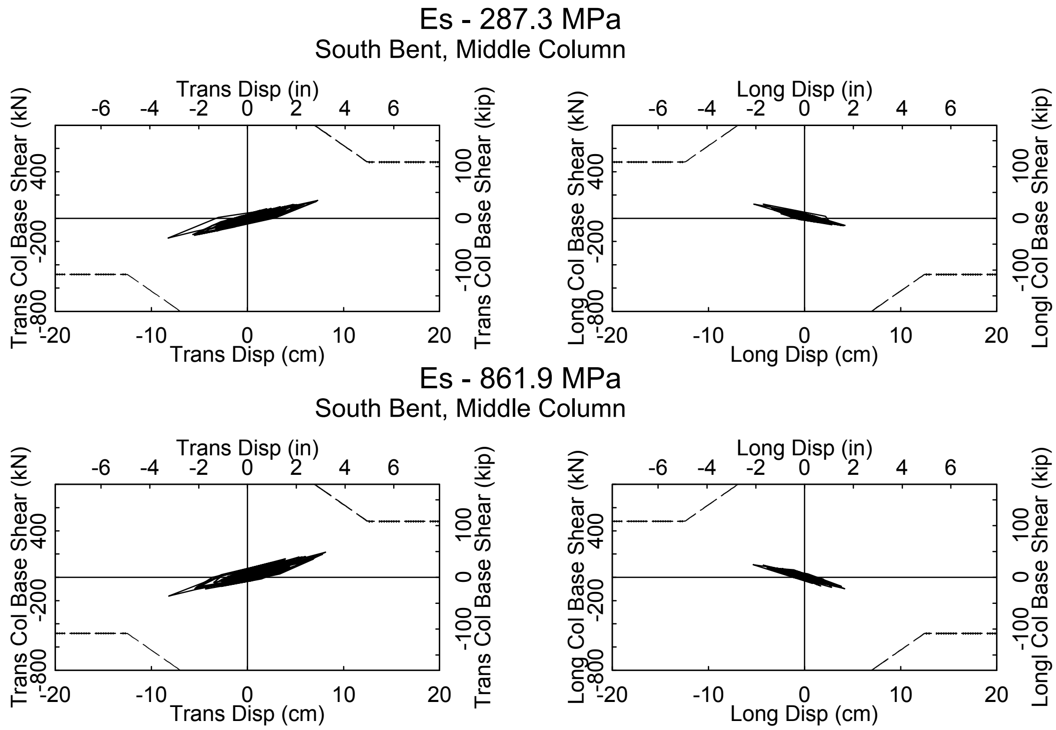

Figure 6.3-7 South Bent, Center Column: Hysteresis Curves for Bridge 5/649E; Olympia 975 EQ; Es=287.3 MPa (6000 ksf); 861.9 MPa (18000 ksf)

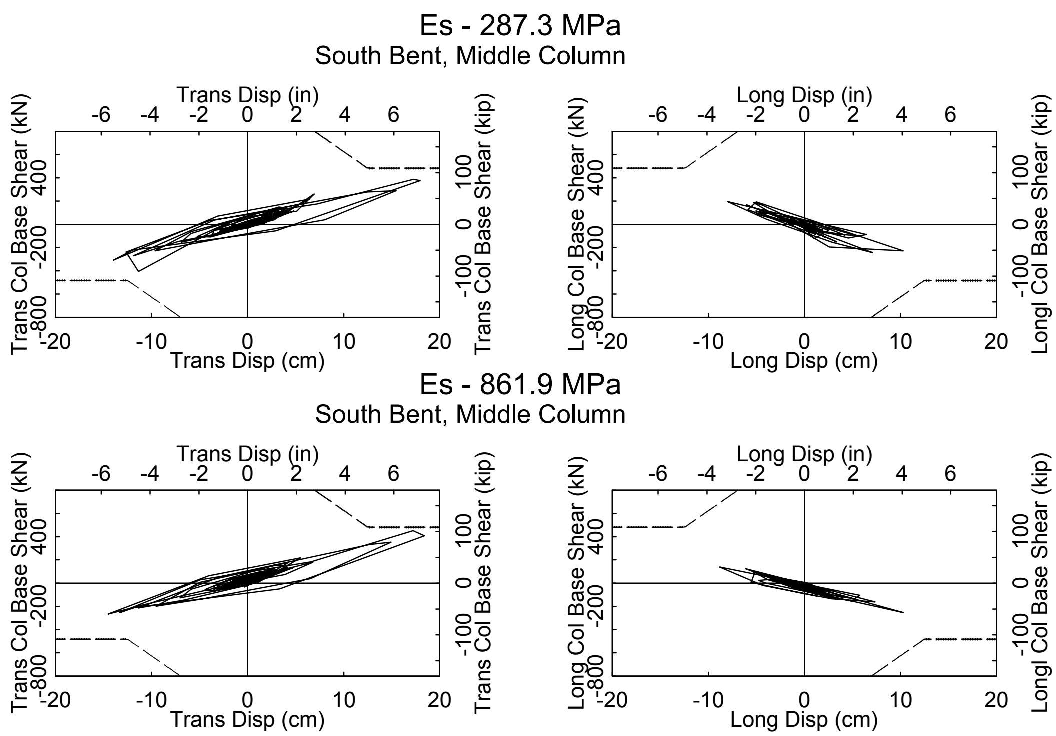

Figure 6.3-8 South Bent, Center Column: Hysteresis Curves for Bridge 5/649E; Chile 2475 EQ; Es=287.3 MPa (6000 ksf); 861.9 MPa (18000 ksf)

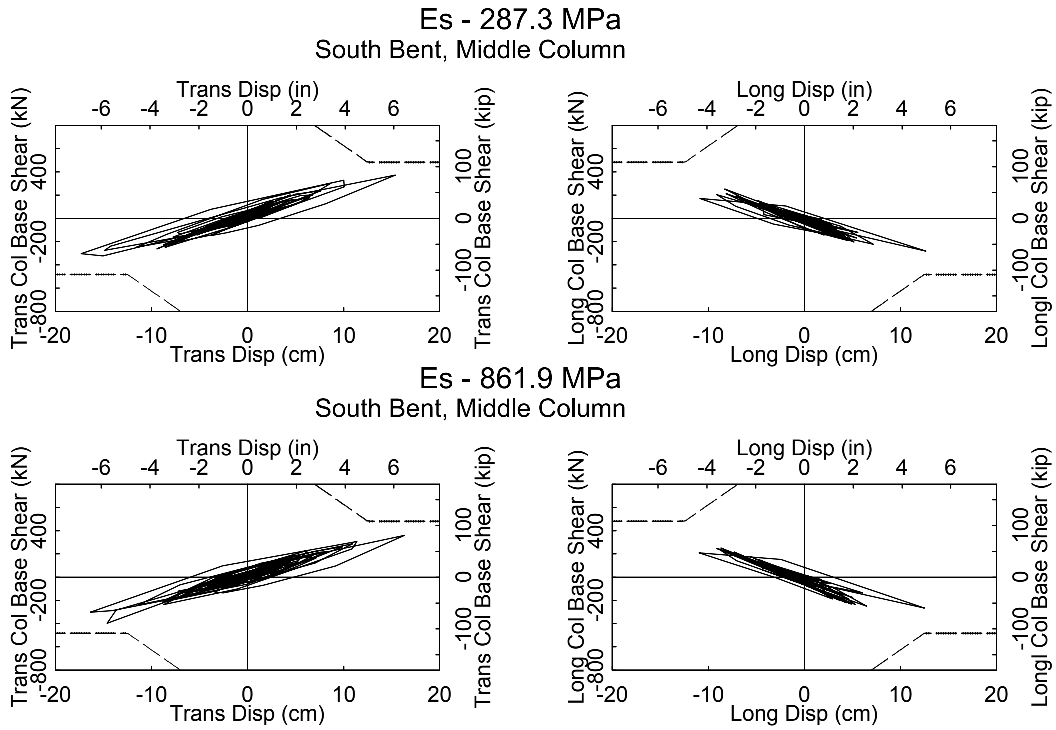

Figure 6.3-9 South Bent, Center Column: Hysteresis Curves for Bridge 5/649E; Peru 2475 EQ; Es=287.3 MPa (6000 ksf); 861.9 MPa (18000 ksf)

The hysteresis curves show that column shear failure is likely to occur under the Chile 2475 earthquake for the 861.9 MPa elastic modulus value model, and comes close to failure for the other boundary conditions under the Chile 2475 earthquake as well as all models under the Peru 2475 earthquake. The hysteresis curves all have similar shapes with larger demands in the transverse direction than in the longitudinal direction.

Displacement time-histories for the Peru 2475 earthquake are shown in figures 6.3-10 and 6.3-11 below. A half cycle occurred at a ductility value almost reaching $4\Delta_y$ indicating that moderate spalling in the hinging region is expected. In addition, the proximity of the force/displacement hysteresis curves to the column shear capacity envelope highlights the probability of column failure.

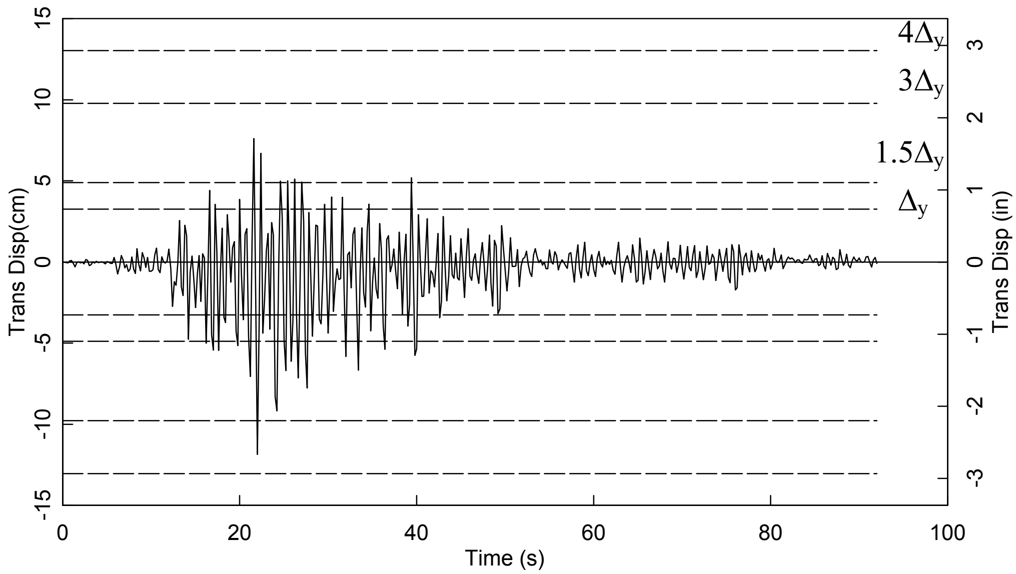

Figure 6.3-10 South Bent, Center Column: Displacement Time History for Bridge 5/649E; Peru 2475 EQ; Es=287.3 MPa

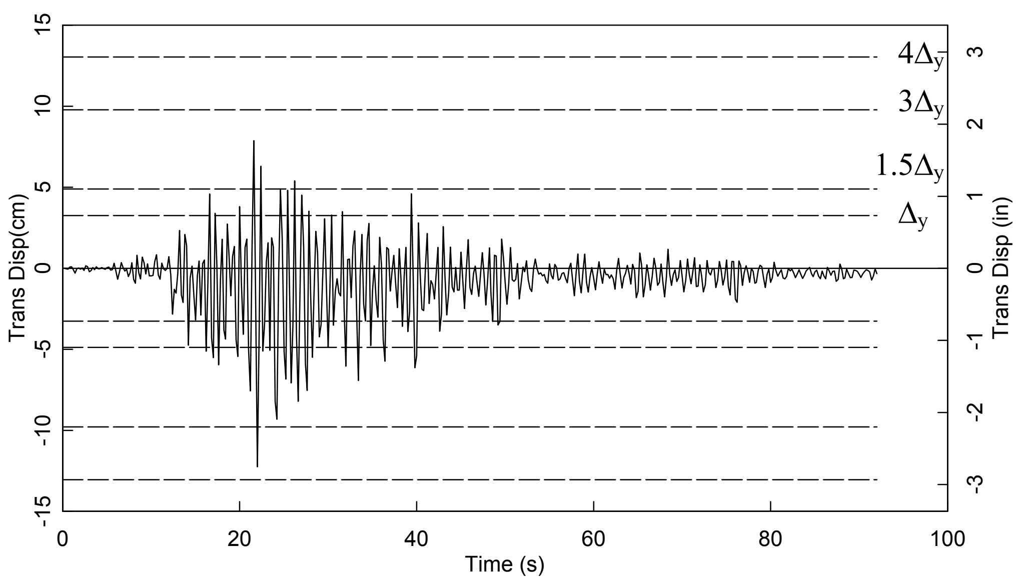

Figure 6.3-11 South Bent, Center Column: Displacement Time History Bridge 5/649E; Peru 2475 EQ; Es=861.9 MPa

The shear force demands in the girder webs at the abutments and in the column footings were investigated for this bridge. The abutments and intermediate bents were built with girder stops on both sides of the I-girders; reducing the transverse force significantly in each girder stop compared to the other two bridges. Therefore, the shear accumulated in each girder web was low and shear failure of the I-girders was not predicted.

The maximum shear force in the column footings was reached for the Chile 2475 earthquake. The shear force demand value was 632 kN (142 kips) in the longitudinal direction and 452 kN (102 kips) in the transverse direction. The shear capacity of the footing is 1876 kN (422 kips) in both directions. Shear failure was not predicted in the column footings or at the abutments. In addition, column/footing joint failure was not investigated here due to the significantly low shear force demands in the footings.

CHAPTER SEVEN

CONCLUSIONS

Recent geological evidence indicates that the potential exists for large earthquakes in the Pacific Northwest as a result of rupturing of the locked interface between the Juan de Fuca and the North American Plate, resulting in long-duration ground motions. To investigate bridge response to long-duration motions, three multi-column bent prestressed concrete bridges, with columns expected to behave primarily in shear, were selected in consultation with the Washington State Department of Transportation (WSDOT). Each bridge is characteristic of pre-1975 WSDOT design specifications and is located in close proximity to Olympia or Seattle. Nonlinear time history analyses were performed using the finite element analysis program, RUAUMOKO 3D, to assess the seismic vulnerability of the bridges. Ten earthquake excitations, six long-duration (Mexico City, Mexico (1985), Lloledo, Chile (1985) and Moquegua, Peru (2001)) and four short duration (Olympia, Washington (1949) and Kobe, Japan (1995)) were modified to fit a target acceleration spectrum for the Seattle area. As a point of reference, the 2001 Nisqually (M=6.8) earthquake was estimated to have a return period between 475 and 2475 years depending on the location in the Puget Sound region and the structure period of interest.

In general, the three bridges experienced light cracking in the column plastic hinge regions under the 475-year return period earthquakes. The 975-year return period earthquakes increased the column damage. In addition, pounding of the expansion joints led to bearing pad failures. Failure of the columns in the center bents of all bridges was predicted by the hysteretic analyses under the 2475-year return period earthquakes, however, displacement time-histories showed that only a small number of cycles reached a ductility level that could lead to failure. For Bridge 5/227, damage was expected to be more significant than for the other two bridges due to a larger number of high-ductility-demand cycles. The damage estimations were based on damage recorded in experimental column testing (Jaradat, 1996).

The column aspect ratios ranged from 2.7 - 3.2 for Bridge 5/649 to 3.4 for Bridge 512/19 to 3 - 3.2 for Bridge 5/227. The largest displacement demands occurred in Bridges 512/19 and 5/649; the lowest displacement demands occurred in Bridge 5/227. The shear demands in the columns were highest for Bridge 5/649 and lowest for Bridge 5/227. Since the column aspect ratios were similar for the three bridges, other bridge characteristics were more influential on the variation of the bridge responses. The bridge deck design, monolithic or non-monolithic, and the bridge geometry greatly influenced the bridge responses. Despite the monolithic deck in Bridge 512/19, the transverse displacement demands were high, especially in the center bent, due to the large longitudinal stiffness of the bridge. Each bridge was unique enough in geometry and design that in order to accurately assess the bridge seismic vulnerability, nonlinear time history analyses were needed rather than basing predictions merely on bridge member detailing, as is often the case due to limited resources.

Shear force demands in the column footings was investigated in this research for all three bridges. It was predicted by the analyses that the footings would not fail in shear. However, studies have shown that the joint shear strength was often a cause of brittle failure in the column/footing connection (McLean, 1999). Due to the significantly low shear forces in the column footings, this failure mode was not investigated in this research but should however be taken into consideration as a potential governing failure mode for future studies.

Modeling the soil-structure interaction was necessary to obtain realistic results and to accurately predict the behavior of the bridges. The trends in the displacement and shear force demands varied with each bridge as the soil-structure-interaction parameters varied. However, the global seismic assessment of the bridges was not altered due to variation in the soil-structure-interaction. Conversely, a significant difference in behavior occurred when the footing and abutment soil-structure-interaction conditions were changed from spring boundary conditions to fixed column base and roller abutment boundary conditions. Displacement and force demands changed for all three bridges, leading to inaccurate results that were either overly conservative or unconservative.

The effect of a 45 degree skew on the overall behavior of bridge 5/649 was also investigated. There was a change of approximately 20% in the displacement and 40% in the shear force demands between the skew and non-skew models. The rest of the bridge response variables did not vary as significantly. Overall, the skew had a large enough effect on the bridge response that it needed to be considered in the modeling process. This particular study was based on the behavior of one bridge. Expanding the study to several bridges with different skew angles is needed to generalize the results and conclusions.

Overall, long-duration earthquakes created more damage in the three bridges than short-duration earthquakes. For the smaller earthquakes, the duration had little effect on the bridge response since multiple cycles at low ductility demands did not lead to damage of the columns. Without significant ductility demands, the duration of the earthquake was of little significance. As the intensity of the earthquake increases, the duration tends to increase as well. Therefore, both earthquake intensity and ground motion duration affect the bridge response; however, large intensity alone can lead to significant demand on the bridges, while duration is not influential on the bridge demand unless the intensity is high as well.

REFERENCES

Abrahamson, N. and Silva, W.J, (1996) "Empirical Ground Motion Models". *Draft Report Prepared for Brookhaven National Laboratory*.

Bozorgnia, Y., Bertero, V. (2003). "Damage Spectra: Characteristics and Applications to Seismic Risk Reduction". *Journal of Structural Engineering, ASCE*, Vol. 129, No. 10, 1330-1340.

Cox, C.J. (2005). "Seismic Assessment and Retrofit of Existing Multi-Column Bent Bridges". *Masters Thesis*, Washington State University.

Dobry, R., Idriss, I. M., and NG, E. (1978). "Duration Characteristics of Horizontal Components of Strong-Motion Earthquake Records." *Bulletin of the Seismology Society of America*, Vol. 68, No. 5, 1487-1520.

Housner, G. W. (1975). "Measures of severity of earthquake ground shaking", *Proc. Natl. Conf. Earthquake Engineering*, Ann Harbor, Michigan.

Jeong, G.D., and Iwan, W.D. (1988) "Effect of Earthquake Duration on the Damage of Structures." *Earthquake Engineering and Structural Dynamics*, Vol. 16, No. 8, 1201-1211.

Jaradat, O.A. (1996). "Seismic Evaluation of Existing Bridge Columns". *PhD Dissertation*, Washington State University.

Kowalsky, M.J., Priestley, M.J.N. (2000). "Improved Analytical Model for Shear Strength of Circular Reinforced Concrete Columns in Seismic Regions." *ACI Structural Journal,* 97 (3), 388-397.

Lindt, J.W., Goh, G. (2004). "Earthquake Duration Effect on Structural Reliability." *Journal of Structural Engineering, ASCE*, Vol. 129, No.5, 821-826.

McLean, D.I., Marsh, M.L. (1999) “Seismic Retrofitting of Bridge Foundations.” *ACI Structural Journal,* 96 (2), 174-182.

PanGEO Incorporated, geotechnical and earthquake engineering consultant firm in Seattle, WA. Information online at: http://pangeoinc.com/

PNSN (2005). “Deep Quakes in Washington and Oregon”. Pacific Northwest Seismograph Network, University of Washington. Accessed online at: http://www.pnsn.org//INFO_GENERAL/platecontours.html

Priestley, M.J.N, Seible, F., Calvi, G.M (1996). *Seismic Design and Retrofit of Bridges*. New York. John Wiley & Sons.

Priestley, M.J.N (2003). “Myths and Fallacies in Earthquake Engineering, Revisited.” *The Mallet Milne Lecture. Rose School*, Pavia, Italy.

Stapleton, S.E. (2004) “Performance of Poorly Confined Reinforced Concrete Columns in Long-Duration Earthquakes.” *Masters Thesis*, Washington State University.

Williamson, E. B. (2003). “Evaluation of Damages and P-Delta Effects for Systems under Earthquake Excitation.” *Journal of Structural Engineering, ASCE*, Vol. 129, No. 8, 1036-1046.

Youngs, R.R., Chiou, S.J., Silva, W.J. and Humphrey, J.R. (1997). “Strong Ground Motion Attenuation Relationships for Subduction Zone Earthquakes”. *Seismological Research Letter*, 68 (1), 58-73.

APPENDICES

APPENDIX A-1

Bridge 5/227 – inner column, center bent:

Scaling from Experimental Data to Model:

aspect ratio of exp: $\frac{L_{ex}}{D_{ex}} = a_{ex}$ $\quad L_{ex} := \frac{70}{24}$ $\quad D_{ex} := \frac{10}{12}$

aspect ratio of model: $\frac{L_{mod}}{D_{mod}} = a_{mod}$ $\quad L_{mod} := \frac{18.62}{2}$ $\quad D_{mod} := 3$

Forces and moments:

$F_{ex} = \frac{M_{ex}}{L_{ex}}$ with $M_{ex} = A_{s.ex} \cdot f_y \cdot \left(D_{ex} - \frac{a}{2}\right)$

$F_{mod} = \frac{M_{mod}}{L_{mod}}$ with $M_{mod} = A_{s.mod} \cdot f_y \cdot \left(D_{mod} - \frac{a}{2}\right)$

$$A_{s.mod} = \left(\frac{D_{mod}}{D_{ex}}\right)^2 \cdot A_{s.ex}$$

$$D_{mod} - \frac{a}{2} = \frac{D_{mod}}{D_{ex}}\left(D_{ex} - \frac{a}{2}\right)$$

$$M_{mod} = \left(\frac{D_{mod}}{D_{ex}}\right)^2 \cdot A_{s.ex} \cdot f_y \cdot \left[\frac{D_{mod}}{D_{ex}}\left(D_{ex} - \frac{a}{2}\right)\right] \qquad M_{mod} = \left(\frac{D_{mod}}{D_{ex}}\right)^3 \cdot A_{s.ex} \cdot f_y \cdot \left(D_{ex} - \frac{a}{2}\right)$$

$$\boxed{M_{mod} = \left(\frac{D_{mod}}{D_{ex}}\right)^3 \cdot M_{ex}}$$

Therefore

$$F_{mod} = \frac{M_{mod}}{L_{mod}} = \left(\frac{D_{mod}}{D_{ex}}\right)^3 \cdot \frac{M_{ex}}{L_{mod}}$$

$$\boxed{F_{mod} = \left(\frac{D_{mod}}{D_{ex}}\right)^3 \cdot \frac{L_{ex}}{L_{mod}} \cdot F_{ex}} \qquad \left(\frac{D_{mod}}{D_{ex}}\right)^3 \cdot \frac{L_{ex}}{L_{mod}} = 14.617$$

Displacements:

Use the actual clear height of the column for the scaling of the displacements. $L_{mod} := \frac{18.62}{2}$

$$\Delta_{y.ex} = \frac{\phi_{y.ex} \cdot L_{ex}^2}{3} \qquad \Delta_{y.mod} = \frac{\phi_{y.mod} \cdot L_{mod}^2}{3}$$

$$\phi_{y.mod} = \phi_{y.ex} \cdot \frac{D_{ex}}{D_{mod}}$$

and $\phi_{y.ex} = 2.25 \cdot \frac{\varepsilon_y}{D_{ex}}$ $\qquad \phi_{y.mod} = 2.25 \cdot \frac{\varepsilon_y}{D_{mod}}$

$$\Delta_{y.mod} = \frac{D_{ex}}{D_{mod}} \cdot \left(\frac{L_{mod}^2}{L_{ex}^2} \right) \cdot \Delta_{y.ex} \qquad \frac{D_{ex}}{D_{mod}} \cdot \left(\frac{L_{mod}^2}{L_{ex}^2} \right) = 2.83$$

$$\Delta_p = \left(\frac{M_u}{M_n} - 1 \right) \cdot \Delta_y + L_p \cdot \left(\phi_u - \phi_y \right) \cdot \left(L - \frac{L_p}{2} \right)$$

$$L_p = 0.08 \cdot \frac{L}{2} + 0.15 \cdot f_y \cdot d_b \qquad L_p = 0.08 \cdot \frac{L}{2} + 0.022 \cdot f_y \cdot d_b$$

Test : $L_{pex} := 0.08 \cdot L_{ex} \cdot ft + 0.15 \cdot 53.8 \cdot \frac{3}{8} \cdot in$ $\qquad L_{pex} = 5.826in$

$$\left(L_{ex} \cdot ft - \frac{L_{pex}}{2} \right) = 32.087in$$

Model : $L_{pmod} := 0.08 \cdot L_{mod} \cdot ft + 0.15 \cdot 53.8 \cdot \frac{9}{8} \cdot in$ $\qquad L_{pmod} = 18.016in$

$$\left(L_{mod} \cdot ft - \frac{L_{pmod}}{2} \right) = 102.712in$$

ratio : $\dfrac{\left(L_{mod} \cdot ft - \frac{L_{pex}}{2} \right)}{\left(L_{ex} \cdot ft - \frac{L_{pmod}}{2} \right)} = 4.186$

ratios for Δp: $\dfrac{L_{pmod} \cdot D_{ex} \cdot \left(L_{mod} \cdot ft - \frac{L_{pex}}{2} \right)}{L_{pex} \cdot D_{mod} \cdot \left(L_{ex} \cdot ft - \frac{L_{pmod}}{2} \right)} = 3.596$

Finally, to scale displacements, use :

$\Delta \le \Delta_y \qquad \Delta_{mod} = 2.83 \cdot \Delta_{ex}$

$\Delta \ge \Delta_y \qquad \Delta_{mod} = 2.83 \cdot \Delta_{yex} + 3.596\left(\Delta_{ex} - \Delta_{yex}\right)$

<u>Axial load:</u>

$$P_{mod} = \left(\frac{D_{mod}}{D_{ex}}\right)^2 \cdot P_{ex} \qquad \left(\frac{D_{mod}}{D_{ex}}\right)^2 = 12.96$$

Appendix A-1 Scaling calculations for the center column, center bent of Bridge 5/227.

APPENDIX A-2

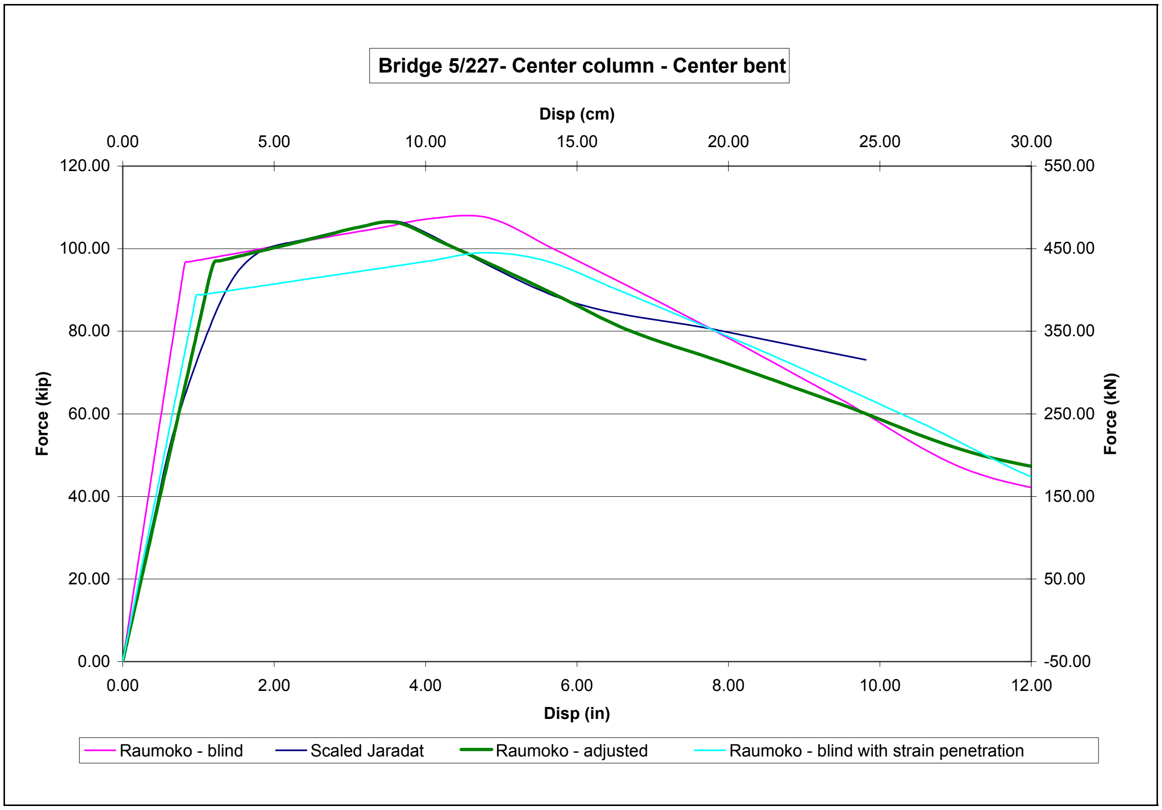

Appendix A-2 Model of the center column, center bent of Bridge 5/227 fitted to Jaradat T2 specimen scaled up and blind model without adjustments to fit T2.

A-2-1 Ruaumoko 3D Input File Calculations

Ruaumoko 3D is an "Inelastic Dynamic Analysis" software developed by Carr at the University of Canterbury, New Zealand in October 2004. The input file can be divided into six parts.

- Input parameters: These define the analysis options (Pushover, time-history), the control parameters (number of nodes, elements…), the iteration parameters (duration of analysis, time-step).
- The nodes: This is where the geometry of the structure is defined: the lengths of each element through nodal coordinates and boundary conditions.
- The elements: This is where the elements are defined by using the nodes determined in the previous section, the member property each element refers to and their orientation in space.
- Member properties: Ruaumoko 3D can model several different types of elements (frame, spring, tendon, masonry…). In this section, each specific property of the member is defined: inertia, cross-sectional area, weight. Also, for a frame member for example, the P-M interaction values must be defined, the plastic hinge lengths and a loss model can be input to account for a particular strength degradation behavior.
- The weights and loads on the structure for each node.
- The excitation: Ruaumoko 3D can run earthquakes as a separate text files with accelerations and time or a standard pushover loading can also be input.

Below are examples of input files for all three bridges.

A-2-1 Bridge 5/227 Ruaumoko Input File

```
227 BRIDGE MODEL; k-ft; Es=6000 ksf=287.3 MPa; Peru
2 1 0 1 3 2 0 0                             ! Analysis Options
1 0 0 0 1 0 0 0 1                            ! EQ Trans. (Mode Shapes
for 95% Mass Part.)
77 81 29 30 1 30 32.2 5 5 0.01 92 1.0        ! Frame Control Par
0 10 10 10 1 1 1 1                           ! Output Control
-.866 .866 0 .5 .5 1                         ! Plot Axes Tran
10 0  0.001                                  ! Iteration Control

NODES 1
1    0       -96.250   0        0 0 0 0 0 0      ! West Ramp
2    0       -88.792   0        0 0 0 0 0 0      ! West Ramp
3    0       -81.333   0        0 0 0 0 0 0      ! West Ramp
4    0       -73.875   0        0 0 0 0 0 0      ! West Ramp
5    0       -66.417   0        0 0 0 0 0 0      ! West Ramp
6    0       -58.958   0        0 0 0 0 0 0      ! West Ramp
7    0       -51.5417  0        0 0 0 0 0 0      ! West Pier Gap (W)
8    0       -51.4583  0        0 0 0 0 0 0      ! West Pier Gap (E)
9    0       -42.917   0        0 0 0 0 0 0      ! West Deck
10   0       -34.333   0        0 0 0 0 0 0      ! West Deck
11   0       -25.750   0        0 0 0 0 0 0      ! West Deck
12   0       -17.167   0        0 0 0 0 0 0      ! West Deck
13   0       -8.583    0        0 0 0 0 0 0      ! West Deck
14   0       -0.0417   0        0 0 0 0 0 0      ! Cntr Pier Gap (W)
15   0       0.0417    0        0 0 0 0 0 0      ! Cntr Pier Gap (E)
16   0       7.250     0        0 0 0 0 0 0      ! East Deck
17   0       14.500    0        0 0 0 0 0 0      ! East Deck
18   0       21.75     0        0 0 0 0 0 0      ! East Deck
19   0       29.00     0        0 0 0 0 0 0      ! East Deck
20   0       36.25     0        0 0 0 0 0 0      ! East Deck
21   0       43.4583   0        0 0 0 0 0 0      ! East Pier Gap (W)
22   0       43.5417   0        0 0 0 0 0 0      ! East Pier Gap (E)
23   0       50.959    0        0 0 0 0 0 0      ! East Ramp
24   0       58.417    0        0 0 0 0 0 0      ! East Ramp
25   0       65.875    0        0 0 0 0 0 0      ! East Ramp
26   0       73.333    0        0 0 0 0 0 0      ! East Ramp
27   0       80.792    0        0 0 0 0 0 0      ! East Ramp
28   0       88.25     0        0 0 0 0 0 0      ! East Ramp
29   -15.583 -51.500   -2.53    2 2 2 0 0 0 39   ! West Col Top (S)
(slaved)
30   0       -51.500   -2.53    2 2 2 0 0 0 40   ! West Col Top (C)
(slaved)
31   15.583  -51.500   -2.53    2 2 2 0 0 0 41   ! West Col Top (N)
(slaved)
32   -15.583 0         -2.53    2 2 2 0 0 0 42   ! Cntr Col Top (S)
(slaved)
33   0       0         -2.53    2 2 2 0 0 0 43   ! Cntr Col Top (C)
(slaved)
34   15.583  0         -2.53    2 2 2 0 0 0 44   ! Cntr Col Top (N)
(slaved)
```

```
35   -15.583 43.500    -2.53    2 2 2 0 0 0 45  ! East Col Top (S)
(slaved)
36   0       43.500    -2.53    2 2 2 0 0 0 46  ! East Col Top (C)
(slaved)
37   15.583  43.500    -2.53    2 2 2 0 0 0 47  ! East Col Top (N)
(slaved)
38   0       -96.333   0        0 0 0 0 0 0     ! West Abut Gap Node
39   -15.583  -51.500   0        0 0 0 0 0 0     ! West Pier X-beam (S)
40   0        -51.500   0        0 0 0 0 0 0     ! West Pier X-beam (C)
41   15.583   -51.500   0        0 0 0 0 0 0     ! West Pier X-beam (N)
42   -15.583  0         0        0 0 0 0 0 0     ! Cntr Pier X-beam (S)
43   0        0         0        0 0 0 0 0 0     ! Cntr Pier X-beam (C)
44   15.583   0         0        0 0 0 0 0 0     ! Cntr Pier X-beam (N)
45   -15.583  43.500    0        0 0 0 0 0 0     ! East Pier X-beam (S)
46   0        43.500    0        0 0 0 0 0 0     ! East Pier X-beam (C)
47   15.583   43.500    0        0 0 0 0 0 0     ! East Pier X-beam (N)
48   0        88.333    0        0 0 0 0 0 0     ! East Abut Gap Node
49   -15.583  -51.500   -21.95   0 0 0 0 0 0     ! West Col bottom (S)
50    0       -51.500   -21.45   0 0 0 0 0 0     ! West Col bottom (C)
51   15.583   -51.500   -21.95   0 0 0 0 0 0     ! West Col bottom (N)
52   -15.583  0         -21.65   0 0 0 0 0 0     ! Cntr Col bottom (S)
53    0       0         -21.15   0 0 0 0 0 0     ! Cntr Col bottom (C)
54    15.583  0         -21.65   0 0 0 0 0 0     ! Cntr Col bottom (N)
55    -15.583 43.500    -20.67   0 0 0 0 0 0     ! East Col bottom (S)
56    0       43.500    -20.17   0 0 0 0 0 0     ! East Col bottom (C)
57    15.583  43.500    -20.67   0 0 0 0 0 0     ! East Col bottom (N)
58    0       -96.333   0        1 1 1 1 1 1     ! West Abutment Spring
59    -15.583 -51.500   -23.95   1 1 1 1 1 1     ! West Col Spring (S)
60    0       -51.500   -23.45   1 1 1 1 1 1     ! West Col Spring (C)
61    15.583  -51.500   -23.95   1 1 1 1 1 1     ! West Col Spring (N)
62    -15.583 0         -23.65   1 1 1 1 1 1     ! Cntr Col Spring (S)
63    0       0         -23.15   1 1 1 1 1 1     ! Cntr Col Spring (C)
64    15.583  0         -23.65   1 1 1 1 1 1     ! Cntr Col Spring (N)
65    -15.583 43.500    -22.67   1 1 1 1 1 1     ! East Col Spring (S)
66    0       43.500    -22.17   1 1 1 1 1 1     ! East Col Spring (C)
67    15.583  43.500    -22.67   1 1 1 1 1 1     ! East Col Spring (N)
68    0       88.333    0        1 1 1 1 1 1     ! East Abutment Spring
69    -15.583 -51.500   -23.95   0 0 0 0 0 0     ! West Col FDN (S)
70    0       -51.500   -23.45   0 0 0 0 0 0     ! West Col FDN (C)
71    15.583  -51.500   -23.95   0 0 0 0 0 0     ! West Col FDN (N)
72    -15.583 0         -23.65   0 0 0 0 0 0     ! Cntr Col FDN (S)
73    0       0         -23.15   0 0 0 0 0 0     ! Cntr Col FDN (C)
74    15.583  0         -23.65   0 0 0 0 0 0     ! Cntr Col FDN (N)
75    -15.583 43.500    -22.67   0 0 0 0 0 0     ! East Col FDN (S)
76    0       43.500    -22.17   0 0 0 0 0 0     ! East Col FDN (C)
77    15.583  43.500    -22.67   0 0 0 0 0 0     ! East Col FDN (N)

ELEMENTS 1
1       2       1   2   0 0 X   ! Long Links: Western Ramp
2       1       2   3   0 0 X
3       1       3   4   0 0 X
4       1       4   5   0 0 X
5       1       5   6   0 0 X
6       3       6   7   0 0 X
7       5       8   9   0 0 X   ! Long Links: Western Deck
8       4       9   10  0 0 X
9       4       10  11  0 0 X
```

```
10      4       11  12  0 0 X
11      4       12  13  0 0 X
12      6       13  14  0 0 X
13      8       15  16  0 0 X   ! Long Links: Eastern Deck
14      7       16  17  0 0 X
15      7       17  18  0 0 X
16      7       18  19  0 0 X
17      7       19  20  0 0 X
18      9       20  21  0 0 X
19      2       22  23  0 0 X   ! Long Links: Eastern Ramp
20      1       23  24  0 0 X
21      1       24  25  0 0 X
22      1       25  26  0 0 X
23      1       26  27  0 0 X
24      3       27  28  0 0 X
25      10      39  29  0 0 Y   ! West Bent Vertical (S)
26      10      40  30  0 0 Y   !                    (C)
27      10      41  31  0 0 Y   !                    (N)
28      10      42  32  0 0 Y   ! Cntr Bent Vertical (S)
29      10      43  33  0 0 Y   !                    (C)
30      10      44  34  0 0 Y   !                    (N)
31      10      45  35  0 0 Y   ! East Bent Vertical (S)
32      10      46  36  0 0 Y   !                    (C)
33      10      47  37  0 0 Y   !                    (N)
34      11      39  40  0 0 Y   ! West Bent Transverse (S)
35      11      40  41  0 0 Y   !                      (N)
36      12      42  43  0 0 Y   ! Cntr Bent Transverse (S)
37      12      43  44  0 0 Y   !                      (N)
38      13      45  46  0 0 Y   ! Cntr Bent Transverse (S)
39      13      46  47  0 0 Y   !                      (N)
40      14      29  49  0 0 Y   ! West Column (S)
41      15      30  50  0 0 Y   !             (C)
42      14      31  51  0 0 Y   !             (N)
43      16      32  52  0 0 Y   ! Cntr Column (S)
44      17      33  53  0 0 Y   !             (C)
45      16      34  54  0 0 Y   !             (N)
46      18      35  55  0 0 Y   ! East Column (S)
47      19      36  56  0 0 Y   !             (C)
48      18      37  57  0 0 Y   !             (N)
49      20      38  1   0 0 X   ! West Abutment Bearing Pad
50      20      7   40  0 0 X   ! West Bearing Pad (W)
51      20      40  8   0 0 X   !                  (E)
52      20      14  43  0 0 X   ! Cntr Bearing Pad (W)
53      20      43  15  0 0 X   !                  (E)
54      20      21  46  0 0 X   ! East Bearing Pad (W)
55      20      46  22  0 0 X   !                  (E)
56      20      28  48  0 0 X   ! East Abutment Bearing Pad
57      21      38  1   0 0 X   ! West Abutment Gap
58      21      7   8   0 0 X   ! West Gap
59      21      14  15  0 0 X   ! Cntr Gap
60      21      21  22  0 0 X   ! East Gap
61      21      28  48  0 0 X   ! East Abutment Gap
62      22      59  69  0 0 X   ! West PIER Spring (South)
63      23      60  70  0 0 X   ! West PIER Spring (Center)
64      22      61  71  0 0 X   ! West PIER Spring (North)
65      24      62  72  0 0 X   ! Cntr PIER Spring (South)
66      25      63  73  0 0 X   ! Cntr PIER Spring (Center)
```

```
67      24      64  74  0 0 X   ! Cntr PIER Spring (North)
68      26      65  75  0 0 X   ! East PIER Spring (South)
69      27      66  76  0 0 X   ! East PIER Spring (Center)
70      26      67  77  0 0 X   ! East PIER Spring (North)
71      28      38  58  0 0 X   ! West Abut Spring 1
72      29      48  68  0 0 X   ! East Abut Spring 5
73      11      49  69  0 0 Y   ! West Col FDN (S)
74      11      50  70  0 0 Y   !              (C)
75      11      51  71  0 0 Y   !              (N)
76      12      52  72  0 0 Y   ! Cntr Col FDN (S)
77      12      53  73  0 0 Y   !              (C)
78      12      54  74  0 0 Y   !              (N)
79      13      55  75  0 0 Y   ! East Col FDN (S)
80      13      56  76  0 0 Y   !              (C)
81      13      57  77  0 0 Y   !              (N)


PROPS
1 FRAME                                                 ! Longitudinal
Deck Beams (west & east ramp)
1 0 0 0 0 0 0                                           !
6.358E5 2.54E5 33.54 3161 40.401 3161 33.54 33.54       !
E,G,A,J,Izz,Ixx,Asz,Asy (K,FT)
0.0                                                     ! End Properties

2 FRAME                                                 ! Longitudinal
Deck Beams (west & east ramp)
1 1 1 0 0 0 0                                           ! Moment releases
6.358E5 2.54E5 33.54 3161 40.401 3161 33.54 33.54       !
E,G,A,J,Izz,Ixx,Asz,Asy (K,FT)
0.0                                                     ! End Properties

3 FRAME                                                 ! Longitudinal
Deck Beams (west & east ramp)
1 2 2 0 0 0 0                                           ! Moment released
6.358E5 2.54E5 33.54 3161 40.401 3161 33.54 33.54       !
E,G,A,J,Izz,Ixx,Asz,Asy (K,FT)
0.0                                                     ! End Properties

4 FRAME                                                 ! Longitudinal
Deck Beams (west deck)
1 0 0 0 0 0 0                                           !
6.358E5 2.54E5 33.54 3161 40.401 3161 33.54 33.54       !
E,G,A,J,Izz,Ixx,Asz,Asy (K,FT)
0.0                                                     ! End Properties

5 FRAME                                                 ! Longitudinal
Deck Beams (west deck)
1 1 1 0 0 0 0 0                                         ! Moment releases
6.358E5 2.54E5 33.54 3161 40.401 3161 33.54 33.54       !
E,G,A,J,Izz,Ixx,Asz,Asy (K,FT)
0.0                                                     ! End Properties

6 FRAME                                                 ! Longitudinal
Deck Beams (west deck)
1 2 2 0 0 0 0 0                                         ! Moment releases
```

```
6.358E5 2.54E5 33.54 3161 40.401 3161 33.54 33.54     !
E,G,A,J,Izz,Ixx,Asz,Asy (K,FT)
0.0                                                    ! End Properties

7 FRAME                                                ! Longitudinal
Deck Beams (east deck)
1 0 0 0 0 0 0                                          !
6.358E5 2.54E5 33.54 3161 40.401 3161 33.54 33.54     !
E,G,A,J,Izz,Ixx,Asz,Asy (K,FT)
0.0                                                    ! End Properties

8 FRAME                                                ! Longitudinal
Deck Beams (east deck)
1 1 1 0 0 0 0 0                                        ! Moment releases
6.358E5 2.54E5 33.54 3161 40.401 3161 33.54 33.54     !
E,G,A,J,Izz,Ixx,Asz,Asy (K,FT)
0.0                                                    ! End Properties

9 FRAME                                                ! Longitudinal
Deck Beams (east deck)
1 2 2 0 0 0 0 0                                        ! Moment releases
6.358E5 2.54E5 33.54 3161 40.401 3161 33.54 33.54     !
E,G,A,J,Izz,Ixx,Asz,Asy (K,FT)
0.0                                                    ! End Properties

10 FRAME                                               ! Rigid Piers
(Vert)
1 0 0 0 0 0 0 0                                        ! Linear Elastic
1E7 1E7 1E3 1E5 1E3 1E6 1E3 1E3                        !
E,G,A,J,Izz,Iyy,Asz,Asy (K,FT)
0                                                      !

11 FRAME                                               ! West Pier (bent)
1 0 0 0 0 0 0 0                                        ! Linear Elastic
1E7 1E7 1E3 1E5 1E3 1E6 1E3 1E3                        !
E,G,A,J,Izz,Iyy,Asz,Asy (K,FT)
0                                                      !

12 FRAME                                               ! Cntr Pier (bent)
1 0 0 0 0 0 0 0                                        ! Linear Elastic
1E7 1E7 1E3 1E5 1E3 1E6 1E3 1E3                        !
E,G,A,J,Izz,Iyy,Asz,Asy (K,FT)
0                                                      !

13 FRAME                                               ! Cntr Pier (bent)
1 0 0 0 0 0 0 0                                        ! Linear Elastic
1E7 1E7 1E3 1E5 1E3 1E6 1E3 1E3                        !
E,G,A,J,Izz,Iyy,Asz,Asy (K,FT)
0                                                      !

14 FRAME                                               ! West Outer
Column
2 0 0 0 4 0 0 0                                        !
6.358E5 2.543E5 7.07 1.168 0.826 0.826 7.07 7.07      !
E,G,A,J,Izz,Iyy,Asz,Asy (.22*I) (K,FT)
0.0 0.0 0.0 0.0                                        ! Ends
0.04 0.04 0.04 0.04                                    ! r0
```

```
1.464 1.464 1.464 1.464                                ! Plastic Hinge
Length
0.0 0.0 1.55 1.0 0.0                                   ! Interaction
-6612 -1575 1790 1790 445.9                            ! Yield
Forces/Moments
! 4.2 11 0.3 15                                        ! Refined Loss
Model
0.5 0.1 1 1                                            ! Modified Takeda
Hyst.

15 FRAME                                               ! West Inner
Column
2 0 0 0 4 0 0 0                                        !
6.358E5 2.543E5 7.069 1.167 0.825 0.825 7.07 7.07      !
E,G,A,J,Izz,Iyy,Asz,Asy (.25*I) (K,FT)
0.0 0.0 0.0 0.0                                        ! Ends
0.04 0.04 0.04 0.04                                    ! r0
1.444 1.444 1.444 1.444                                ! Plastic Hinge
Length
0.0 0.0 1.5 1.15 0.0                                   ! Interaction
-6612 -1575 1790 1790 445.9                            ! Yield
Forces/Moments
! 4.2 11 0.3 15                                        ! Refined Loss
Model
0.5 0.1 1 1                                            ! Modified Takeda
Hyst.

16 FRAME                                               ! Mid Outer Column
2 0 0 0 4 0 0 0                                        !
6.358E5 2.543E5 7.069 1.169 0.827 0.827 7.07 7.07      !
E,G,A,J,Izz,Iyy,Asz,Asy (.22*I) (K,FT)
0.0 0.0 0.0 0.0                                        ! Ends
0.04 0.04 0.04 0.04                                    ! r0
1.452 1.452 1.452 1.452                                ! Plastic Hinge
Length
0.0 0.0 1.5 1.15 0.0                                   ! Interaction
-6612 -1575 1790 1790 445.9                            ! Yield
Forces/Moments
! 4.2 11 0.3 15                                        ! Refined Loss
Model
0.5 0.1 1 1                                            ! Modified Takeda
Hyst.

17 FRAME                                               ! Mid Inner Column
2 0 0 0 4 0 0 0                                        !
6.358E5 2.543E5 7.069 1.169 0.827 0.827 7.07 7.07      !
E,G,A,J,Izz,Iyy,Asz,Asy (.25*I) (K,FT)
0.0 0.0 0.0 0.0                                        ! Ends
0.04 0.04 0.04 0.04                                    ! r0
1.432 1.432 1.432 1.432                                ! Plastic Hinge
Length
0.0 0.0 1.5 1.15 0.0                                   ! Interaction
-6612 -1575 1790 1790 445.9                            ! Yield
Forces/Moments
! 4.2 11 0.3 15                                        ! Refined Loss
Model
```

```
0.5 0.1 1 1                                           ! Modified Takeda
Hyst.

18 FRAME                                              ! East Outer
Column
2 0 0 0 4 0 0 0                                       !
6.358E5 2.543E5 7.069 1.169 0.826 0.826 7.07 7.07     !
E,G,A,J,Izz,Iyy,Asz,Asy (.21*I) (K,FT)
0.0 0.0 0.0 0.0                                       ! Ends
0.04 0.04 0.04 0.04                                   ! r0
1.393 1.393 1.393 1.393                               ! Plastic Hinge
Length
0.0 0.0 1.5 1.15 0.0                                  ! Interaction
-6612 -1575 1790 1790 445.9                           ! Yield
Forces/Moments
! 4.2 11 0.3 15                                       ! Refined Loss
Model
0.5 0.1 1 1                                           ! Modified Takeda
Hyst.

19 FRAME                                              ! East Inner
Column
2 0 0 0 4 0 0 0                                       !
6.358E5 2.543E5 7.069 1.168 0.826 0.826 7.07 7.07     !
E,G,A,J,Izz,Iyy,Asz,Asy (.23*I) (K,FT)
0.0 0.0 0.0 0.0                                       ! Ends
0.04 0.04 0.04 0.04                                   ! r0
1.413 1.413 1.413 1.413                               ! Plastic Hinge
Length
0.0 0.0 1.5 1.15 0.0                                  ! Interaction
-6612 -1575 1790 1790 445.9                           ! Yield
Forces/Moments
! 4.2 11 0.3 15                                       ! Refined Loss
Model
0.5 0.1 1 1                                           ! Modified Takeda
Hyst.

20 SPRING                                             ! Bridge Deck
Bearing Pads
1 0 0 0 0 0                                           ! Control
Parameters
1479.6 2E7 3E6 8E7 8E4 8E4 0 .3 .3                    ! Section
Properties

21 MULTISPRING                                        ! Bridge Gap
Elements
1 0 0 0 10 2 31 0                                     ! Control
Parameters
3.265E3 0 0 0 0 0 .3                                  ! Section
Properties
0 -9.265E9 0 0 0 0 0 0 0 0 0                          ! Section Yield
Prop.

22 SPRING                                             ! SOIL SPRING WI
1 0 0 0 0 0                                           ! Control Par.
1.2177E5 1.2177E5 2.0210E5 5.3777E6 3.7637E6 5.2783E6 0 .33 .33 !
Section Prop.
```

```
23 SPRING                                                      ! SOIL SPRING WO
1 0 0 0 0 0                                                    ! Control Par.
1.2177E5 1.2177E5 2.0210E5 5.3777E6 3.7637E6 5.2783E6 0 .33 .33 !
Section Prop.

24 SPRING                                                      ! SOIL SPRING CI
1 0 0 0 0 0                                                    ! Control Par.
1.2177E5 1.2177E5 2.0210E5 5.3777E6 3.7637E6 5.2783E6 0 .33 .33 !
Section Prop.

25 SPRING                                                      ! SOIL SPRING CO
1 0 0 0 0 0                                                    ! Control Par.
1.2177E5 1.2177E5 2.0210E5 5.3777E6 3.7637E6 5.2783E6 0 .33 .33 !
Section Prop.

26 SPRING                                                      ! SOIL SPRING EI
1 0 0 0 0 0                                                    ! Control Par.
1.2177E5 1.2177E5 2.0210E5 5.3777E6 3.7637E6 5.2783E6 0 .33 .33 !
Section Prop.

27 SPRING                                                      ! SOIL SPRING EO
1 0 0 0 0 0                                                    ! Control Par.
1.2177E5 1.2177E5 2.0210E5 5.3777E6 3.7637E6 5.2783E6 0 .33 .33 !
Section Prop.

28 SPRING                                                      ! Secant SOIL SPR
W abt
1 0 0 0 0 0                                                    ! Control Par.
4.6272E5 4.6580E5 7.1459E5 3.5529E7 4.3135E7 3.74E7 0 .33 .33  ! Section
Prop.

29 SPRING                                                      ! Secant SOIL SPR
E abt
1 0 0 0 0 0                                                    ! Control Par.
4.6272E5 4.6580E5 7.1459E5 3.5529E7 4.3135E7 3.74E7 0 .33 .33  ! Section
Prop.


WEIGHTS 0
1        17.979   17.979      17.979    ! West Ramp
2        35.958   35.958      35.958
3        35.958   35.958      35.958
4        35.958   35.958      35.958
5        35.958   35.958      35.958
6        35.958   35.958      35.958
7        17.979   17.979      17.979
8        20.73    20.73       20.73    ! West Deck
9        41.46    41.46       41.46
10       41.46    41.46       41.46
11       41.46    41.46       41.46
12       41.46    41.46       41.46
13       41.46    41.46       41.46
14       20.73    20.73       20.73
15       17.496   17.496      17.496    ! East Deck
16       34.993   34.993      34.993
17       34.993   34.993      34.993
```

```
18        34.993   34.993      34.993
19        34.993   34.993      34.993
20        34.993   34.993      34.993
21        17.496   17.496      17.496
22        17.979   17.979      17.979    ! East Ramp
23        35.958   35.958      35.958
24        35.958   35.958      35.958
25        35.958   35.958      35.958
26        35.958   35.958      35.958
27        35.958   35.958      35.958
28        17.979   17.979      17.979
29        20.591   20.591      20.591    ! West Column (s)
30        20.061   20.061      20.061    !             (c)
31        20.591   20.591      20.591    !             (n)
32        20.273   20.273      20.273    ! Cntr Column (s)
33        19.743   19.743      19.743    !             (c)
34        20.273   20.273      20.273    !             (n)
35        19.764   19.764      19.764    ! East Column (s)
36        19.234   19.234      19.234    !             (c)
37        19.764   19.764      19.764    !             (n)
38        76.5     76.5        76.5      ! West Abutment
39        14.025   14.025      14.025    ! West X-beam
40        28.049   28.049      28.049
41        14.025   14.025      14.025
42        14.025   14.025      14.025    ! Cntr X-Beam
43        28.049   28.049      28.049
44        14.025   14.025      14.025
45        14.025   14.025      14.025    ! East X-Beam
46        28.049   28.049      28.049
47        14.025   14.025      14.025
48        76.5     76.5        76.5      ! East Abutment
77

LOADS
1          0   0    -17.9799  ! West Ramp
2          0   0    -35.958
3          0   0    -35.958
4          0   0    -35.958
5          0   0    -35.958
6          0   0    -35.958
7          0   0    -17.979
8          0   0    -20.73    ! West Deck
9          0   0    -41.46
10         0   0    -41.46
11         0   0    -41.46
12         0   0    -41.46
13         0   0    -41.46
14         0   0    -20.73
15         0   0    -17.496    ! East Deck
16         0   0    -34.993
17         0   0    -34.993
18         0   0    -34.993
19         0   0    -34.993
20         0   0    -34.993
21         0   0    -17.496
22         0   0    -17.979    ! East Ramp
23         0   0    -35.958
```

```
24         0   0    -35.958
25         0   0    -35.958
26         0   0    -35.958
27         0   0    -35.958
28         0   0    -17.979
29         0   0    -20.591    ! West Column (s)
30         0   0    -20.061    !             (c)
31         0   0    -20.591    !             (n)
32         0   0    -20.273    ! Cntr Column (s)
33         0   0    -19.743    !             (c)
34         0   0    -20.273    !             (n)
35         0   0    -19.764    ! East Column (s)
36         0   0    -19.234    !             (c)
37         0   0    -19.764    !             (n)
38         0   0    -76.5      ! West Abutment
39         0   0    -14.025    ! West X-beam
40         0   0    -28.049
41         0   0    -14.025
42         0   0    -14.025    ! Cntr X-Beam
43         0   0    -28.049
44         0   0    -14.025
45         0   0    -14.025    ! East X-Beam
46         0   0    -28.049
47         0   0    -14.025
48         0   0    -76.5      ! East Abutment
77

EQUAKE NSPeru9.txt
5  1  0.01  1  -1                        ! File Parameters

EQUAKE EWPeru9.txt
5  1  0.01  1  -1                        ! File Parameters

EQUAKE UPPeru9.txt
5  1  0.01  1  -1                        ! File Parameters
```

A-2-2 Bridge 512/19 Ruamoko Input File

```
512-19 bridge with skew;units kip-ft; Es=6000 ksf=287.3 MPa; Peru-Half
Data
2  1  0  0  3  2  0  0                         ! Analysis Options
1 0 0 0 1 0 0 0 -1                             ! Earthquake Transformation
78 77 13 29 1 23 32.2 5 5 0.01 92 1.0          ! Frame Control Par
0  20  10  3  1  1  1  1                       ! Output Control
.866 -.866 0 -.5 -.5 -1                        ! Plot Axes Tran
10 0  0.0001                                   ! Iteration Control

Nodes 1
1   -125.5   0     0          0 0 0 0 0 0       !north abutment
2   -125.0   0     0          0 0 0 0 0 0 !north ramp
3   -100.5   0     0          0 0 0 0 0 0
4   -76.000  0     0          0 0 0 0 0 0 !north deck
5   -50.670  0     0          0 0 0 0 0 0
6   -25.330  0     0          0 0 0 0 0 0
7   0.000    0     0          0 0 0 0 0 0 !middle deck
8   25.330   0     0          0 0 0 0 0 0 !south deck
9   50.670   0     0          0 0 0 0 0 0
10  76.000   0     0          0 0 0 0 0 0 !south ramp
11  99.500   0     0          0 0 0 0 0 0
12  123.000  0     0          0 0 0 0 0 0
13  123.500  0     0          0 0 0 0 0 0 !south abutment
14  -75.517 -35.5  4.375      0 0 0 0 0 0 !north bent
15  -75.839 -11.83 4.375      0 0 0 0 0 0
16  -76.000 0      4.375      0 0 0 0 0 0
17  -76.161 11.83  4.375      0 0 0 0 0 0
18  -76.483 35.5   4.375      0 0 0 0 0 0
19   0.483  -35.5  4.375      0 0 0 0 0 0 !middle bent
20   0.161  -11.83 4.375      0 0 0 0 0 0
21   0.000  0      4.375      0 0 0 0 0 0
22  -0.483  11.83  4.375      0 0 0 0 0 0
23  -0.483  35.5   4.375      0 0 0 0 0 0
24  76.483  -35.5  4.375      0 0 0 0 0 0 !south bent
25  76.161  -11.83 4.375      0 0 0 0 0 0
26  76.000  0      4.375      0 0 0 0 0 0
27  75.839  11.83  4.375      0 0 0 0 0 0
28  75.517  35.5   4.375      0 0 0 0 0 0
29  -75.517 -35.5  6.1875     2 2 2 0 0 0 14    !ne col top
30  -75.517 -35.5  26.2875    0 0 0 0 0 0 !col bot
31  -75.517 -35.5  27.2875    0 0 0 0 0 0 !col footing
32  -75.839 -11.83 6.1875     2 2 2 0 0 0 15    !nme col top
33  -75.839 -11.83 26.2875    0 0 0 0 0 0 !col bot
34  -75.839 -11.83 27.2875    0 0 0 0 0 0 !col footing
35  -76.161 11.83  6.1875     2 2 2 0 0 0 17    !nmw  col top
36  -76.161 11.83  26.2875    0 0 0 0 0 0 !col bot
37  -76.161 11.83  27.2875    0 0 0 0 0 0 !col footing
38  -76.483 35.5   6.1875     2 2 2 0 0 0 18    !nw   col top
39  -76.483 35.5   26.2875    0 0 0 0 0 0 !col bot
40  -76.483 35.5   27.2875    0 0 0 0 0 0 !col footing
41  0.483   -35.5  6.1875     2 2 2 0 0 0 19    !me   col top
42  0.483   -35.5  26.2875    0 0 0 0 0 0 !col bot
```

```
43  0.483   -35.5  27.2875    0 0 0 0 0 0 !col footing
44  0.161   -11.83 6.1875     2 2 2 0 0 0 20    !mme  col top
45  0.161   -11.83 26.2875    0 0 0 0 0 0 !col bot
46  0.161   -11.83 27.2875    0 0 0 0 0 0 !col footing
47  -0.483  11.83  6.1875     2 2 2 0 0 0 22    !mmw  col top
48  -0.483  11.83  26.2875    0 0 0 0 0 0 !col bot
49  -0.483  11.83  27.2875    0 0 0 0 0 0 !col footing
50  -0.483  35.5   6.1875     2 2 2 0 0 0 23    !mw   col top
51  -0.483  35.5   26.2875    0 0 0 0 0 0 !col bot
52  -0.483  35.5   27.2875    0 0 0 0 0 0 !col footing
53  76.483  -35.5  6.1875     2 2 2 0 0 0 24    !se   col top
54  76.483  -35.5  26.2875    0 0 0 0 0 0 !col bot
55  76.483  -35.5  27.2875    0 0 0 0 0 0 !col footing
56  76.161  -11.83 6.1875     2 2 2 0 0 0 25    !sme  col top
57  76.161  -11.83 26.2875    0 0 0 0 0 0 !col bot
58  76.161  -11.83 27.2875    0 0 0 0 0 0 !col footing
59  75.839  11.83  6.1875     2 2 2 0 0 0 27    !smw  col top
60  75.839  11.83  26.2875    0 0 0 0 0 0 !col bot
61  75.839  11.83  27.2875    0 0 0 0 0 0 !col footing
62  75.517  35.5   6.1875     2 2 2 0 0 0 28    !sw   col top
63  75.517  35.5   26.2875    0 0 0 0 0 0 !col bot
64  75.517  35.5   27.2875    0 0 0 0 0 0 !col footing
65  -125.5  0      0          1 1 1 1 1 1 !north abutment spring
66  123.500 0      0          1 1 1 1 1 1 !south abutment spring
67  -75.517 -35.5  27.2875    1 1 1 1 1 1 !col footing spring
68  -75.839 -11.83 27.2875    1 1 1 1 1 1 !col footing spring
69  -76.161 11.83  27.2875    1 1 1 1 1 1 !col footing spring
70  -76.483 35.5   27.2875    1 1 1 1 1 1 !col footing spring
71  0.483   -35.5  27.2875    1 1 1 1 1 1 !col footing spring
72  0.161   -11.83 27.2875    1 1 1 1 1 1 !col footing spring
73  -0.483  11.83  27.2875    1 1 1 1 1 1 !col footing spring
74  -0.483  35.5   27.2875    1 1 1 1 1 1 !col footing spring
75  76.483  -35.5  27.2875    1 1 1 1 1 1 !col footing spring
76  76.161  -11.83 27.2875    1 1 1 1 1 1 !col footing spring
77  75.839  11.83  27.2875    1 1 1 1 1 1 !col footing spring
78  75.517  35.5   27.2875    1 1 1 1 1 1 !col footing spring

Elements 1
1     1     65    2     0     0     Y     !north abutment
2     1     2     3     0     0     Y     !north deck
3     1     3     4     0     0     Y
4     1     4     5     0     0     Y
5     1     5     6     0     0     Y
6     1     6     7     0     0     Y
7     1     7     8     0     0     Y     !south deck
8     1     8     9     0     0     Y
9     1     9     10    0     0     Y
10    1     10    11    0     0     Y
11    1     11    12    0     0     Y
12    1     12    66    0     0     Y     !south abutment
13    2     14    15    0     0     X     !north bent
14    2     15    16    0     0     X
15    2     16    17    0     0     X
16    2     17    18    0     0     X
17    2     19    20    0     0     X     !middle bent
18    2     20    21    0     0     X
19    2     21    22    0     0     X
```

20	2	22	23	0	0	X	
21	2	24	25	0	0	X	!south bent
22	2	25	26	0	0	X	
23	2	26	27	0	0	X	
24	2	27	28	0	0	X	
25	3	4	16	0	0	X	!vert link deck-bent (N)
26	3	14	29	0	0	X	!vert link cap-col (Ne)
27	5	29	30	0	0	X	! Col (Ne)
28	4	30	31	0	0	X	!vert link col-foot (Ne)
29	3	15	32	0	0	X	!vert link cap-col (Nme)
30	5	32	33	0	0	X	! Col (Nme)
31	4	33	34	0	0	X	!vert link col-foot (Nme)
32	3	17	35	0	0	X	!vert link cap-col (Nmw)
33	5	35	36	0	0	X	! Col (Nmw)
34	4	36	37	0	0	X	!vert link col-foot (Nmw)
35	3	18	38	0	0	X	!vert link cap-col (Nw))
36	5	38	39	0	0	X	! Col (Nw)
37	4	39	40	0	0	X	!vert link col-foot (Nw)
38	3	7	21	0	0	X	!vert link deck-bent (M)
39	3	19	41	0	0	X	!vert link cap-col (Me)
40	5	41	42	0	0	X	! Col (Me)
41	4	42	43	0	0	X	!vert link col-foot (Me)
42	3	20	44	0	0	X	!vert link cap-col (Mme)
43	5	44	45	0	0	X	! Col (Mme)
44	4	45	46	0	0	X	!vert link col-foot (Mme)
45	3	22	47	0	0	X	!vert link cap-col (Mmw)
46	5	47	48	0	0	X	! Col (Mmw)
47	4	48	49	0	0	X	!vert link col-foot (Mmw)
48	3	23	50	0	0	X	!vert link cap-col (Mw)
49	5	50	51	0	0	X	! Col (Mw)
50	4	51	52	0	0	X	!vert link col-foot (Mw)
51	3	10	26	0	0	X	!vert link deck-bent (S)
52	3	24	53	0	0	X	!vert link cap-col (Se)
53	5	53	54	0	0	X	! Col (Se)
54	4	54	55	0	0	X	!vert link col-foot (Se)
55	3	25	56	0	0	X	!vert link cap-col (Sme)
56	5	56	57	0	0	X	! Col (Sme)
57	4	57	58	0	0	X	!vert link col-foot (Sme)
58	3	27	59	0	0	X	!vert link cap-col (Smw)
59	5	59	60	0	0	X	! Col (Smw)
60	4	60	61	0	0	X	!vert link col-foot (Smw)
61	3	28	62	0	0	X	!vert link cap-col (Sw)
62	5	62	63	0	0	X	! Col (Sw)
63	4	63	64	0	0	X	!vert link col-foot (Sw)
64	12	65	1	0	0	X	!north abutment spring
65	13	66	13	0	0	X	!south abutment spring
66	6	31	67	0	0	X	!col footing spring
67	7	34	68	0	0	X	!col footing spring
68	7	37	69	0	0	X	!col footing spring
69	6	40	70	0	0	X	!col footing spring
70	8	43	71	0	0	X	!col footing spring
71	9	46	72	0	0	X	!col footing spring
72	9	49	73	0	0	X	!col footing spring
73	8	52	74	0	0	X	!col footing spring
74	10	55	75	0	0	X	!col footing spring
75	11	58	76	0	0	X	!col footing spring
76	11	61	77	0	0	X	!col footing spring

```
77    10    64    78    0     0     X     !col footing spring


PROPS
1 FRAME                                      ! Deck
1 0 0 0 0 0 0 0                              !
6.358E5 2.54E5 86.755 56170 56170 231.802   ! E,G,A,J,Izz,Iyy (K,FT)
0

2 FRAME                                      ! Capbeam
1 0 0 0 0 0 0 0                              !
6.358E5 2.54E5  1E10 1E10 1E10 1E10          ! E,G,A,J,Izz,Iyy (K,FT)
0

3 FRAME                                      ! Vertical links btw deck+col
1 0 0 0 0 0 0 0                              !
1E10 1E10 1E4 2E7 1E7 1E2                    ! E,G,A,J,Izz,Iyy (K,FT)
0

4 FRAME                                      ! vertical links btw
col+footing
1 0 0 0 0 0 0 0                              !
1E10 1E10 1E4 2E7 1E7 1E2                    ! E,G,A,J,Izz,Iyy (K,FT)
0

5 FRAME
2 0 0 0 4 0 0                                !14a. Section Control
6.35E5 2.54E5 7.069 1.205 0.852 0.852        !14b. Section prop
E,G,A,J,Izz,Iyy
0.0                                          !14c. End Properties
0.04 0.04 0.04 0.04                          !14d. Member bilinear factor
1.423 1.423 1.423 1.423                      !14e. Plastic Hinge Length
0 0 1.0 1.0 0                                !14l. Interaction param
-4900 -1203 1475 1475 591.4                  !14m. P-M interaction
! 5.5 17 0.9 0                               ! Loss Model(page 145-
appendix A)
0.5 0.1 1 1

6 SPRING                                                     ! SOIL SPRING
NO
1 0 0 0 0 0                                                  ! Control
Par.
9.4921E4 9.4921E4 9.8085E4 4.4837E6 2.7516E6 4.9144E6 0 .33 .33        !
Section Prop.

7 SPRING                                                     ! SOIL SPRING
NI
1 0 0 0 0 0                                                  ! Control
Par.
9.4921E4 9.4921E4 9.8085E4 4.4837E6 2.7516E6 4.9144E6 0 .33 .33        !
Section Prop.

8 SPRING                                                     ! SOIL SPRING
CO
1 0 0 0 0 0                                                  ! Control
Par.
```

```
9.8059E4 9.8059E4 1.0320E5 4.8277E6 3.5006E6 4.6821E6 0 .33 .33        !
Section Prop.

9 SPRING                                                   ! SOIL SPRING
CI
1 0 0 0 0 0                                                ! Control
Par.
9.8059E4 9.8059E4 1.0320E5 4.8277E6 3.5006E6 4.6821E6 0 .33 .33        !
Section Prop.

10 SPRING                                                     ! SOIL
SPRING SO
1 0 0 0 0 0                                                   ! Control
Par.
9.1220E4 9.1220E4 9.4760E4 4.1780E6 2.0881E6 4.4245E6 0 .33 .33  !
Section Prop.

11 SPRING                                                     ! SOIL
SPRING SI
1 0 0 0 0 0                                                   ! Control
Par.
9.1220E4 9.1220E4 9.4760E4 4.1780E6 2.0881E6 4.4245E6 0 .33 .33  !
Section Prop.

12 SPRING                                                 ! SOIL SPRING
N Abt.
1 0 0 0 0 0                                               ! Control Par.
8.4002E5 8.4002E5 8.7782E5 2.4497E7 6.7001E7 5.1069E7 0 .33 .33        !
Section Prop.

13 SPRING                                                 ! SOIL SPRING
S Abt.
1 0 0 0 0 0                                               ! Control Par.
3.3819E5 3.3819E5 3.5341E5 9.8626E6 2.6974E7 2.0560E7 0 .33 .33        !
Section Prop.

Weights 0
1     1.767       1.767            1.767                   !north
abutment
2     88.359      88.359           88.359                  !north ramp
3     173.184     173.184          173.184
4     176.12      176.12           176.12                  !north deck
5     179.051     179.051          179.051
6     179.051     179.051          179.051
7     179.051     179.051          179.051                 !middle deck
8     179.051     179.051          179.051                 !south deck
9     179.051     179.051          179.051
10    172.584     172.584          172.584                 !south ramp
11    166.116     166.116          166.116
12    84.825      84.825           84.825
13    1.767       1.767            1.767                   !south
abutment
14    165.881     165.881          165.881                 !north bent
15    118.857     118.857          118.857
16    107.97      107.97           107.97
17    118.857     118.857          118.857
18    165.881     165.881          165.881
```

```
19    149.534     149.534           149.534                 !middle bent
20    107.959     107.959           107.959
21    97.071      97.071            97.071
22    107.959     107.959           107.959
23    149.534     149.534           149.534
24    162.909     162.909           162.909                 !south bent
25    116.875     116.875           116.875
26    105.988     105.988           105.988
27    116.875     116.875           116.875
28    162.909     162.909           162.909
30    21.312      21.312            21.312                  !column bot
33    21.312      21.312            21.312
36    21.312      21.312            21.312
39    21.312      21.312            21.312
42    21.312      21.312            21.312
45    21.312      21.312            21.312
48    21.312      21.312            21.312
51    21.312      21.312            21.312
54    21.312      21.312            21.312
57    21.312      21.312            21.312
60    21.312      21.312            21.312
63    21.312      21.312            21.312
77

Loads
1     0           0           -1.767            !north abutment
2     0           0           -88.359           !north ramp
3     0           0           -173.184
4     0           0           -176.118          !north deck
5     0           0           -179.051
6     0           0           -179.051
7     0           0           -179.051          !middle deck
8     0           0           -179.051          !south deck
9     0           0           -179.051
10    0           0           -172.584          !south ramp
11    0           0           -166.116
12    0           0           -84.825
13    0           0           -1.767            !south abutment
14    0           0           -165.881          !north bent
15    0           0           -118.857
16    0           0           -107.97
17    0           0           -118.857
18    0           0           -165.881
19    0           0           -149.534          !middle bent
20    0           0           -107.959
21    0           0           -97.071
22    0           0           -107.959
23    0           0           -149.534
24    0           0           -162.909          !south bent
25    0           0           -116.875
26    0           0           -105.988
27    0           0           -116.875
28    0           0           -162.909
30    0           0           -21.312           !column bot
33    0           0           -21.312
36    0           0           -21.312
39    0           0           -21.312
```

```
42     0           0           -21.312
45     0           0           -21.312
48     0           0           -21.312
51     0           0           -21.312
54     0           0           -21.312
57     0           0           -21.312
60     0           0           -21.312
63     0           0           -21.312
77


EQUAKE NSPERU9.TXT
5  1  0.01  1  -1                          ! File Parameters

EQUAKE EWPERU9.TXT
5  1  0.01  1  -1                          ! File Parameters

EQUAKE UPPERU9.TXT
5  1  0.01  1  -1                          ! File Parameters
```

A-2-3 Bridge 5/649 Ruaumoko Input File

```
5-649E east bridge with skew;units kip-ft; Es=6000 ksf=287.3 MPa; Peru;
Half Data
2  1  0  0  3  2  0  0                         ! Analysis Options
-1 0 0 0 -1 0 0 0 -1                           ! Earthquake Transformation
57 60 25 30 1 30 32.2 5 5 0.01 92 1.0          ! Frame Control Par
0  20  10  10  3  1  1  1                      ! Output Control
.866 -.866 0 -.5 -.5 -1                        ! Plot Axes Tran
10 0  0.0001                                   ! Iteration Control

NODES 1
1      0.000   0.000     0.000  0 0 0 0 0 0      !deck (north half)
2      12.00   0.000     0.000  0 0 0 0 0 0
3      24.00   0.000     0.000  0 0 0 0 0 0
4      36.00   0.000     0.000  0 0 0 0 0 0
5      47.91   0.000     0.000  0 0 0 0 0 0      !north ramp exp joint
6      48.09   0.000     0.000  0 0 0 0 0 0      !north ramp
7      67.25   0.000     0.000  0 0 0 0 0 0
8      86.50   0.000     0.000  0 0 0 0 0 0
9      105.75  0.000     0.000  0 0 0 0 0 0
10     125.00  0.000     0.000  0 0 0 0 0 0      !north abutment
11     125.05  0.000     0.000  1 1 1 1 1 1      !north abutment gap
12     -120.05 0.000     0.000  1 1 1 1 1 1      !south abutment gap
13     -120.00 0.000     0.000  0 0 0 0 0 0      !south abutment
14     -102.00 0.000     0.000  0 0 0 0 0 0      !south ramp
15     -84.000 0.000     0.000  0 0 0 0 0 0
16     -66.000 0.000     0.000  0 0 0 0 0 0
17     -47.906 0.000     0.000  0 0 0 0 0 0      !south ramp exp joint
18     -48.094 0.000     0.000  0 0 0 0 0 0      !deck (south half)
19     -36.000 0.000     0.000  0 0 0 0 0 0
20     -24.000 0.000     0.000  0 0 0 0 0 0
21     -12.000 0.000     0.000  0 0 0 0 0 0
22     -67.450 -20.142   0.000  0 0 0 0 0 0      !south-west bent
23     -57.725 -10.071   0.000  0 0 0 0 0 0      !mid south-west bent
24     -48.000 0.000     0.000  0 0 0 0 0 0      !center south bent
25     -38.275 10.071    0.000  0 0 0 0 0 0      !mid south-east bent
26     -28.550 20.142    0.000  0 0 0 0 0 0      !mid south-east bent
27     28.550  -20.142   0.000  0 0 0 0 0 0      !north-west bent
28     38.275  -10.071   0.000  0 0 0 0 0 0      !mid north-west bent
29     48.000  0.000     0.000  0 0 0 0 0 0      !center north bent
30     57.725  10.071    0.000  0 0 0 0 0 0      !mid north-east bent
31     67.450  20.142    0.000  0 0 0 0 0 0      !mid north-east bent
32     -67.450 -20.142   8.354  2 2 2 0 0 0 22   !west col south bent top
(slaved)
33     -67.450 -20.142   26.334 0 0 0 0 0 0      !west col south bent bot
34     -67.450 -20.142   27.959 1 1 1 1 1 1      !west col south bent ftg
35     -48.000 0.000     8.354  2 2 2 0 0 0 24   !mid col south bent top
(slaved)
36     -48.000 0.000     27.054 0 0 0 0 0 0      !mid col south bent bot
37     -48.000 0.000     28.679 1 1 1 1 1 1      !mid col south bent ftg
38     -28.550 20.142    8.354  2 2 2 0 0 0 26   !east col south bent top
(slaved)
39     -28.550 20.142    27.584 0 0 0 0 0 0      !east col south bent bot
40     -28.550 20.142    29.209 1 1 1 1 1 1      !east col south bent ftg
```

```
41    28.550  -20.142   8.354  2 2 2 0 0 0 27   !west col north bent top
(slaved)
42    28.550  -20.142   24.704 0 0 0 0 0 0      !west col north bent bot
43    28.550  -20.142   26.329 1 1 1 1 1 1      !west col north bent ftg
44    48.000  0.000     8.354  2 2 2 0 0 0 29   !mid col north bent top
                                                                (slaved)
45    48.000  0.000     25.504 0 0 0 0 0 0      !mid col north bent bot
46    48.000  0.000     27.129 1 1 1 1 1 1      !mid col north bent ftg
47    67.450  20.142    8.354  2 2 2 0 0 0 31   !east col north bent top
(slaved)
48    67.450  20.142    26.094 0 0 0 0 0 0      !east col north bent bot
49    67.450  20.142    27.719 1 1 1 1 1 1      !east col north bent ftg
50    -67.450 -20.142   27.959 0 0 0 0 0 0      !west col south bent sp
51    -48.000 0.000     28.679 0 0 0 0 0 0      !mid col south bent sp
52    -28.550 20.142    29.209 0 0 0 0 0 0      !east col south bent sp
53    28.550 -20.142    26.329 0 0 0 0 0 0      !west col north bent sp
54    48.000 0.000      27.129 0 0 0 0 0 0      !mid col north bent sp
55    67.450 20.142     27.719 0 0 0 0 0 0      !east col north bent sp
56    125.050 0.000     0.000  0 0 0 0 0 0      !north abutment spring
57    -120.05 0.000     0.000  0 0 0 0 0 0      !south abutment spring

ELEMENTS 1
1     6     1     2     0     0     Y     !north deck
2     6     2     3     0     0     Y     !north deck
3     6     3     4     0     0     Y     !north deck
4     5     4     5     0     0     Y     !north deck
5     1     6     7     0     0     Y     !north ramp
6     3     7     8     0     0     Y     !north ramp
7     3     8     9     0     0     Y     !north ramp
8     2     9     10    0     0     Y     !north ramp
9     1     13    14    0     0     Y     !south ramp
10    3     14    15    0     0     Y     !south ramp
11    3     15    16    0     0     Y     !south ramp
12    2     16    17    0     0     Y     !south ramp
13    4     18    19    0     0     Y     !south deck
14    6     19    20    0     0     Y     !south deck
15    6     20    21    0     0     Y     !south deck
16    6     21    1     0     0     Y     !south deck
17    7     24    23    0     0     X     !south-west bent
18    7     23    22    0     0     X
19    7     24    25    0     0     X     !south-east bent
20    7     25    26    0     0     X
21    7     29    28    0     0     X     !north-west bent
22    7     28    27    0     0     X
23    7     29    30    0     0     X     !north-east bent
24    7     30    31    0     0     X
25    8     22    32    0     0     X     !vert link deck-col
26    10    32    33    0     0     X     !west col south bent
27    9     33    50    0     0     X     !vert link col-foot
28    8     24    35    0     0     X     !vert link deck-col
29    11    35    36    0     0     X     !mid col south bent
30    9     36    51    0     0     X     !vert link col-foot
31    8     26    38    0     0     X     !vert link deck-col
32    12    38    39    0     0     X     !east col south bent
33    9     39    52    0     0     X     !vert link col-foot
34    8     27    41    0     0     X     !vert link deck-col
35    13    41    42    0     0     X     !west col north bent
```

```
36    9     42    53    0     0     X     !vert link col-foot
37    8     29    44    0     0     X     !vert link deck-col
38    14    44    45    0     0     X     !mid col north bent
39    9     45    54    0     0     X     !vert link col-foot
40    8     31    47    0     0     X     !vert link deck-col
41    15    47    48    0     0     X     !east col north bent
42    9     48    55    0     0     X     !vert link col-foot
43    16    5     29    0     0     Y     !north bent bearing pad (S)
44    16    29    6     0     0     Y     !north bent bearing pad (N)
45    16    17    24    0     0     Y     !south bent bearing pad (S)
46    16    24    18    0     0     Y     !south bent bearing pad (N)
47    16    10    56    0     0     Y     !north abutment bearing pad
48    16    13    57    0     0     Y     !south abutment bearing pad
49    17    5     6     0     0     Y     !north bent gap
50    17    17    18    0     0     Y     !south bent gap
51    17    10    56    0     0     Y     !north abutment gap
52    17    13    57    0     0     Y     !south abutment gap
53    21    34    50    0     0     X     !west col south bent footing
54    22    37    51    0     0     X     !mid col south bent sp ftg
55    23    40    52    0     0     X     !east col south bent sp ftg
56    18    43    53    0     0     X     !west col north bent sp ftg
57    19    46    54    0     0     X     !mid col north bent sp ftg
58    20    49    55    0     0     X     !east col north bent sp ftg
59    24    11    56    0     0     Y     !north abutment spring
60    25    12    57    0     0     Y     !south abutment spring


PROPS
1 FRAME                                  ! Deck 72ft (south ramp) w/
mbr release end 1
1 1 1 0 0 0 0                            ! Deck 77ft (north ramp)
6.358E5 2.54E5 63 3177 3176 237.5 63 63    ! E,G,A,J,Izz,Iyy,Asy,Asz
(K,FT)
0.0 0.0 0.0 0.0

2 FRAME                                  ! Deck 72ft (south ramp) w/
mbr release end 2
1 2 2 0 0 0 0                            ! Deck 77ft (north ramp)
6.358E5 2.54E5 63 3177 3176 237.5 63 63    ! E,G,A,J,Izz,Iyy,Asy,Asz
(K,FT)
0.0 0.0 0.0 0.0

3 FRAME                                  ! Deck 72ft (south ramp)
1 0 0 0 0 0 0                            ! Deck 77ft (north ramp)
6.358E5 2.54E5 63 3177 3176 237.5 63 63    ! E,G,A,J,Izz,Iyy,Asy,Asz
(K,FT)
0.0 0.0 0.0 0.0

4 FRAME                                  ! Deck 96ft (deck) w/ mbr
release end 1
1 1 1 0 0 0 0
6.358E5 2.54E5 70.6 34330 34330 292.334 70.6 70.6  !
E,G,A,J,Izz,Iyy,Asy,Asz (K,FT)
0.0 0.0 0.0 0.0

5 FRAME                                 ! Deck 96ft (deck) w/ mbr
release end 2
```

```
1 2 2 0 0 0 0                                          !
6.358E5 2.54E5 70.6 34330 34330 292.334 70.6 70.6      !
E,G,A,J,Izz,Iyy,Asy,Asz (K,FT)
0.0 0.0 0.0 0.0

6 FRAME                                ! Deck 96ft (deck)
1 0 0 0 0 0 0                                          !
6.358E5 2.54E5 70.6 34330 34330 292.334 70.6 70.6      !
E,G,A,J,Izz,Iyy,Asy,Asz (K,FT)
0.0 0.0 0.0 0.0

7 FRAME                                                ! Capbeam
1 0 0 0 0 0 0                                          !
6.358E5 2.54E5 1E2 1E4 1E2 1E5 1E2 1E2                 !
E,G,A,J,Izz,Iyy,Asy,Asz (K,FT)
0.0 0.0 0.0 0.0

8 FRAME                                  ! Vertical links btw deck+col
1 0 0 0 0 0 0                                          ! linear elastic
1E7 1E7 1E3 1E5 1E3 1E6 1E3 1E3                        !
E,G,A,J,Izz,Iyy,Asy,Asz (K,FT)
0.0 0.0 0.0 0.0

9 FRAME                                ! vertical links btw col+footing
1 0 0 0 0 0 0                                          ! linear elastic
1E7 1E7 1E3 1E5 1E3 1E6 1E3 1E3                        !
E,G,A,J,Izz,Iyy,Asy,Asz (K,FT)
0.0 0.0 0.0 0.0

10 FRAME                                                 !South-west column
2 0 0 0 4 0 0 0                                      !14a. Section Control
6.358E5 2.543E5 7.069 1.168 0.826 0.826 7.069 7.069  !14b. Section prop
E,G,A,J,Izz,Iyy
0.0 0.0 0.0 0.0                                      !14c. End Properties
0.07 0.07 0.07 0.07                             !14d. Member bilinear factor
1.338 1.338 1.338 1.338                         !14e. Plastic Hinge Length
0 0 1.0 1.1 0.0                                 !14l. Interaction param
-6556 -1555 1770 1770 483.7                     !14m. P-M interaction
! 5 8 0.7                                       ! Loss Model(appendix A)
0.5 0.1 1 1                                     ! Modified Takeda

11 FRAME                                       !South-mid column
2 0 0 0 4 0 0 0                                !14a. Section Control
6.358E5 2.543E5 7.069 1.168 0.826 0.826 7.069 7.069  !14b. Section prop
E,G,A,J,Izz,Iyy
0.0 0.0 0.0 0.0                                !14c. End Properties
0.07 0.07 0.07 0.07                            !14d. Member bilinear factor
1.367 1.367 1.367 1.367                        !14e. Plastic Hinge Length
0 0 1.0 1.1 0.0                                !14l. Interaction param
-6556 -1555 1770 1770 483.7                    !14m. P-M interaction
! 5 8 0.7                                      ! Loss Model(appendix A)
0.5 0.1 1 1                                    ! Modified Takeda


12 FRAME                                      ! South-east Column
2 0 0 0 4 0 0 0                               !14a. Section Control
```

```
6.358E5 2.543E5 7.069 1.168 0.826 0.826 7.069 7.069  !14b. Section prop
E,G,A,J,Izz,Iyy
0.0 0.0 0.0 0.0                           !14c. End Properties
0.07 0.07 0.07 0.07                       !14d. Member bilinear factor
1.388 1.388 1.388 1.388                   !14e. Plastic Hinge Length
0 0 1.0 1.1 0.0                           !14l. Interaction param
-6556 -1555 1770 1770 483.7               !14m. P-M interaction
! 5 8 0.7                                 ! Loss Model(appendix A)
0.5 0.1 1 1                               ! Modified Takeda

13 FRAME                                  !North-west Column
2 0 0 0 4 0 0 0                           !14a. Section Control
6.358E5 2.543E5 7.069 1.168 0.826 0.826 7.069 7.069  !14b. Section prop
E,G,A,J,Izz,Iyy
0.0 0.0 0.0 0.0                           !14c. End Properties
0.07 0.07 0.07 0.07                       !14d. Member bilinear factor
1.273 1.273 1.273 1.273                   !14e. Plastic Hinge Length
0 0 1.0 1.1 0.0                           !14l. Interaction param
-6556 -1555 1770 1770 483.7               !14m. P-M interaction
! 5 8 0.7                                 ! Loss Model(appendix A)
0.5 0.1 1 1                               ! Modified Takeda

14 FRAME                                  !North-Mid Column
2 0 0 0 4 0 0 0                           !14a. Section Control
6.358E5 2.543E5 7.069 1.168 0.826 0.826 7.069 7.069   !14b. Section prop
E,G,A,J,Izz,Iyy
0.0 0.0 0.0 0.0                           !14c. End Properties
0.07 0.07 0.07 0.07                       !14d. Member bilinear factor
1.305 1.305 1.305 1.305                   !14e. Plastic Hinge Length
0 0 1.0 1.1 0.0                           !14l. Interaction param
-6556 -1555 1770 1770 483.7               !14m. P-M interaction
! 5 8 0.7                                 ! Loss Model(appendix A)
0.5 0.1 1 1                               ! Modified Takeda

15 FRAME                                  !North-East Column
2 0 0 0 4 0 0 0                           !14a. Section Control
6.358E5 2.543E5 7.069 1.168 0.826 0.826 7.069 7.069   !14b. Section prop
E,G,A,J,Izz,Iyy
0.0 0.0 0.0 0.0                           !14c. End Properties
0.07 0.07 0.07 0.07                       !14d. Member bilinear factor
1.328 1.328 1.328 1.328                   !14e. Plastic Hinge Length
0 0 1.0 1.1 0.0                           !14l. Interaction param
-6556 -1555 1770 1770 483.7               !14m. P-M interaction
! 5 8 0.7                                 ! Loss Model(appendix A)
0.5 0.1 1 1                               ! Modified Takeda

16 SPRING                                 ! Bridge Deck Bearing Pads
1 0 0 0 0 0                               ! Control Parameters
1479.6 2E7 3E6 8E6 8E4 8E4 0 .3 .3        ! Section Properties

17 MULTISPRING                            ! Bridge Gap Elements
1 0 0 0 10 2 31 0                         ! Control Parameters
3.265E3 0 0 0 0 0 .3                      ! Section Properties
0 -9.265E15 0 0 0 0 0 0 0 0 0

18 SPRING                                 ! SOIL SPRING NW
1 0 0 0 0 0                               ! Control Par.
```

```
1.2091E5 1.2091E5 1.6626E5 7.3084E6 7.3084E6 1.0268E7 0 .33 .33        !
Section Prop.

19 SPRING                                                   ! SOIL SPRING NM
1 0 0 0 0 0                                                 ! Control Par.
1.2091E5 1.2091E5 1.6626E5 7.3084E6 7.3084E6 1.0268E7 0 .33 .33        !
Section Prop.

20 SPRING                                                   ! SOIL SPRING NE
1 0 0 0 0 0                                                 ! Control Par.
1.2091E5 1.2091E5 1.6626E5 7.3084E6 7.3084E6 1.0268E7 0 .33 .33        !
Section Prop.

21 SPRING                                                   ! SOIL SPRING SW
1 0 0 0 0 0                                                 ! Control Par.
1.3339E5 1.3339E5 1.6626E5 7.3106E6 7.3106E6 1.0268E7 0 .33 .33        !
Section Prop.

22 SPRING                                                   ! SOIL SPRING SM
1 0 0 0 0 0                                                 ! Control Par.
1.3339E5 1.3339E5 1.6626E5 7.3106E6 7.3106E6 1.0268E7 0 .33 .33        !
Section Prop.

23 SPRING                                     ! SOIL SPRING SE
1 0 0 0 0 0                                                 ! Control Par.
1.3339E5 1.3339E5 1.6626E5 7.3106E6 7.3106E6 1.0268E7 0 .33 .33        !
Section Prop.

24 SPRING                                     ! Secant SOIL SPRING BENT North
1 0 0 0 0 0                                                 ! Control Par.
2.0057E5 2.0718E5 3.3608E5 3.5240E6 6.0453E7 4.7215E7 0 .33 .33  !
Section Prop.

25 SPRING                                     ! Secant SOIL SPRING BENT South
1 0 0 0 0 0                                                 ! Control Par.
1.8966E5 1.9628E5 3.2071E5 3.5198E6 6.0449E7 4.7215E7 0 .33 .33  !
Section Prop.

WEIGHTS 1
1      127.126     127.126     127.126
2      127.126     127.126     127.126
3      127.126     127.126     127.126
4      127.126     127.126     127.126
5      63.563      63.563      63.563
6      91          91          91
7      182.014     182.014     182.014
8      182.014     182.014     182.014
9      182.014     182.014     182.014
10     91          91          91
13     85.1        85.1        85.1
14     170.195     170.195     170.195
15     170.195     170.195     170.195
16     170.195     170.195     170.195
17     85.10       85.10       85.10
18     63.563      63.563      63.563
19     127.126     127.126     127.126
20     127.126     127.126     127.126
```

21	127.126	127.126	127.126
22	13.65	13.65	13.65
23	27.3	27.3	27.3
24	27.3	27.3	27.3
25	27.3	27.3	27.3
26	13.65	13.65	13.65
27	13.65	13.65	13.65
28	27.3	27.3	27.3
29	27.3	27.3	27.3
30	27.3	27.3	27.3
31	13.65	13.65	13.65
32	19.064	19.064	19.064
35	19.827	19.827	19.827
38	20.389	20.389	20.389
41	17.336	17.336	17.336
44	18.184	18.184	18.184
47	18.81	18.81	18.81
56	321.294	321.294	321.294
57	309.244	309.244	309.244

LOADS

1	0	0	-127.126
2	0	0	-127.126
3	0	0	-127.126
4	0	0	-127.126
5	0	0	-63.563
6	0	0	-91
7	0	0	-182.014
8	0	0	-182.014
9	0	0	-182.014
10	0	0	-91
13	0	0	-85.1
14	0	0	-170.195
15	0	0	-170.195
16	0	0	-170.195
17	0	0	-85.097
18	0	0	-63.563
19	0	0	-127.126
20	0	0	-127.126
21	0	0	-127.126
22	0	0	-13.65
23	0	0	-27.3
24	0	0	-27.3
25	0	0	-27.3
26	0	0	-13.65
27	0	0	-13.65
28	0	0	-27.3
29	0	0	-27.3
30	0	0	-27.3
31	0	0	-13.65
32	0	0	-19.064
35	0	0	-19.827
38	0	0	-20.389
41	0	0	-17.336
44	0	0	-18.184
47	0	0	-18.81

```
56    0     0     -321.294
57    0     0     -309.244


EQUAKE NSPeru9.txt
5  1  0.01  1  -1                           ! File Parameters

EQUAKE EWPeru9.txt
5  1  0.01  1  -1                           ! File Parameters

EQUAKE UPPeru9.txt
5  1  0.01  1  -1                           ! File Parameters
```

Once Ruaumoko has been run a *'filename'*.RAS is generated and another software is used to sort the data: pwave. This software was developed by Visual Numerics, Inc. in 1997. It reads a script (reader_*'filename'*.pro) which will read the unformatted data of the .RAS file and store it as a matrix in a .txt file. The .pro file can be modified to fit the geometry of the analyzed structure (Enter the node, member numbers that define the structure, enter the number defining the analyses to be run (1=X-disp, 27=Z-shear at top, etc…)). Two commands need to be entered to run pwave:

At the prompt: WAVE>

Type: .rnew reader_*'filename'* (without the .pro extension)

Type: *'filename'* (without the .RAS extension)

This will execute the .pro file and create a 'filename'.txt file. After that, this text file can be used as a matrix of data in any program to plot and sort the data. S-Plus 2000 (MathSoft, Inc.) is a powerful software to plot numerous data variables at once, once an S-Plus script has been created.

APPENDIX A-3

Spring stiffness values for all bridges in US units.

		Translational Springs			Rotational Springs		
Bridge 512	Es (ksf)	K11 (Trans) k/ft	K22 (Long.) k/ft	K33 (Vert.) k/ft	K44 (Trans.) k-ft/rad	K55 (Long.) k-ft/rad	K66 (Vert.) k-ft/rad
North Abut	1000	1.40E+05	1.40E+05	1.46E+05	4.08E+06	1.12E+07	8.51E+06
	6000	8.40E+05	8.40E+05	8.78E+05	2.45E+07	6.70E+07	5.11E+07
	18000	2.52E+06	2.52E+06	2.63E+06	7.35E+07	2.01E+08	1.53E+08
North Pier	1000	1.58E+04	1.58E+04	1.63E+04	7.47E+05	4.59E+05	8.19E+05
	6000	9.49E+04	9.49E+04	9.81E+04	4.48E+06	2.75E+06	4.91E+06
	18000	2.85E+05	2.85E+05	2.94E+05	1.35E+07	8.25E+06	1.47E+07
Center Pier	1000	1.63E+04	1.63E+04	1.72E+04	8.05E+05	5.83E+05	7.80E+05
	6000	9.81E+04	9.81E+04	1.03E+05	4.83E+06	3.50E+06	4.68E+06
	18000	2.94E+05	2.94E+05	3.10E+05	1.45E+07	1.05E+07	1.40E+07
South Pier	1000	1.52E+04	1.52E+04	1.58E+04	6.96E+05	3.48E+05	7.37E+05
	6000	9.12E+04	9.12E+04	9.48E+04	4.18E+06	2.09E+06	4.42E+06
	18000	2.74E+05	2.74E+05	2.84E+05	1.25E+07	6.26E+06	1.33E+07
South Abut	1000	5.64E+04	5.64E+04	5.89E+04	1.64E+06	4.50E+06	3.43E+06
	6000	3.38E+05	3.38E+05	3.53E+05	9.86E+06	2.70E+07	2.06E+07
	18000	1.01E+06	1.01E+06	1.06E+06	2.96E+07	8.09E+07	6.17E+07

Bridge 227	Es (ksf)	Translational Springs			Rotational Springs		
West Abut	5	7.87E+04	8.48E+04	3.20E+05	1.38E+07	1.38E+07	3.12E+04
	1000	1.42E+05	1.48E+05	3.85E+05	1.74E+07	1.86E+07	6.23E+06
	6000	4.63E+05	4.66E+05	7.15E+05	3.55E+07	4.31E+07	3.74E+07
	18000	1.23E+06	1.23E+06	1.50E+06	7.91E+07	1.02E+08	1.12E+08
West Pier	5	1.98E+04	1.98E+04	9.33E+04	5.34E+05	5.33E+05	4.40E+03
	1000	3.68E+04	3.68E+04	1.11E+05	1.34E+06	1.07E+06	8.80E+05
	6000	1.22E+05	1.22E+05	2.02E+05	5.38E+06	3.76E+06	5.28E+06
	18000	3.26E+05	3.26E+05	4.20E+05	1.51E+07	1.02E+07	1.58E+07
Center Pier	5	1.98E+04	1.98E+04	9.33E+04	5.34E+05	5.33E+05	4.40E+03
	1000	3.68E+04	3.68E+04	1.11E+05	1.34E+06	1.07E+06	8.80E+05
	6000	1.22E+05	1.22E+05	2.02E+05	5.38E+06	3.76E+06	5.28E+06
	18000	3.26E+05	3.26E+05	4.20E+05	1.51E+07	1.02E+07	1.58E+07
East Pier	5	1.98E+04	1.98E+04	9.33E+04	5.34E+05	5.33E+05	4.40E+03
	1000	3.68E+04	3.68E+04	1.11E+05	1.34E+06	1.07E+06	8.80E+05
	6000	1.22E+05	1.22E+05	2.02E+05	5.38E+06	3.76E+06	5.28E+06
	18000	3.26E+05	3.26E+05	4.20E+05	1.51E+07	1.02E+07	1.58E+07
East Abut	5	7.87E+04	8.48E+04	3.20E+05	1.38E+07	1.38E+07	3.12E+04
	1000	1.42E+05	1.48E+05	3.85E+05	1.74E+07	1.86E+07	6.23E+06
	6000	4.63E+05	4.66E+05	7.15E+05	3.55E+07	4.31E+07	3.74E+07
	18000	1.23E+06	1.23E+06	1.50E+06	7.91E+07	1.02E+08	1.12E+08

Bridge 649	Es (ksf)	Translational Springs			Rotational Springs		
South Abut	1000	7.43E+04	8.09E+04	1.82E+05	6.15E+05	1.01E+07	7.87E+06
	6000	1.90E+05	1.96E+05	3.21E+05	3.52E+06	6.04E+07	4.72E+07
	18000	4.67E+05	4.73E+05	6.55E+05	1.05E+07	1.81E+08	1.42E+08
South Pier	1000	3.37E+04	3.37E+04	6.36E+04	1.22E+06	1.22E+06	1.71E+06
	6000	1.33E+05	1.33E+05	1.66E+05	7.31E+06	7.31E+06	1.03E+07
	18000	3.73E+05	3.73E+05	4.13E+05	2.19E+07	2.19E+07	3.08E+07
North Pier	1000	2.12E+04	2.12E+04	6.36E+04	1.22E+06	1.22E+06	1.71E+06
	6000	1.21E+05	1.21E+05	1.66E+05	7.31E+06	7.31E+06	1.03E+07
	18000	3.60E+05	3.60E+05	4.13E+05	2.19E+07	2.19E+07	3.08E+07
North Abut	1000	8.52E+04	9.18E+04	1.97E+05	6.19E+05	1.01E+07	7.87E+06
	6000	2.01E+05	2.07E+05	3.36E+05	3.52E+06	6.05E+07	4.72E+07
	18000	4.77E+05	4.84E+05	6.70E+05	1.05E+07	1.81E+08	1.42E+08

Appendix A-3 Spring values for all bridges in US units

APPENDIX A-4

1. <u>Bridge 5/227</u>

Footings - Transverse Shear Force Demands | **Longitudinal Shear Force Demands**

Bridge 227 - Φ Vn = 1641 kN (369 kips) | **Bridge 227 - Φ Vn = 2185 kN (492 kips)**

		Center bent - Center Column (Transverse)				Center bent - Center Column (Longitudinal)			
EQ	Spring Es values (MPa)	North dir. Shear (kips)	North dir. Shear (kN)	South dir. Shear	South dir. Shear (kN)	North dir. Shear (kips)	North dir. Shear (kN)	South dir. Shear (kips)	South dir. Shear (kN)
Kobe 475	47.9	65	289	-69	-309	42	187	-36	-160
	861.9	66	295	-77	-345	39	175	-40	-179
	fixed	65	290	-85	-377	62	277	-60	-269
Mexico 475	47.9	60	269	-64	-287	37	167	-44	-195
	861.9	56	249	-60	-268	49	220	-50	-221
	fixed	71	314	-59	-263	54	239	-42	-186
Olympia 475	47.9	43	191	-52	-232	28	124	-37	-163
	861.9	70	312	-72	-320	35	156	-47	-210
	fixed	67	296	-52	-230	20	89	-57	-255
Chile 475	47.9	59	263	-66	-292	30	133	-36	-161
	861.9	80	355	-67	-297	33	146	-38	-171
	fixed	41	181	-33	-145	46	203	-50	-220
Peru 475	47.9	47	207	-52	-230	38	169	-48	-215
	861.9	49	218	-59	-264	42	189	-47	-207
	fixed	94	417	-62	-276	86	383	-44	-196
Kobe 975	47.9	58	256	-68	-303	67	298	-75	-334
	861.9	63	278	-58	-258	66	293	-66	-291
	fixed	81	362	-80	-354	83	371	-56	-248
Mexico 975	47.9	66	292	-69	-308	40	178	-30	-135
	861.9	62	276	-66	-292	41	181	-66	-292
	fixed	71	315	-94	-418	46	205	-89	-395
Olympia 975	47.9	61	271	-65	-288	42	185	-47	-208
	861.9	58	259	-56	-251	44	197	-46	-204
	fixed	73	325	-60	-266	50	223	-54	-242
Chile 2475	47.9	66	295	-62	-275	49	217	-51	-228
	861.9	72	321	-68	-303	51	225	-52	-230
	fixed	45	199	-56	-249	52	230	-54	-241
Peru 2475	47.9	79	352	-75	-335	52	231	-53	-237
	861.9	89	395	-89	-394	59	263	-62	-278
	fixed	90	400	-75	-334	107	476	-62	-276

Transverse Shear Force in Girder-webs at the Abutments

Bridge 227 - Φ Vn = 1312 kN (295 kips)

		West abut				East Abut.			
EQ	Spring Es values	North dir.		South dir.		North dir.		South dir.	
		kips	kN	kips	kN	kips	kN	kips	kN
Kobe975	47.9	51	227	-51	-225	55	243	-48	-215
	861.9	58	258	-56	-249	55	246	-39	-172
Mexico 975	47.9	39	174	-48	-214	52	229	-52	-230
	861.9	40	178	-48	-213	48	214	-54	-242
Olympia 975	47.9	51	226	-51	-228	53	235	-51	-227
	861.9	45	198	-54	-239	45	200	-43	-191
Peru 2475	47.9	72	322	-72	-320	70	313	-59	-262
	861.9	61	271	-53	-236	72	320	-64	-286
Chile 2475	47.9	76	338	-60	-266	72	320	-49	-219
	861.9	65	291	-52	-231	65	289	-54	-242

2. Bridge 512/19

Footings - Transverse Shear Force Demands

Bridge 512 - Φ Vn = 972 kN (219 kips)

EQ	Spring Es values (ksf)	Center bent - Middle-East Column West dir. Shear (kips)	West dir. Shear (kN)	East dir. Shear (kips)	East dir. Shear (kN)
Kobe 475	1000	57	252	-52	-231
	18000	48	214	-47	-207
	fixed	34	152	-37	-163
Mexico 475	6000	51	228	-49	-216
	18000	52	230	-47	-210
	fixed	37	165	-38	-170
Olympia 475	1000	54	239	-56	-251
	18000	45	201	-45	-198
	fixed	40	177	-32	-141
Chile 475	6000	51	226	-53	-237
	18000	51	226	-52	-233
	fixed	49	218	-40	-180
Peru 475	6000	52	229	-50	-223
	18000	50	224	-48	-215
	fixed	36	160	-60	-268
Kobe 975	6000	60	268	-58	-257
	18000	54	239	-53	-235
	fixed	49	218	-46	-205
Mexico 975	6000	53	237	-61	-270
	18000	51	225	-54	-239
	fixed	51	228	-32	-142
Olympia 975	6000	49	217	-65	-290
	18000	61	273	-51	-225
	fixed	34	152	-48	-214
Chile 2475	6000	62	276	-65	-288
	18000	65	291	-73	-326
	fixed	63	280	-63	-278
Peru 2475	6000	74	330	-79	-350
	18000	76	338	-83	-367
	fixed	79	350	-91	-404

Longitudinal Shear Force Demands

Bridge 512 - Φ Vn = 972 kN (219 kips)

Center bent - Middle-East Column West dir. Shear (kips)	West dir. Shear (kN)	East dir. Shear (kips)	East dir. Shear (kN)
1	2	-1	-3
3	12	-2	-11
34	150	-36	-161
7	32	-1	-4
3	14	-4	-17
28	124	-37	-166
1	4	-1	-6
1	4	-9	-38
28	125	-41	-181
1	5	-1	-4
8	36	-1	-5
32	142	-41	-182
1	3	-1	-5
1	4	-1	-5
45	199	-58	-259
1	6	-12	-55
1	6	-2	-7
40	177	-31	-139
8	37	-7	-33
12	52	-9	-40
34	149	-39	-176
11	48	-2	-8
2	7	-8	-36
36	160	-39	-175
2	7	-23	-100
13	56	-15	-69
84	372	-64	-286
17	76	-10	-45
3	15	-13	-58
73	324	-82	-365

Transverse Shear Force in Girder-webs at the Abutments

Bridge 512 - Φ Vn = 2096 kN (471 kips)

EQ	Spring Es values	North abut West dir. Shear kips	kN	East dir. kips	kN	South Abut. West dir. kips	kN	East dir. Shear kips	kN
Peru 2475	47.9	309	1372	-272	-1208	273	1213	-270	-1203
	861.9	304	1351	-282	-1254	261	1162	-269	-1198

3. Bridge 5/649

Footings - Transverse Shear Force Demands

Bridge 649 with skew - Φ Vn = 1876 kN (422 kips)

		South bent - Center Column (54 - 28)			
EQ	Spring Es values (ksf)	West dir. Shear (kips)	West dir. Shear (kN)	East dir. Shear (kips)	East dir. Shear (kN)
Kobe 475	6000	34	152	-24	-107
	18000	34	151	-21	-94
	fixed	42	188	-22	-96
Mexico 475	6000	27	122	-21	-95
	18000	24	108	-21	-91
	fixed	25	111	-37	-164
Olympia 475	6000	21	92	-29	-129
	18000	26	116	-26	-114
	fixed	31	136	-32	-141
Chile 475	6000	37	166	-42	-187
	18000	38	170	-33	-146
	fixed	45	198	-55	-245
Peru 475	6000	39	172	-41	-182
	18000	47	208	-30	-132
	fixed	46	206	-46	-203
Kobe 975	6000	45	199	-33	-145
	18000	42	189	-33	-147
	fixed	51	227	-35	-156
Mexico 975	6000	36	160	-29	-127
	18000	25	111	-37	-165
	fixed	25	112	-53	-237
Olympia 975	6000	34	153	-38	-170
	18000	48	215	-36	-161
	fixed	41	184	-48	-214
Chile 2475	6000	87	386	-91	-405
	18000	102	452	-60	-265
	fixed	89	395	-88	-391
Peru 2475	6000	83	371	-73	-322
	18000	81	360	-89	-396
	fixed	102	452	-83	-369

Longitudinal Shear Force Demands

Bridge 649 with skew - Φ Vn = 1876 kN (422 kips)

South bent - Center Column (54 - 28)			
West dir. Shear (kips)	West dir. Shear (kN)	East dir. Shear (kips)	East dir. Shear (kN)
16	72	-13	-58
16	69	-11	-49
34	150	-23	-103
21	93	-17	-77
19	85	-11	-49
30	135	-19	-85
22	98	-14	-62
25	111	-8	-36
29	129	-31	-137
12	53	-29	-130
23	102	-22	-96
42	185	-77	-341
32	144	-21	-92
30	133	-25	-110
54	238	-45	-201
28	126	-18	-80
28	122	-17	-75
37	163	-34	-152
37	166	-20	-89
22	96	-32	-141
50	223	-31	-136
27	122	-15	-64
25	109	-22	-98
36	158	-39	-173
44	195	-55	-243
31	140	-57	-252
106	471	-142	-632
57	253	-63	-281
56	251	-60	-265
122	544	-91	-406

Transverse Shear Force in Girder-webs at the Abutments

Bridge 649 - Φ Vn = 2041 kN (548.76 kips)

		North abut				South Abut.			
EQ	Spring Es values	West dir. Shear		East dir.		West dir.		East dir. Shear	
		kips	kN	kips	kN	kips	kN	kips	kN
Kobe975	47.9	32	144	-23	-102	41	182	-32	-143
	861.9	30	132	-22	-100	38	171	-31	-138
Mexico 975	47.9	20	91	-42	-186	18	80	-27	-118
	861.9	22	97	-40	-177	18	79	-27	-120
Olympia 975	47.9	33	146	-29	-131	33	148	-32	-143
	861.9	30	132	-27	-121	29	128	-29	-130
Peru 2475	47.9	34	149	-32	-141	37	162	-43	-192
	861.9	29	131	-27	-120	33	148	-38	-168
Chile 2475	47.9	35	156	-27	-120	38	167	-32	-143
	861.9	35	156	-27	-120	38	167	-32	-143